THE INFLUENCE OF SWIMMING ON THE VERTICAL AND HORIZONTAL DISTRIBUTION OF MARINE INVERTEBRATE LARVAE

by

Rémi M. Daigle

Submitted in partial fulfilment of the requirements
for the degree of Doctor of Philosophy

at

Dalhousie University
Halifax, Nova Scotia
June 2013

For my loving wife, Katy, who has always been there through the good times and the bad.

And to my family, for your never ending love and support.

TABLE OF CONTENTS

LIST OF TABLES

LIST OF FIGURES

ABSTRACT

This thesis aims to increase our understanding of mechanisms that influence larval dispersal in marine benthic invertebrates, particularly in the absence of strong oceanographic features (e.g. estuarine plumes, upwelling events, or markedly different water masses). Laboratory experiments identified behavioural mechanisms that regulate the vertical distribution of larvae in response to thermal stratification, and field studies in St. George's Bay, Nova Scotia (NS), Canada, examined the relationship between larval abundance and physical variables (temperature, salinity, fluorescence, etc) and identified mechanisms that regulate larval distributions *in situ*. In the laboratory, I demonstrated that thermal stratification affects the vertical distribution of larvae by acting as a barrier to migration, or through temperature-dependent vertical swimming velocities. I also developed a random walk based model which highlighted that the key to successfully simulating larval response to temperature was 1) determining the temperature-dependent distribution of vertical swimming velocities and 2) the temporal autocorrelation in these velocities. In the field, the most striking pattern was that the larval distributions for species with similar swimming abilities were significantly correlated to one another at all scales (0.5 to 40 km). This suggests a common mechanism, related to larval swimming ability, which greatly influences the horizontal larval distribution. I found that the spatial scale of variability in larval distributions (~ 3 km) matches that in both the environmental variables and of coherent structures in current velocities (i.e. the tidal excursion). Results from an aggregation-diffusion model suggest that horizontal larval swimming could not be responsible for the observed level of aggregation in the larval horizontal distributions. I suggest that these horizontal patterns are the result of 1) an aggregative process (i.e. larvae swimming against a vertical current and maintaining their vertical position) and 2) a diffusive process which scales the aggregations to the scale of the coherent structures in current velocity (i.e. tidal excursion). In conclusion, this thesis increases our understanding of larval behaviour and its effects on larval dispersal. The results will be particularly useful to those who are interested in mechanisms regulate population connectivity, particularly those using bio-physical models to model dispersal trajectories.

LIST OF ABBREVIATIONS AND SYMBOLS USED

Abbreveation/ Symbol	Definition	Units
ΔT	the temperature difference between layers	°C
Δt	time step	s
ε_T	random error based on a normal distribution	m
ρ	seawater density	g ml^{-1}
μ	dynamic viscosity of seawater	cP
λ	exponential decay rate	s^{-1}
ADCP	Acoustic Doppler Current Profilers	
Ar	*Asterias rubens*	
Ai	*Argopecten irradians*	
B	temperature in the bottom water layer	°C
Bv	bivalves	
Bv1	*Mytilus* spp.	
Bv2	Other bivalves	
Bz	bryozoans	
Bz1	*Electra pilosa*	
CGS M	Alexander Graham Bell Canada Graduate Scholarships (Master's level)	
CHONe	Canadian Healthy Oceans Network	
CTD	Conductivity-Temperature-Depth recorder	
d	distance class	km

Abbreveation/ Symbol	**Definition**	**Units**
DNA	Deoxyribonucleic acid	
D	diffusion index	$m^2 s^{-1}$
Dp	decapods	
Dp1	*Cancer irroratus*	
Dp2	*Crangon septemspinosa*	
Gp	gastropods	
Gp1	*Astyris lunata*	
Gp2	*Margarites* spp	
I	Moran's I	
I_D	index of dispersion	
I_M	Morisita's index	
MPA	Marine Protected Areas	
NS	Nova Scotia	
NSERC	Natural Sciences and Engineering Research Council of Canada	
p	probability of changing velocity	
P	larval position	mm
PDF	probability distribution functions	
PGS D	Postgraduate Scholarships	
p_i	proportion of larvae at depth interval i	
PLD	pelagic larval duration	

Abbreveation/ Symbol	Definition	Units
q_i	numerical constant that depends on dimensionality	
s	larval swimming speed	mm s^{-1}
Sd	*Strongylocentrotus droebachiensis*	
SD	Standard deviation	
SL	simulated larvae	
t	time at which measurements are made	s
V_a	variance of the measured acceleration	$(mm\ s^{-1})^2$
w	vertical velocity	mm s^{-1}
W	sum of w_{hi}	
w_{hi}	the weights for sites h and i	
x_i	larval abundance at site i	Ind. m^{-3}
y_h and y_i	values of the variable (abundance or physical variables) at sites h and i	
ZCM	the center of larval mass	
z	larval depth	
z_i	median depth at interval i	

ACKNOWLEDGEMENTS

Firstly, I thank my supervisor Dr. Anna Metaxas for her guidance, encouragement and mentorship. Her dedication to her students is outstanding and I am forever grateful. My committee members, Drs. Christopher Taggart, Paul Snelgrove and Joël Chassé, have also provided very helpful advice, discussion and suggestions. Also, anonymous reviewers have provided constructive feedback that has improved those manuscripts.

I would like to thank John Lindley, Colette Feehan and Kira Krumhansl for collecting adult echinoderms and Barry Macdonald for providing larvae of *A. irradians*. I am grateful for the assistance from Amy Roy, Jessie Short, Jim Eddington and the staff at Dalhousie University's Aquatron during larval rearing and experiments. I would also like to thank Michelle Lloyd, Ryan Stanley, Stacey Henderson, Jessie Short, Donny Ross, and Jack Foley for help with field work and Keith Thompson, Eric Oliver, Jean-Pierre Auclair and Kim Davies for assistance with Matlab.

Funding for this research was provided by Natural Sciences and Engineering Research Council of Canada (NSERC) grants to Anna Metaxas: Discovery and the Strategic Network for the Canadian Healthy Oceans Network (CHONe). I would also like to thank all the people involved in the CHONe network, this experience would not have been the same without you. Funding to Rémi Daigle was through a NSERC CGS M and PGS D, as well as Graduate Scholarships and President Awards from Dalhousie University.

Last but certainly not least, I'd like to thank my wife, my family and my friends for supporting me.

CHAPTER 1: INTRODUCTION

The life cycle of marine benthic invertebrates includes a benthic adult phase which is often sessile, and a planktonic larval phase that can disperse large distances (McEdward 1995; Levin 2006; Cowen et al. 2007). Spatial and temporal variability in larval recruitment to adult populations affects overall population dynamics (Underwood and Fairweather 1989a). Conversely, spatial and temporal variability in adult populations also affects larval supply (Grosberg and Levitan 1992). For marine benthic invertebrates, this intergenerational dependence is essential for population connectivity, which is the exchange of individuals among populations (Cowen and Sponaugle 2009). Due to demographics, local oceanographic conditions, and geographic location, some populations may act as a source of individuals while others may act as a sink and thus not contribute to the long term survival of the species.

The study of larval dispersal is difficult because of the small size of the larvae, and complex interactions with physical features in a vast ocean (Levin 2006; Cowen and Sponaugle 2009). While useful insights into larval dispersal have been gained from studies using elemental fingerprinting, genetic and physical models, all these techniques have limitations. Elemental fingerprinting allows the discrimination of larval source from a distinct trace-elemental signature in tissues that were formed in the natal habitat. This technique is limited by the spatial scale of detectable differences in elemental fingerprints due to local geology, habitat type, pollution, runoff and local oceanography (*e.g.* upwelling), as well as by the availability and accuracy of an atlas of elemental fingerprints from potential source locations (DiBacco and Levin 2000; Miller et al. 2013).

Genetic studies are useful to detect realised genetic structure in adults or the lineage of new settlers when the genetic structure is known. However, the utility of genetics studies is generally limited to larger spatial and temporal scales since the genetic structure detected by these studies is the result of population interactions over multiple generations (Palumbi 2003; Weersing and Toonen 2009). Physical models, which are either general circulation models or advection-diffusion models, are used to quantify the effects of the physical properties of the ocean (*e.g.* general circulation patterns, tides, wind-driven circulation) on biological components such as larval behaviour and dispersal. However, bio-physical models generally only simulate processes that are known to affect larval dispersal and have been parameterized (Metaxas and Saunders 2009).

Given that invertebrate larvae are weak swimmers compared to horizontal current velocities (Chia et al. 1984), larvae have been mostly considered passively drifting particles when modelling dispersal (Petrie and Drinkwater 1978; Banse 1986; Miller and Emlet 1997). Intuitively, larvae with longer pelagic larval duration (PLD), should be advected further, and be associated with longer dispersal distances and more homogeneous genetic structure all else being equal (same larval behaviour, same temperature regime, etc). Conversely, larvae with short PLD should be less influenced by advection, and show greater retention and genetic differentiation (Palumbi 2003; Levin 2006; Shanks 2009). However, observations of the spread of invasive species, genetic studies of population structure, direct observations, and experimental estimates of dispersal distances do not support this hypothesis (Shanks 2009; Weersing and Toonen 2009). Species with a short PLD can be associated with a surprisingly homogeneous population structure and species with a longer PLD can be retained locally. While some

of this variability may be explained by the biases related to the methods used to quantify PLD, dispersal or genetic structure (*e.g.* microsatellites versus mitochondrial DNA), there is certainly variability in the PLD/dispersal distance relationship that is due to larval behaviour and interactions with oceanographic features.

A classic example of such a behavioural interaction is selective tidal stream transport (DiBacco et al. 2001; Forward Jr et al. 2003; Tamaki et al. 2010). The larvae of certain species migrate vertically with the same periodicity as the tidal cycle, migrating towards the surface for flood tide and towards the bottom for ebb tide, taking advantage of the differential transport to reach the head of the estuary. This type of behavioural mechanism allows larval dispersal to deviate substantially from the dispersal path of a passive particle. Studying the prevalence, variety and consequence of these behavioural mechanisms are central to explaining variation in larval dispersal.

Studying population connectivity and, by extension, larval dispersal is critical in the management of marine benthic invertebrate populations. Source-sink population dynamics and their spatial scale are critical in the design of marine protected areas (MPA), managing commercially important stocks, maintaining biodiversity and understanding the spread of invasive species (Kinlan et al. 2005; Kaplan 2006; Edwards et al. 2007). The probability density function of the dispersal distances from a source population is the dispersal kernel; and is affected by many factors including PLD, larval behaviour (*e.g.* vertical migration), as well as spatiotemporal variability in circulation patterns (O'Connor et al. 2007; Shanks 2009; Corell et al. 2012). For example, the spatial scale of these dispersal kernels will affect the efficiency of a network of MPA. In an MPA which is smaller than the mean dispersal distance of a particular organism, local

larval retention will be very low, whereas a larger MPA can contain largely self-seeding populations (Botsford et al. 2003; Halpern 2003). Similarly, when the distance between MPAs is smaller than the maximum dispersal distance of a particular organism, there is potential for population connectivity to be high, whereas there will be no exchange of individuals between MPAs that are separated by greater distances.

While there is some contention regarding size, shape and efficiency of MPAs, the intended role of a network of MPAs (*e.g.* protection of biodiversity, insurance policy for commercially valuable species or enhance recovery of a threatened species) will affect the spatial design of such a network (Halpern 2003; Palumbi 2004; O'Connor et al. 2007; López-Duarte et al. 2012). The design of these networks may produce variable results due to their different intended roles; however, it is clear that larval dispersal and population connectivity will affect the population dynamics and resilience within the network (Cowen et al. 2002; Browman et al. 2004). At present, bio-physical models are the best way to experimentally compare the effects of different management options, such as the population connectivity within different MPA networks. Therefore, if the role of the MPA network is species specific, then species specific ecology, behaviour and dispersal properties should be used when designing the network. However, if the role of the MPA network is to protect biodiversity, or maintain ecosystem structure, function and services, then a multi-species approach is required.

1.1 Objectives

Broadly, this thesis aims to increase our understanding of mechanisms that influence larval dispersal in marine benthic invertebrates, particularly in the absence of strong oceanographic features (e.g. estuarine plumes, upwelling events, or markedly

different water masses). To measure key aspects of larval behaviour and distributions, I have conducted: 1) laboratory experiments to identify behavioural mechanisms regulating the vertical distribution of larvae in response to thermal stratification, and 2) field observations to examine the relationship between larval abundance and physical variables (temperature, salinity, fluorescence, etc) and identify mechanisms that determine larval distributions *in situ*. I have included complementary modelling components to explore the role of potential mechanisms affecting the observed larval distributions for both the laboratory and field components. The field work was conducted in St. George's Bay, Nova Scotia (NS), Canada.

This thesis is part of a larger project within the Canadian Healthy Oceans Network (CHONe) under the theme of Population Connectivity. This project (Project 3.2.1 "Population connectivity and dispersal in contrasting species") partly addresses the goal of comparing metapopulation connectivity among marine populations using different metrics of larval dispersal. To address these questions, several studies were conducted in St. George's Bay concurrently: 1) a high temporal frequency study of larval vertical distributions (Lloyd et al. 2012a; b), 2) a survey of potential larval predators and their prey selectivity (Short et al. 2012), 3) a study focused on lobster (*Homarus americanus*) larval distribution and dispersal (Stanley and Snelgrove, unpublished data), 4) a study using magnetically attractive particles (micro drifters) as larval mimics (Hrycik and Taggart, unpublished data). The synthesis of all these studies should address poignant questions regarding population connectivity.

This thesis is arranged in 6 chapters (including this Introduction), **Chapters 2-5** address the research objectives, and are intended as standalone manuscripts for

publication in the primary literature. Consequently, there is necessarily some repetition among the chapters. **Chapters 2** and **3** have been published (Daigle and Metaxas 2011, 2012) and **Chapters 4** and **5** have been submitted for publication. In **Chapter 2**, I examine the influence of thermal stratification on the larval vertical distribution of a number of model species, the sea urchin *Strongylocentrotus droebachiensis*, the sea star *Asterias rubens*, and the scallop *Argopecten irradians*. I further develop the hypothesis that temperature affects vertical distribution by acting on vertical swimming velocity in **Chapter 3** using *Strongylocentrotus droebachiensis* as a model organism. I parameterized a random walk based model of larval swimming with video observations of larval swimming. In **Chapters 4** and **5**, I describe studies based on sampling larval distributions in the field and comparing those distributions to physical variables (temperature, salinity, fluorescence, etc) to identify mechanisms that affect larval distributions *in situ*. In **Chapter 4,** I examine processes at smaller scales (0.5 to 10 km) than in **Chapter 5** (5 to 40 km). In **Chapters 4** and **5,** I have deliberately attempted to identify broadly applicable mechanisms that may explain larval distributions and expand the existing suite of conceptual models. In **Chapter 6,** I provide final conclusions from the thesis and a prescriptive prelude to a future standalone manuscript for publication in the primary literature that is intended to serve as a capstone piece to **Chapters 2-5**. This manuscript, which is in development, will examine the role of larval vertical swimming behaviour and vertical distributions in larval dispersal and the formation of larval aggregations using a bio-physical model.

CHAPTER 2: VERTICAL DISTRIBUTION OF MARINE INVERTEBRATE LARVAE IN RESPONSE TO THERMAL STRATIFICATION IN THE LABORATORY[1]

2.1 Abstract

I investigated the effect of the presence of an experimentally generated thermocline on the vertical distribution of larval *Strongylocentrotus droebachiensis*, *Asterias rubens* and *Argopecten irradians*. Vertical distributions were recorded over 90 minutes in rectangular plexiglass thermocline chambers designed to regulate the temperature of a central observation compartment to the desired temperature(s). The temperature in the bottom water layer (B) and the temperature difference between layers (ΔT) were manipulated in an orthogonal design. I used, for *S. droebachiensis*: 4 levels of ΔT (0, 3, 6 and 12 °C) and 3 levels of B (3, 6 and 9 °C); for *A. rubens*: 3 levels ΔT (0, 6 and 12 °C) and 2 levels of B (6 and 12 °C); and for *A. irradians*: 3 levels of ΔT (0, 5 and 11 °C) and 2 levels of B (5 and 11 °C). The difference in temperature between water layers did not affect the vertical distribution of echinoderms consistently, while the distribution of *A. irradians* was limited to the bottom layer when any thermal stratification was present regardless of strength. My results suggest that the vertical position of larvae of *S. droebachiensis* and *A. rubens* are related the temperatures of the surface layer and that the presence alone or the steepness of the thermocline have less influence on their distribution. Consequently, in the field, echinoderm larvae would

---

[1] Daigle, R. M., and A. Metaxas. 2011. Vertical distribution of marine invertebrate larvae in response to thermal stratification in the laboratory. Journal of Experimental Marine Biology and Ecology 409: 89–98.

My coauthor Dr. Anna Metaxas supervised the study design and analyses, and edited the manuscript.

aggregate at the surface unless temperature extremes were encountered. In contrast, the position of *A. irradians* was limited to the bottom layer in the presence of a thermocline of at least 5 °C (the shallowest used in my study). Such thermoclines are common in a natural setting and could affect the vertical distribution and horizontal dispersal of larvae by acting as a barrier to vertical migration.

2.2 Introduction

Population dynamics and persistence are affected by dispersal and connectivity, which in the case of benthic invertebrates, is largely mediated by the larval phase (Levin 2006; Cowen and Sponaugle 2009). Invertebrate larvae are relatively poor swimmers and the role of directed horizontal swimming in dispersal has been often ignored until recently (Bradbury and Snelgrove 2001); ocean currents have been considered the main mechanism for larval horizontal transport.

Because current velocity and direction can vary with depth, larval vertical position in the water column can affect transport distance and direction (Scheltema 1986; Bradbury and Snelgrove 2001; Cowen and Sponaugle 2009; Metaxas and Saunders 2009). For example, several species of decapods display vertical migration related to the tidal cycle and can be effectively retained, exported or imported into estuaries depending on behaviour type (Epifanio et al. 1984; Cronin and Forward Jr 1986; López-Duarte and Tankersley 2007; Banas et al. 2009). Vertical distribution of larvae can also be affected by ontogenetic stage (Gallager et al. 1996; Tamaki et al. 2010; Tapia et al. 2010). For example, larvae of the giant scallop P*lacopecten* magellanicus were found to cross the thermocline only after they had reached a shell length of about 200 µm. Additionally, invertebrate larvae can alter their vertical distribution in response to numerous biological

and physical cues such as salinity, temperature and food (Boudreau et al. 1992; Young 1995; Gallager et al. 1996; Metaxas and Young 1998; Sameoto and Metaxas 2008b).

The thermal structure of the water column can regulate the vertical distribution of several species of invertebrates. For example, larvae of *Mytilus edulis* have been found predominantly between the thermocline and the sea surface in the White Sea (Dobretsov and Miron 2001), and larvae of *Dendraster excentricus* above 6 m depth in Eastsound, WA (Pennington and Emlet 1986). Similarly, aggregations of larvae of the scallop *Placopecten magellanicus* between 5 and 20 m in the NW Atlantic were found to be associated with the presence of a thermocline (Tremblay and Sinclair 1988). Also, an increase in the strength of thermal stratification was associated with a decrease in the number of mid-stage IV lobster larvae (*Homarus americanus*) crossing the thermocline (Boudreau et al. 1992), effectively delaying or preventing settlement.

Temperature can affect larval dispersal in ways other than by influencing vertical distribution. It influences planktonic larval duration (*i.e.* the amount of time larvae spend in the water column) by directly affecting metabolism and growth rate (O'Connor et al. 2007). Similarly, temperature can alter larval swimming ability directly, as its effects on biochemical reactions can, in turn influence physiological processes resulting in the modification of the ciliary beat rate (Jørgensen et al. 1990; Larsen et al. 2008). Additionally, density and viscosity, which are linked to the temperature of the water, can also affect larval swimming by altering buoyancy, sinking rates and propulsive forces (Podolsky and Emlet 1993).

In this study, I investigated the effect of the presence of an experimentally generated thermocline in the laboratory on the vertical distribution of larval *Strongylocentrotus droebachiensis, Asterias rubens* and *Argopecten irradians*. These species represent commonly occurring invertebrates in the NW Atlantic, and their larvae (particularly of *S. droebachiensis* and *A. rubens*) have been used extensively in previous studies on factors affecting behaviour and survival (Stephens 1972; Meidel and Scheibling 1998; Burdett-Coutts and Metaxas 2004; Metaxas and Burdett-Coutts 2006; Sameoto and Metaxas 2008a; b). I examined the effects of the temperature of the bottom layer and the difference in temperature between the 2 layers on larval vertical distributions. In Nova Scotia, larvae of *S. droebachiensis* normally experience temperatures between 5 and 10 °C in the spring and up to 18 °C during autumn spawnings (Meidel and Scheibling 1998). In St. Margarets Bay, NS, in the spring, temperature below 30 m is ~2 °C and in the surface mixed layer (top 20 m) can reach up to 10 °C. In contrast, in autumn, the temperature below 50 m is ~4 °C, and the surface mixed layer (top 30 m) can reach up to 18 °C (Gregory 2004). Larvae of *A. rubens* normally experience temperatures between 10 and 18 °C from April to July(Harper and Hart 2005) and a wide range of thermal structures, ranging from a uniformely structured water column of 4°C to the stratification in autumn described above (Gregory 2004). While there is no local wild population of *A. irradians*, temperature in their native range is between 15 and 28 °C (Tettelbach and Rhodes 1981). The temperatures I used in my experiments ranged from 3 to 24 °C, and were selected to reflect those in the habitat of the species (coasts of Nova Scotia for *S. droebachiensis* and *A. rubens,* and the US eastern seaboard for *A. irradians*). I also measured mortality of *S. droebachiensis* at

different temperatures, to explore relationships between the response of larval vertical distribution at a particular temperature and physiological tolerance. Addressing these questions in the laboratory allowed us to control the experimental conditions and to eliminate other confounding variables. These experiments can provide a first order estimate of behaviours that cannot be measured in the field (Metaxas and Saunders 2009).

2.3 Methods

2.3.1 Fertilization and larval rearing

Adults of *Strongylocentrotus droebachiensis* and Asterias *rubens* were collected from the shallow subtidal zone at Splitnose Point, NS, in Mar 2009 and Duncan's Cove, NS, in Jul 2009, respectively. They were maintained in ambient seawater flow-through tanks in the Aquatron facility at Dalhousie University and fed kelp (*Saccharina longicruris* and *Laminaria digitata*) and mussels (*Mytilus sp.*), respectively, *ad libitum*. Spawning was induced by injecting 2-4 ml of 0.55 M KCl through the peristomal membrane for *S. droebachiensis*, and 3-5 ml of 100 µM 1-methyladenine into the coelomic cavity for *A. rubens*. For each replicate of a set of treatments, eggs and sperm from 3 males and 3 females were combined in 0.45 µm-filtered seawater. Fertilization success, determined as the proportion of eggs with elevated perivitelline membranes, varied between 94 and 100% (n = 50). Larvae of *Argopecten irradians* (4-d old) were obtained from a spawning stock maintained at the Bedford Institute of Oceanography, Department of Fisheries and Oceans-Canada, Dartmouth, NS.

All zygotes and larvae were transferred into 4-L culture jars containing 0.45 µm-filtered seawater, which were maintained in a temperature-controlled room at 10 ± 1 °C

for *S. droebachiensis*, 12 ± 1 °C for *A. rubens* and 20 ± 1 °C for *A. irradians*. Water was gently stirred with slowly rotating paddles and was changed every other day. Larvae of all species were kept at a maximum density of 4 larvae ml^{-1} and were fed a mixture of *Isochrysis galbana* (from Tahiti) and *Chaetoceros muelleri* at a total concentration of 5000 cells ml^{-1} for *S. droebachiensis* and *A. rubens,* and 30,000 cells ml^{-1} for *A. irradians*.

Larvae of *S. droebachiensis* and *A. rubens* were used in the experiments once they reached the 4-arm (6-d old) and bipinnaria (10-d old) stages, respectively. These larval stages were chosen because they represent the dominant dispersal stage for these species. Larvae of *A. irradians* were used as soon as they were visible to the naked eye (9-d old). For the experiments with *A. irradians* and *A. rubens*, all replicates and treatments were conducted using 1 mixed-progeny cohort (18 hermaphroditic possible parents and 4 parental pairs, respectively). The experiment with *S. droebachiensis* was conducted using 1 cohort from 1 parental pair for each replicate.

2.3.2 Generation of experimental thermoclines

In the laboratory, thermoclines were generated in rectangular plexiglass chambers based on those in (McConnaughey and Sulkin 1984) (Figure 2.1). Each chamber included a central observation compartment (10x10x50 cm) where the larvae could swim freely, surrounded by a water jacket (5-cm wide around observation compartment) separated into 3 sections (2 12.5-cm tall and 1 25-cm tall). Continuous flow of water at a particular temperature through each section allowed the manipulation of the temperatures in the adjacent observation compartment, and by using different temperatures in different sections of the water jacket, I could generate thermal structure in the water column. Once the water flow in the different sections of the water jacket was established, I allowed

equilibration of the temperature of the water in the observation compartment for at least 4 h to generate stable thermal stratification. In all cases, the bottom two sections of the water jacket were used as 1 continuous section. Temperature was measured before and after the experiment at the surface, 15 cm, every cm between 20-30, 35 and 50 cm depth, using a Marina Digital Thermometer with a 90-cm cable (accuracy ± 0.1°C). The gradient in temperature occurred over 10 cm centered at 25 cm depth, and these thermoclines remained stable for > 24 hours. Preliminary measurements showed that the thermoclines were not disturbed by either the temperature measurements or the introduction of larvae.

2.3.3 Experimental protocol

I manipulated both the temperature in the bottom water layer (B) and the temperature difference between layers (ΔT) in an orthogonal design. I used, for *S. droebachiensis* (n = 5): 4 levels of ΔT (0, 3, 6 and 12 °C) and 3 levels of B (3, 6 and 9 °C); for *A. rubens* (n = 4): 3 levels ΔT (0, 6 and 12 °C) and 2 levels of B (6 and 12 °C); and for *A. irradians* (n = 4): 3 levels of ΔT (0, 5 and 11 °C) and 2 levels of B (5 and 11 °C). These combinations of factors were chosen to represent the conditions in the local environment. Since there were up to 12 treatment combinations for a particular species and I only had 4 thermocline chambers, not all replicates could be run simultaneously. For *S. droebachiensis*, different cohorts (from unique parental pairs) were blocked in time and all treatments were completed in 3 randomized groups of 4 within 26 h. For the other species, all replicates of all treatments were conducted in randomized order with a single larval cohort (from multiple parental pairs) within 48 h. Due to limitations of the seawater system at the time, the surface water was ~ 20 °C rather than 21 °C in the

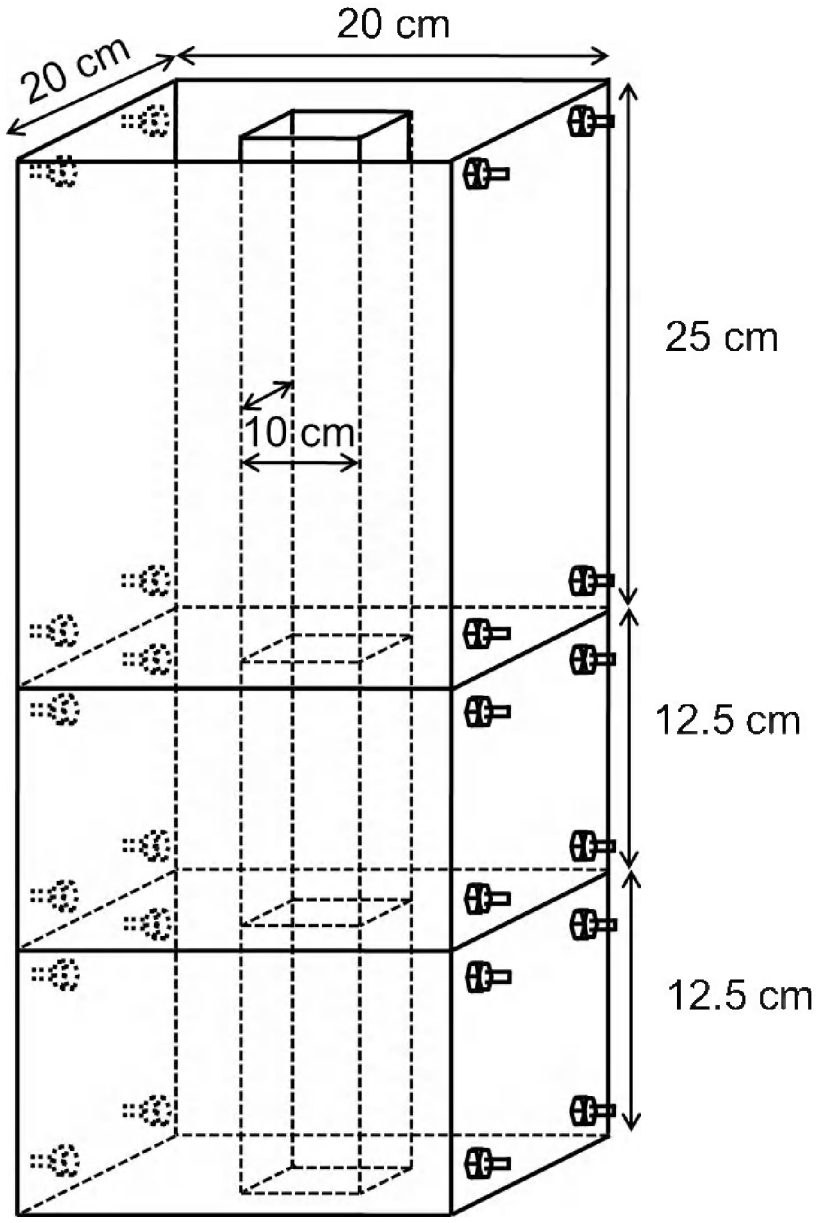

Figure 2.1: Diagram of plexiglass thermocline chamber. An open central observation chamber (10x10x50 cm) surrounded by a water jacket (5 cm thick perimeter), in turn separated into 3 chambers (2 are 12.5 cm high and 1 is 25 cm high) Each jacket chamber had 8 nylon 6-mm barbed fittings to allow water input/output. In all cases, water of the same temperature was circulated through the 2 bottom jacket chambers; therefore, thermal stratification (if present) was centered at 25 cm depth

treatment combination of $\Delta T = 12$ °C and B = 9 °C for *S. droebachiensis*.

Once the thermoclines were established, 50 ml of seawater containing 250-350 larvae were introduced to each chamber within 1 cm from the bottom of the observation compartment (filled with 0.45 µm-filtered seawater) by gently pouring into a funnel attached to a small tube (2-mm inner diameter). Before being introduced to the experimental chamber, larvae were acclimated to the respective bottom temperature for 15 min. Larval position was visually determined to the nearest cm at 5, 15, 30, 45, 60 and 90 min after introduction for *S. droebachiensis* and *A. irradians,* and at 10, 30, 60 and 90 min for *A. rubens*. Larvae in the entire 50 cm water columns were counted in < 2 min, making repeat counts of individual larvae highly unlikely.

2.3.4 Effect of temperature on larval survival

I measured larval mortality for *S. droebachiensis* at 3 different temperatures (3, 10 and 21 °C) reared in 4-L culture jars (n = 3). Temperatures in the jars were maintained either by placing them in a water bath (3 and 21 °C) or in a temperature-controlled room (10 °C). These temperatures encompass ambient and the extreme temperatures used in the experimental thermoclines. Six-day old larvae (each replicate was from a single parental pair, and reared at 10 °C) were used for this experiment. To quantify mortality, 30 larvae from every treatment for each replicate were transferred to a Petri dish at 0, 24 and 48 h, and categorized as live if swimming was observed using a Nikon SMZ 1500 dissecting microscope.

2.3.5 Statistical analyses

The effect of time on larval vertical distribution was examined using a 3-way ANOVA with B (3, 6 or 9 °C) and ΔT (0, 3, 6 or 12 °C) as fixed factors and repeated measures on time. In this case, the vertical distribution of larvae was represented by the center of larval mass (ZCM), calculated as

$$ZCM = \sum p_i z_i \tag{2.1}$$

where p_i is the proportion of larvae at depth interval i and z_i is the median depth of that interval. To determine the time after which the ZCM did not change any further, pairwise comparisons (Tukey's HSD test) were done on the within-subject factor (Time).

Log-linear models were used to examine the independence between larval position (P), temperature in the bottom layer (B) and temperature difference between layers (ΔT). Since the 3-way models fit the data poorly ($P < 0.0001$), I examined the fit of 2-way models within each level of B or ΔT, respectively. These analyses were conducted on larval vertical positions at 60 min because it was determined that the ZCM did not change significantly after 30 min. Where applicable, I used 2-way models to compare pairs of treatments. To reduce the number of categories for position and fulfill the assumptions of the tests, I pooled the numbers of vertical positions into 3 or 4 functional positions ("surface" = < 1, <5 cm or not used and "above the thermocline" = 1-19, 6-19 or <19 cm for *S. droebachiensis*, *A. rubens* and *A. irradians*, respectively; "thermocline" = 20-30 cm; "below thermocline" = 31-50 cm, for all species). The "surface" category was used to differentiate surface aggregations, which did not form in the experiments for

A. irradians. The "thermocline" was defined as the depth range over which temperature was changing from the temperature of the top layer to that of the bottom layer. I also pooled the number of observations at each depth across replicates because the order of treatments was randomly assigned to replicates to avoid any bias associated with the timing during the experimental period. Since the replicates were not blocked across time for *A.rubens* and *A. irradians*, it is not possible to use "replicate" as a factor. I have chosen to pool the replicates for all species to incorporate natural variability associated with variability among different batches of larvae in my tests. For these tests, a more conservative Bonferroni-adjusted P_{crit} was used, given the large number of comparisons ($P_{crit} = 0.05/n$, where n is the number of comparisons within each set of models).

Because of the great sensitivity of the analysis by contingency tables to the frequency of observations, and the large number of observations in my experiments, I elected to use an ecologically meaningful effect size for the interpretation of differences between treatments. This effect size was selected to be greater than the variability among replicates within treatments, and was more conservative than the statistically detected effect based on P_{crit} even after Bonferroni-adjustments. To determine an effective difference, I identified the maximum standard deviation in mean proportion of larvae of any position within each replicate of each treatment. I defined an ecologically meaningful difference as a difference in the mean proportion of larvae within a particular position category (*i.e.* surface, above, at, or below the thermocline) that was greater than the maximum standard deviation.

The effect of temperature on larval survival was examined using a 2-way ANOVA, with temperature as a fixed factor (3 levels: 3, 10 and 21 °C) and repeated

measures on time (3 levels: 0, 24 and 48 h). Percent mortality was arcsine-transformed to fulfill the assumption of normality (Zar 1999). Differences between temperatures were identified using multiple comparisons (Tukey's HSD test).

2.4 Results

The center of larval mass (ZCM) of *Strongylocentrotus droebachiensis* and *Asterias rubens* increased significantly over time (Figure 2.2, Table 2.1). The ZCM of *A. irradians* did not vary significantly over time (Figure 2.2, Table 2.1), suggesting that stable vertical distributions where achieved in less than 5 min from the introduction of larvae into the experimental chambers. Post-hoc multiple comparisons showed no significant differences in ZCM after 30 min (Table 2.2) for all species, indicating that larval distribution had stabilized after this time. For *S. droebachiensis*, there are significant interactions with time (Table 2.1), but there also were no significant differences after 30 min for any treatment combinations. Consequently, all further analyses are done on the distributions at 60 min after the initiation of the experiments.

The poor fit of the 3-way log-linear model (Table 2.3) indicates that, for all species, the larval position in the thermocline chambers (*P*) was dependent upon the temperature in the bottom layer (B), the temperature difference between layers (ΔT) and their interactions. Due to significant 2-way interactions ([B $\times$ P] and [ΔT $\times$ P]) in the 3-way models, I used 2-way contingency tables to examine the independence of: 1) position and bottom temperature within each level of ΔT; and 2) position and temperature difference between layers for each level of B.

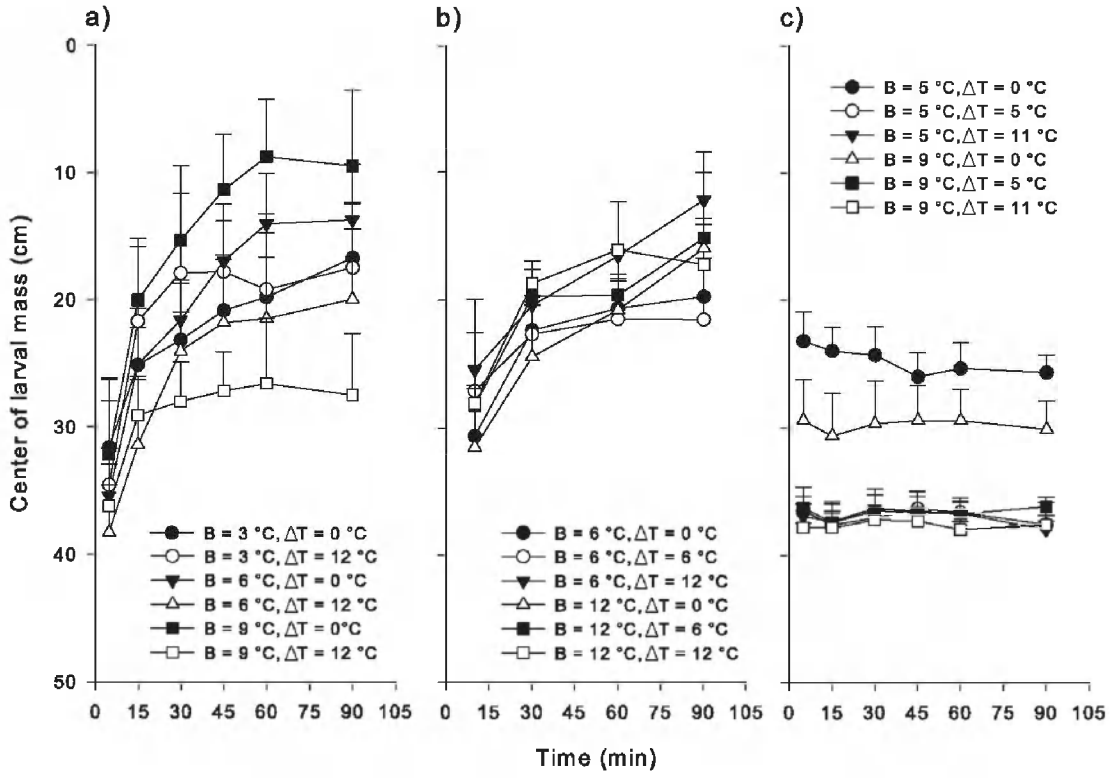

Figure 2.2: Mean (± SD) center of larval mass over time for larvae of a) *Strongylocentrotus droebachiensis*, b) *Asterias rubens* and c) *Argopecten irradians* for treatments of different bottom temperature (B) and temperature differences between layers (ΔT)

Table 2.1: Results of ANOVA examining the effects of bottom temperature (B) and temperature difference (ΔT) on mean center of larval mass (ZCM) and repeated measures on time for *Strongylocentrotus droebachiensis* (Sd), *Asterias rubens* (Ar) and *Argopecten irradians* (Ai). Asterisks indicate significant values.

Strongylocentrotus droebachiensis				
Between Subject	**df**	**MS**	**F**	**p**
B	2	129.2	1.2	0.299
ΔT	3	691.8	6.6	<0.001*
B*ΔT	6	265.7	2.5	0.032*
Error	48	104.4		
Within Subject				
Time	5	3392.7	283.9	<0.001*
Time*B	10	23	1.9	0.043*
Time*ΔT	15	40	3.3	<0.001*
Time*B*ΔT	30	20.5	1.7	0.014*
Error	240	11.9		
Asterias rubens				
Between Subject	**df**	**MS**	**F**	**p**
B	1	4.6	0.1	<0.001*
ΔT	2	127.7	2.9	0.751
B*ΔT	2	31.1	0.7	0.081
Error	18	44.1		0.508
Within Subject				
Time	3	11.6	54.4	<0.001*
Time*B	3	8.2	1.1	0.377
Time*ΔT	6	8.2	0.7	0.622
Time*B*ΔT	6	19.6	1.7	0.124
Error	54	11.1		
Argopecten irradians				
Between Subject	**df**	**MS**	**F**	**p**
B	1	114.7	6.8	0.017*
ΔT	2	1548.6	92	<0.001*
B*ΔT	2	95.9	5.7	0.012*
Error	18	16.8		
Within Subject				
Time	5	2.7	1.8	0.113
Time*B	5	1.7	1.2	0.327
Time*ΔT	10	1.2	0.8	0.589
Time*B*ΔT	10	1.4	0.9	0.497
Error	90	1.4		

Table 2.2: Post-hoc comparisons (Tukey's HSD test) for significant effects as detected in ANOVAs in Table 2.1 of the center of larval mass (ZCM) between sampling time points for *Strongylocentrotus droebachiensis* (Sd) and *Asterias rubens* (Ar). Asterisks indicate significant values.

Sd		**Ar**	
Time (min)	p	**Time (min)**	p
60 vs 90	0.741	60 vs 90	0.104
45 vs 90	0.372	30 vs 90	0.002*
45 vs 60	0.615	30 vs 60	0.115
30 vs 90	<0.001*	10 vs 90	<0.001*
30 vs 60	<0.001*	10 vs 60	<0.001*
30 vs 45	0.002*	10 vs 30	<0.001*
15 vs 90	<0.001*		
15 vs 60	<0.001*		
15 vs 45	<0.001*		
15 vs 30	<0.001*		
5 vs 90	<0.001*		
5 vs 60	<0.001*		
5 vs 45	<0.001*		
5 vs 30	<0.001*		
5 vs 15	<0.001*		

Table 2.3: Analysis by log-linear models of the independence between larval position in thermocline chambers (P), and bottom temperature (B) and temperature difference (ΔT), for *Strongylocentrotus droebachiensis* (Sd), *Asterias rubens* (Ar) and *Argopecten irradians* (Ai). For all models, P<0.0001

	Sd		**Ar**		**Ai**	
Model	**G**	**df**	**G**	**df**	**G**	**df**
Three-Way Models						
$B + \Delta T + P + [B \times P] + [\Delta T \times P]$	551.9	24	428.5	8	118.2	6
$B + \Delta T + P + [B \times P]$	1221.9	33	1338.5	14	1527.7	10
$B + \Delta T + P + [\Delta T \times P]$	865.4	30	513.9	11	138.2	8

2.4.1 *Strongylocentrotus droebachiensis*

Irrespective of the presence of a thermocline, larvae tended to accumulate at the surface in most treatments (Figure 2.3). Notable exceptions are the warmest treatment (B = 9 and ΔT = 12 °C) in which the larvae were relatively evenly distributed throughout the water column. The magnitude of the temperature difference between layers (ΔT) had a pronounced effect on the vertical distribution of sea urchin larvae (Figure 2.3), since position was dependent on ΔT for all levels of bottom temperature (Table 2.4). However, in the pairwise comparisons, the vertical position of larvae in the treatments where bottom temperature was 3°C showed no consistent pattern with ΔT (Table 2.4). In the single ecologically significant difference, there were fewer larvae at the surface and more below the thermocline at ΔT = 0°C than ΔT= 3°C (Table 2.5). For treatments with temperature in the bottom layer of 6°C, larval distribution varied between all levels of ΔT and ΔT = 12 °C (Figure 2.3, Table 2.4), and fewer larvae were found at the surface at the highest ΔT than the other levels. Lastly, in treatments where the temperature of the bottom layer was 9°C, larval position was dependent on ΔT for all comparisons except one (Figure 2.3, Table 2.4). In these treatments, fewer larvae were found at the surface in the warmest temperatures corresponding to the highest ΔT (Table 2.5).

The vertical distribution of sea urchin larvae (Figure 2.3) was also affected by the temperature in the bottom layer since position was dependent on B for most levels of ΔT (Table 2.6). However, few ecologically significant effects were recorded. For ΔT = 0 °C (no thermocline), larval position varied between 3°C and 9°C, with more larvae found at the surface and fewer below the thermocline at the highest bottom temperature (Table

Figure 2.3: Vertical larval distributions of *Strongylocentrotus droebachiensis* in chambers after 60 min with experimentally generated thermoclines of 3 different temperatures in the bottom layer and 4 different temperature differences between layers. Shown as mean abundance (± SD, n=5) at each 1 cm interval. Superimposed line plot shows temperature profiles averaged across replicates.

Δt = 0 °C
Δt = 3 °C
Δt = 6 °C
Δt = 12 °C
Larvae Abundance (%)
Temperature (°C)
Depth (cm)
Bottom = 3 °C
Bottom = 6 °C
Bottom = 9 °C

Table 2.4: Results of analyses by two-way log-linear models testing the independence between position of larvae of *Strongylocentrotus droebachiensis*, *Asterias rubens* and *Argopecten irradians* in thermocline chambers (P), and temperature difference between layers (ΔT) within each level of bottom temperature (df = 9, 6 and 6, for each species respectively). Individual comparisons within all possible pairs of ΔT are also shown (df = 3, 3 and 2, for each species respectively). P_{crit} is 0.0167 for the 2-way analyses, and 0.0028, 0.0083 and 0.0083 for each of the within-pair comparison, for each species respectively. Asterisks and bold indicate statistical and ecological (>20.76%, >17.78% and >12.46% difference) significance, respectively.

	Bottom Temperature					
S. droebachiensis	**3°C**		**6°C**		**9°C**	
Two-way analyses	**G**	**P**	**G**	**P**	**G**	**P**
(Model ΔT + P)	80.1	<0.0001*	388.1	<0.0001*	746.1	<0.0001*
Within-pair comparisons						
0°C vs 3°C	69.7	**<0.0001***	5.8	0.1220	13.17	0.004
0°C vs 6°C	35.5	<0.0001*	24.9	<0.0001*	161.8	**<0.0001***
0°C vs 12°C	14.6	0.0022*	267.1	**<0.0001***	596.7	**<0.0001***
3°C vs 6°C	7.8	0.0506	16.0	0.0011*	114.1	**<0.0001***
3°C vs 12°C	21.6	<0.0001*	221.7	**<0.0001***	500.8	**<0.0001***
6°C vs 12°C	6.0	0.1098	256.6	**<0.0001***	162.1	**<0.0001***
A. rubens	**6°C**		**12°C**			
Two-way analyses	**G**	**P**	**G**	**P**		
(Model ΔT + P)	216.8	<0.0001*	991.9	<0.0001*		
Within-pair comparisons						
0°C vs 6°C	81.8	<0.0001*	40.7	<0.0001*		
0°C vs 12°C	167.6	<0.0001*	689.9	**<0.0001***		
6°C vs 12°C	79.8	<0.0001*	629.5	**<0.0001***		
A. irradians	**5°C**		**11°C**			
Two-way analyses	**G**	**P**	**G**	**P**		
(Model ΔT + P)	782.6	<0.0001*	672.8	<0.0001*		
Within-pair comparisons						
0°C vs 5°C	523.1	**<0.0001***	467.2	**<0.0001***		
0°C vs 11°C	562.4	**<0.0001***	421.4	**<0.0001***		
5°C vs 11°C	7.0	0.0295	3.6	0.1665		

Table 2.5: Mean proportion of larvae of *Strongylocentrotus droebachiensis* in each position category relative to the thermocline (± standard deviation, n = 5) for all levels of bottom temperature and temperature difference between layers (ΔT).

Bottom	Position	ΔT = 0°C	ΔT = 3°C	ΔT = 6°C	ΔT = 12°C
3°C	Surface	41.92±15.80%	64.16±14.35%	58.34±7.22%	52.29±12.21%
	Above	11.94±4.18%	7.16±4.78%	7.97±8.60%	6.71±4.40%
	At	5.21±3.80%	1.45±1.03%	3.19±2.40%	2.50±2.88%
	Below	40.93±17.21%	27.23±15.67%	30.49±14.63%	38.50±10.85%
6°C	Surface	57.95±8.70%	56.64±11.07%	53.91±10.30%	18.98±7.56%
	Above	9.44±4.69%	14.01±4.04%	13.09±12.46%	31.09±15.65%
	At	8.45±3.47%	7.09±7.92%	2.92±2.56%	22.87±16.37%
	Below	24.16±11.89%	22.25±7.49%	30.08±18.54%	27.05±20.76%
9°C	Surface	73.53±14.15%	66.61±19.37%	37.81±18.46%	11.98±12.47%
	Above	7.90±4.29%	10.37±7.19%	18.23±5.18%	19.03±11.37%
	At	2.36±1.89%	6.98±5.38%	13.52±13.33%	26.52±12.43%
	Below	16.20±10.69%	16.04±7.88%	30.43±7.34%	42.47±18.42%

Table 2.6: Results of analyses by two-way log-linear models testing the independence between position of *Strongylocentrotus droebachiensis*, *Asterias rubens* and *Argopecten irradians* larvae in thermocline chambers (P), and bottom temperature (B) within each level of temperature difference between layers (df = 9, 6 and 6, for each species respectively). Individual comparisons within all possible pairs of B are also shown (df = 3). P_{crit} is 0.0125, 0.0167 and 0.0167 for the 2-way analyses, for each species respectively, and 0.0042 for each of the within-pair comparison. Asterisks and bold indicate statistical and ecological (>20.76%, >17.78% and >12.46% difference) significance, respectively

S. droebachiensis	**Temperature Difference**							
	0°C		**3°C**		**6°C**		**12°C**	
Two-way	**G**	**P**	**G**	**P**	**G**	**P**	**G**	**P**
(Model B + P)	166.8	<0.0001*	74.4	<0.0001*	115.4	<0.0001*	501.1	<0.0001*
Within-pair comparisons								
3°C vs 6°C	61.3	<0.0001*	44.1	<0.0001*	12.4	0.0062	321.4	**<0.0001***
3°C vs 9°C	141.9	**<0.0001***	47.8	<0.0001*	96.5	<0.0001*	384.4	**<0.0001***
6°C vs 9°C	44.0	<0.0001*	22.6	<0.0001*	57.7	<0.0001*	51.4	<0.0001*
A. rubens	**0°C**		**6 °C**		**12°C**			
Two-way	**G**	**P**	**G**	**P**	**G**	**P**		
(Model B + P)	12.637	0.0055*	122.2	<0.0001*	249.3	**<0.0001***		
A. irradians	**0°C**		**5°C**		**11°C**			
Two-way	**G**	**P**	**G**	**P**	**G**	**P**		
(Model B + P)	43.6	**<0.0001***	5.1	0.0785	17.231	0.0002*		

2.5). At ΔT=12 °C, the vertical position of larvae was dependent on bottom temperature, and more larvae were present at the surface when B= 3 °C, than 6 or 9 °C.

The relationship between surface temperature and ZCM was parabolic and peaked at 9 °C (Figure 2.4a). Surface temperatures at 3 °C or above 12 °C were correspond to a deeper ZCM indicating fewer larvae in the surface layer. Larval mortality varied among temperatures ($F_{2,6}$ = 22.19, df = 2, P = 0.002), over time ($F_{2,12}$ = 20.77, P = <0.001) and there was a significant temperature*time interaction ($F_{4,12}$ = 5.26, P = 0.011). Multiple comparisons (Table 2.7) revealed that mortality was significantly greater in 21 °C than in 3 and 10 °C (Figure 2.4b) at 48 h.

2.4.2 *Asterias rubens*

The vertical distributions of larval *A.* rubens were comparable to those of *S. droebachiensis*. Larvae formed aggregations at the surface in most treatments except the warmest (B = 12 and ΔT = 12 °C). In this treatment, there were fewer larvae in the surface and bottom layers, and more above the thermocline than other treatments (Figure 2.5). The magnitude of the temperature difference between layers (ΔT) had a pronounced effect on the vertical distribution of sea star larvae (Figure 2.5), since position was dependent on ΔT for all levels of bottom temperature (Table 2.4). In the pairwise comparisons, the vertical position of larvae was statistically dependent on ΔT in all cases, but only 2 ecologically significant effects were recorded (Table 2.4). At B = 12 °C more larvae were above the thermocline and fewer below the thermocline or at the surface when ΔT was 12 °C than 0 or 6 °C (Tables 2.4&2.8).

The vertical distribution of sea star larvae (Figure 2.5) was also affected by the temperature in the bottom layer. Position was dependent on B for all levels of ΔT (Table 2.6), but only when ΔT = 12 °C was the effect ecologically significant: there were more larvae above the thermocline and fewer at the surface when B was 12 °C than 6 °C (Table 2.8).

2.4.3 *Argopecten irradians*

The presence of a temperature difference between water layers had a strong and consistent effect on the vertical distribution of scallop larvae (Figure 2.6), and position was dependent on ΔT for all levels of bottom temperature (Table 2.4). Pairwise comparisons revealed that the vertical distribution of larvae in a water column with no thermal structure differed from those of all other treatments, for both levels of bottom temperature (Table 2.9). Overall, there were almost no larvae (≤ 5%) at or above the thermocline in the treatments where a thermocline was present. In contrast, larval vertical distribution did not vary consistently with temperature in the bottom layer (Table 2.6).

2.5 Discussion

The presence of thermoclines affected the vertical distribution of larval *S. droebachiensis*, *A. rubens* and *A. irradians,* but the effect was not consistent across species. For larval echinoderms, vertical distributions were particularly modified when larvae were exposed to layers with temperatures at the extremes of the tested range. In contrast, very few larvae of *A. irradians* crossed the thermocline when any stratification was present regardless of the temperature in the bottom or top layers.

Table 2.7: Tukey's multiple comparisons of larval mortality for *Strongylocentrotus droebachiensis*. Asterisks indicate significant differences in mortality between temperatures or times.

Constant time				Constant temperature			
t (h)	T_1 (°C)	T_2 (°C)	P	T (°C)	t_1 (h)	t_2 (h)	P
0	3	10	1.000	3	0	24	0.887
0	3	21	1.000	3	0	48	0.941
0	10	21	1.000	3	24	48	1.000
24	3	10	1.000	10	0	24	0.728
24	3	21	0.035*	10	0	48	0.973
24	10	21	0.061	10	24	48	0.998
48	3	10	1.000	21	0	24	0.004*
48	3	21	0.024*	21	0	48	0.004*
48	10	21	0.019*	21	24	48	1.000

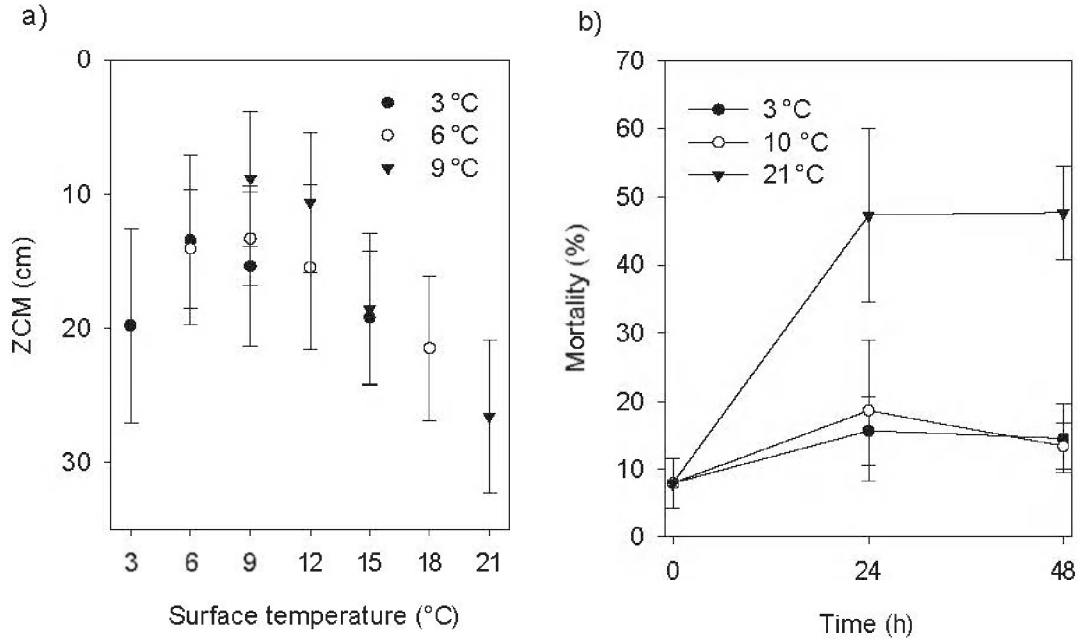

Figure 2.4: a) Mean (± SD, n=5) center of larval mass of *Strongylocentrotus droebachiensis* after 60 min relative to the surface temperature in the thermocline chambers. b) Change in larval mortality rate (± SD, n=3) of *S. droebachiensis* in 3 different temperatures over 48 h.

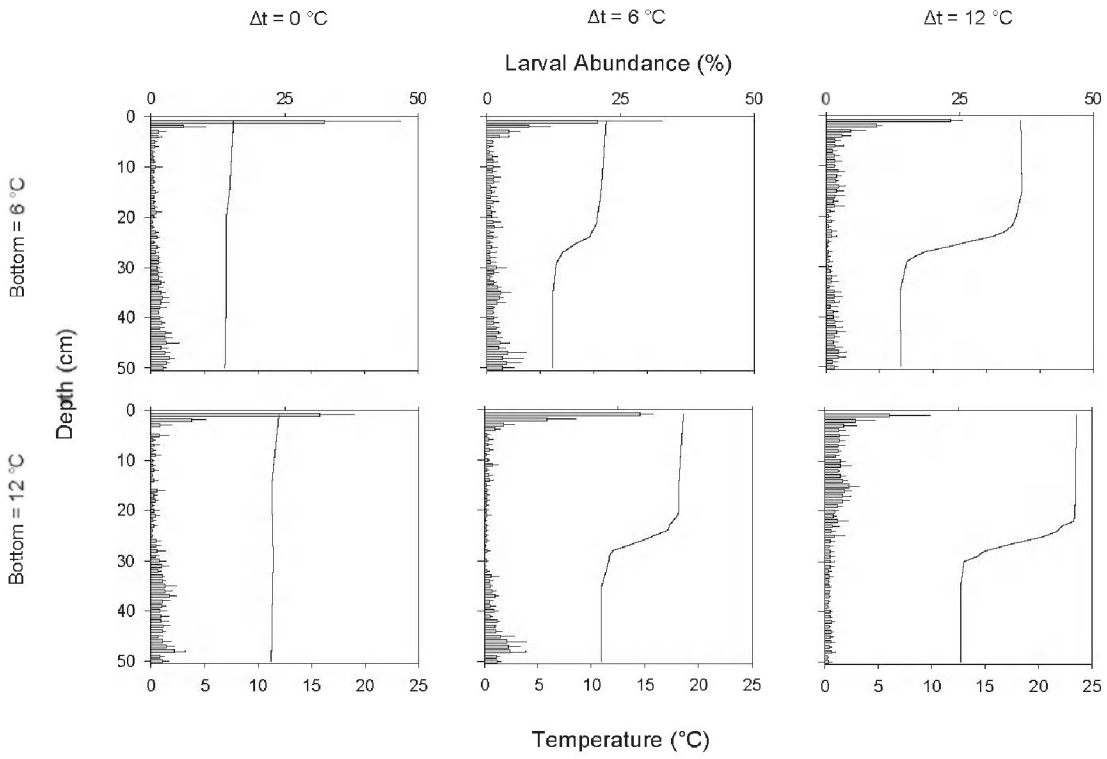

Figure 2.5: Vertical larval distributions of *Asterias rubens* in chambers after 60 min with experimentally generated thermoclines of 3 different temperatures in the bottom layer and 4 different temperature differences between layers. Shown as mean abundance (± SD, n=4) at each 1 cm interval. Superimposed line plot shows temperature profiles averaged across replicates

Table 2.8: Mean proportion of larvae of *Asterias rubens* in each position category relative to the thermocline (± standard deviation, n = 4) for all levels of bottom temperature and temperature difference between layers (ΔT).

Bottom	Position	ΔT = 0°C	ΔT = 6°C	ΔT = 12°C
6°C	Surface	41.79±8.59%	36.13±12.01%	41.84±6.06%
	Above	7.80±3.07%	12.97±11.38%	23.29±10.66%
	At	9.25±2.91%	10.27±9.72%	6.57±4.28%
	Below	41.15±5.56%	40.63±13.15%	28.30±17.78%
12°C	Surface	42.26±5.33%	46.92±6.00%	26.52±10.66%
	Above	6.15±5.82%	9.47±4.50%	41.23±9.87%
	At	7.70±4.30%	3.41±2.65%	14.87±9.13%
	Below	43.88 ±8.19%	40.20±11.49%	17.38±3.99%

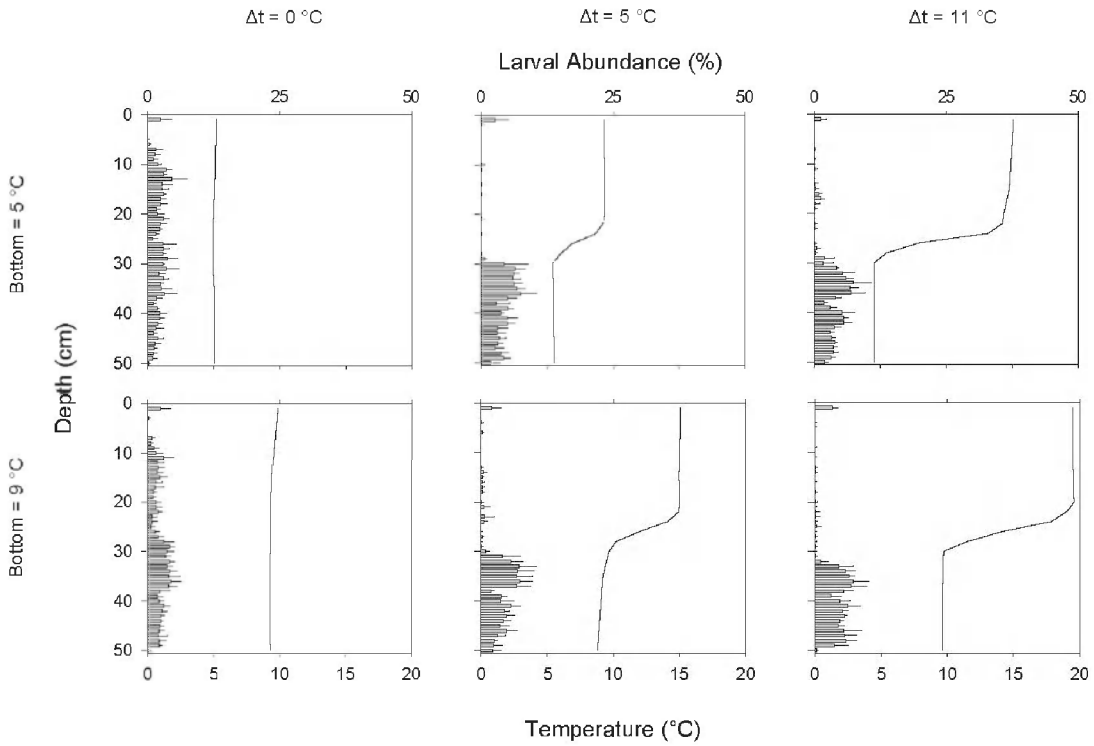

Figure 2.6: Vertical larval distributions of *Argopecten irradians* in chambers after 60 min with experimentally generated thermoclines of 3 different temperatures in the bottom layer and 4 different temperature differences between layers. Shown as mean abundance (± SD, n=4) at each 1 cm interval. Superimposed line plot shows temperature profiles averaged across replicates

Table 2.9: Mean proportion of larvae of *Argopecten irradians* in each position category relative to the thermocline (± standard deviation, n = 4) for all levels of bottom temperature and temperature difference between layers (ΔT).

Bottom	Position	ΔT = 0°C	ΔT = 5°C	ΔT = 11°C
5°C	Above	34.92±8.40%	3.52±2.68%	5.25±3.59%
	At	27.47±1.89%	5.35±4.63%	5.55±4.50%
	Below	37.61±8.25%	91.13±2.28%	89.20±7.12%
9°C	Above	22.96±11.10%	4.01±2.99%	4.69±0.96%
	At	21.54±6.01%	3.70±2.63%	2.56±2.81%
	Below	55.50±12.46%	92.30±4.94%	92.75±2.48%

For echinoderms, the absolute temperature of the water, particularly above the thermocline, appeared to have a greater effect on vertical distribution than the presence of stratification, as supported by the lack of a consistent effect of the temperature difference between layers. In the absence of any structure, larvae of *S. droebachiensis* normally swim up towards the water surface (Sameoto and Metaxas 2008a). Therefore, the fewer larvae observed in the surface layer at high (> 18 °C) and low (3°C) temperatures suggest an avoidance behaviour and retarded swimming, respectively. Similarly for *A. rubens*, increased temperatures in the top layer were associated with greater proportions of larvae above the thermocline; however, there was a decrease in the proportion of larvae at the surface in the warmest treatment (24 °C).

In contrast to echinoderms, the distribution of larval *A. irradians* was greatly influenced by the presence of a thermocline. In the absence of a thermocline, larvae of *A. irradians* were fairly evenly distributed throughout the entire water column. Conversely, in the presence of a thermocline, very few larvae crossed the thermocline. It is important to note that the vertical scale of the thermoclines simulated by these chambers are exaggerated with respect to those found in the field, where a change of 6 or 12 °C in 10 cm or less is unlikely to occur. Nonetheless, other studies have suggested that thermoclines can act as a barrier to the vertical migration of bivalve larvae using more representatively scaled thermoclines both in the laboratory (Gallager et al. 1996; Manuel et al. 2000) and in the field (Tremblay and Sinclair 1988; Dobretsov and Miron 2001). Therefore, it is unlikely that it was the steepness of the thermocline in my experiments that determined the vertical distribution of larval *A. irradians*, but rather its presence. Interestingly, those previous studies found that bivalve larvae were associated with or

distributed above the thermocline, whereas I found the opposite pattern. If thermoclines act as a barrier to vertical migration of bivalve larvae, it is quite possible that the starting position (below the thermocline) of the larvae plays a significant role in their vertical distributions.

Gradients in temperature can influence larval vertical distribution by effecting changes in swimming ability and/or by inducing a behavioural response inherent to the organisms. These gradients result in changes in the density (ρ) of seawater across water layers, which may, in turn, affect larvae buoyancy. In the treatments I used, seawater density ranged from 1.027 g ml^{-1} at 3 °C to 1.022 g ml^{-1} at 24 °C. In these densities, most bivalve larvae are negatively buoyant ($\rho > 1.052$) due to their calcified larval shell (Pennington and Strathmann 1990; Sameoto and Metaxas 2008b), as is *S. droebachiensis* ($\rho \approx 1.06$ g ml^{-1}), while *A. rubens* ($\rho = 1.010$-1.015 g ml^{-1}) is positively buoyant. Consequently, in my experiments *S. droebachiensis* and *A. irradians* should have sank to the bottom and *A. rubens* should have risen to the surface in the absence of swimming. Therefore, my results indicate that the vertical distributions of larvae I observed are the result of active larval swimming and not passive buoyancy-driven processes.

The dynamic viscosity (μ) of seawater, which is inherently linked to temperature, affects both how propulsive forces are translated into motion, as well as the settling velocity of larvae at rest (Podolsky and Emlet 1993). For *S. droebachiensis*, the patterns observed could possibly be in part the result of differential swimming under different viscosities. The increase in ZCM observed between the surface temperatures of 3°C (μ = 1.72 cP for salinity of 34‰; (Sharqawy et al. 2010)) and 9°C (μ = 1.43 cP) may be the result of a decrease in swimming speed in higher viscosity associated with lower

temperature, as was found for the larval sand dollars *Dendraster excentricus* (Podolsky and Emlet 1993). However, an increase from 9°C (μ = 1.43 cP) to 21°C (μ = 1.05 cP) results in further decreases in viscosity that should increase larval swimming speed, as for *Dendraster excentricus* over a similar range (μ = 1.30 to 1.02 cP). The opposite was manifested in the vertical distribution of *S. droebachiensis*.

Temperature could affect larval physiology and, in turn, influence swimming ability through modification of the ciliary beat rate or other propulsive structures such as the muscle-powered appendages of crustaceans (Jørgensen et al. 1990; Larsen et al. 2008). Interestingly, preliminary analysis of larval swimming speeds has revealed that the maximum vertical swimming velocity of larval *S. droebachiensis* does not vary for temperatures between 5 and 20 °C , but the relative probability distribution of swimming velocity does (Daigle and Metaxas 2012). This suggests that the physiological effects on swimming speed are negligible.

Vertical distributions can also be altered by adaptive behaviours that may enhance growth or improve survival (Gallager et al. 1996; Sameoto and Metaxas 2008b). In *P. magellanicus*, larvae have been found to remain above an experimentally generated thermocline when food was present, a behaviour which resulted in enhanced growth (Gallager et al. 1996). Interestingly, when food was present only below the thermocline, the larvae remained above the thermocline and growth was inhibited. However, other species of larvae (*Lytechinus* variegatus and *S. droebachiensis*) can detect food directly (chemosensory mechanisms), and have been found to alter their vertical distribution based on the quantity and quality of the food source (Burdett-Coutts and Metaxas 2004).

Depth-dependant mortality is an additional mechanism that can drive modifications in vertical distributions as a function of a thermal gradient. However, at time scales considered in these experiments, mortality is not likely to have played a direct role. For example, I found that there was significantly higher mortality at 21 °C than 3 or 10 °C, and others have found that *S. droebachiensis* larvae do not develop normally above 10 °C (Stephens 1972). However, in my study mortality differed statistically between 21 °C and 10 °C only after 48 h. Therefore, the avoidance of warm temperatures observed in the thermocline experiments could have been an adaptive short-term response to physiologically stressful temperatures, which can in turn increase long-term survival. Similarly, larvae of *S. droebachiensis* and *A. rubens* exhibit adaptive avoidance behaviours of low salinities, resulting in altered vertical distributions, possibly increasing long-term survival (Sameoto and Metaxas 2008b).

As with mortality, short-term adaptive behaviours which affect vertical distributions can, in turn, influence growth rates over longer periods. For *S. droebachiensis*, the increase in ZCM observed between surface temperatures of 3 and 9°C may be an example of such an adaptive behaviour. Increases in temperature in this range have been found to accelerate growth rates of larval *S. droebachiensis* (Stephens 1972). For *A. rubens*, the rate of larval development of a related species, *Asterias amurensis*, increases from 5 to 17 °C (Kashenko 2005). Given that these 2 species exist in similar temperature regimes and spawn at the same time of year, it is reasonable to assume that *A. rubens* might respond similarly to increases in temperature. This implies that temperature may also affect the vertical distribution of larval *A. rubens* through an adaptive short-term behaviour increasing long-term growth rates.

In the field, larval echinoderms are often associated with the surface layer (top 6 m) or a water mass of specific temperature or salinity (Banse 1986; Pennington and Emlet 1986), suggesting that the patterns I observed in this study support patterns observed in the field. In the northern part of the range of *S. droebachiensis* (Gulf of St. Lawrence and Newfoundland), 21 °C is the maximum annual temperature but this occurs in July-September. Similarly, in the southern part of their range (*e.g.* Cape Cod, MA) and in Nova Scotia, temperatures above 21 °C do occur, but not between December and April, or March and April when the main spawning events of the respective populations occur (Stephens 1972). Therefore, based on my results, larvae of this species could occur at or near the surface based on the expected temperature structure of the water column in the spring (*e.g.* for Nova Scotia, < 8 °C, little or no stratification), when spawning occurs. Interestingly, small summer and autumn spawning events have been reported in local populations (Meidel and Scheibling 1998), when surface temperatures occasionally reach 21 °C and there can be a temperature difference of up to 8 °C between water layers at that time. my results would suggest that larvae from the summer and fall spawning events may avoid the surface mixed layer (≤ 10 m), when stratification is present at the warmest times of year (July-September). While the autumn spawning events may not be as large as the spring ones, these larvae would likely have very different dispersal trajectories.

As for *S. droebachiensis*, the larvae of *A. rubens* avoid the water surface in the warmest temperatures. The larvae of this species, however, are present in the field at the warmest times of year since they spawn from April to July (Harper and Hart 2005). Avoidance of the water surface (top 5 cm) was only observed at 24 °C, a temperature which would occur in Nova Scotia only in extremely rare instances in a protected coastal

embayment. However, surface temperature was only 18 °C in the second warmest treatment. Consequently, larvae could conceivably avoid forming surface aggregations in water that is > 18 °C, a temperature observed in Nova Scotia in summer. Despite the lack of surface aggregation at these high temperatures in the laboratory, larvae exposed to high temperatures remained above the thermocline fairly dispersed in the warm layer. Although larvae of *A. rubens* that are exposed to higher temperatures are in different vertical positions in the water column (surface aggregation vs entire warm layer) and possibly exposed to different horizontal currents, they would be exposed to the same temperature in either case. Therefore, *A. rubens* is not avoiding a particular temperature within the experimental range, but its behaviour varies in response to high temperatures.

In contrast, the position of *A. irradians* was affected by the presence of a thermocline of at least 5 °C (the shallowest used in my study). Thermoclines of this magnitude are common in the native range of this species and the presence of a thermocline could affect larval vertical distribution. These results are in agreement with other studies that have suggested that thermoclines can act as a barrier to the vertical migration of bivalve larvae in the field (Tremblay and Sinclair 1988; Dobretsov and Miron 2001).

Although factors other than the presence of stratification, or extreme temperatures are likely to influence larval vertical distribution of these species in the field, it is important to understand the potential effect that a factor such as temperature can have. Despite the utility of laboratory experiments in providing first order estimates of potential effects, the results must be interpreted with caution. For example, issues of scale,

experimental conditions and other interacting factors would have to be considered when results are extrapolated to the natural setting.

In conclusion, temperature is an important factor to consider in the study of vertical distribution and migration of invertebrate larvae. Not only does it affect dispersal on long time scales (days to weeks) by altering pelagic larval duration (Shanks 2009), but also on short time scales (min to h) by affecting vertical distributions. my results suggest that the vertical position of larvae of *S. droebachiensis* and *A. rubens* are related to the temperatures of the surface layer and that the presence alone or the steepness of the thermocline have less influence on distribution. In low temperatures, vertical distribution is influenced through effects either of viscosity on swimming or of behaviour, whereas in high temperatures, it is affected by short-term adaptive behaviours that may increase long-term growth and survival. The vertical distribution of invertebrate larvae can be affected both by the presence and strength of thermal stratification, as well as by the absolute temperature experienced by the larvae. Such effects on vertical distributions can ultimately affect the trajectories of larval dispersal away from the parental habitat.

CHAPTER 3: MODELLING OF THE LARVAL RESPONSE OF GREEN SEA URCHINS TO THERMAL STRATIFICATION USING A RANDOM WALK APPROACH[2]

3.1 Abstract:

Larval transport in the ocean can be affected by their vertical position in the water column. In biophysical models that are often used to predict larval horizontal dispersal, generally larval vertical positions are either ignored or incorporated as static parameters. Here, I evaluate the ability of one dimensional random walk based model to predict larval vertical distribution of *Strongylocentrotus droebachiensis* in response to thermal stratification. Vertical swimming velocities were recorded at various temperatures and used to parameterize the model. Data from a previous laboratory study on the effects of thermal stratification on larval vertical distribution of *S. droebachiensis* were compared to the model results to evaluate the predictive ability of the model. The model predicts general trends in vertical distribution fairly well, but has a systematic bias which can be explained by un-quantified larval behaviours at the boundaries of the experimental water column. Overall, my behavioural model successfully reproduces the mechanism which regulates larval vertical distribution in response to thermal structure. Collectively, the findings suggest that simple behavioural models parameterized using simple lab experiments can prove useful in estimating the vertical distributions of invertebrate larvae

---

[2] Daigle, R. M., and A. Metaxas. 2012. Modeling of the larval response of green sea urchins to thermal stratification using a random walk approach. Journal of Experimental Marine Biology and Ecology 438: 14–23.

My coauthor Dr. Anna Metaxas supervised the study design and analyses, and edited the manuscript.

in the laboratory and likely in the ocean. Such models can then be linked to bio-physical models to more accurately predict larval dispersal.

3.2 Introduction

For larval marine benthic invertebrates, horizontal swimming speeds are generally considered to have a negligible effect on larval transport since they are much smaller than the velocity of the prevailing currents (Largier 2003). However, larvae are able to alter their vertical position behaviourally, and even weak swimmers, such as gastropods and bivalves, display vertical migration (Lloyd et al. 2012a; b). This vertical migration can be in response to numerous biological and physical cues such as salinity, temperature, turbulence, predators and food (Boudreau et al. 1992; Young 1995; Gallager et al. 1996; Metaxas and Young 1998; Metaxas and Burdett-Coutts 2006; Fuchs et al. 2007; Sameoto and Metaxas 2008b). By vertically migrating, the dispersal pattern of larvae can be altered since different layers can flow in different directions. Consequently, determining the relative importance of these cues, as well as the mechanism and timing of the response, is important in making predictions of larval dispersal.

While it is possible to quantify realized dispersal using geochemical tracers or genetic studies, bio-physical modeling is the only method currently used to predict trajectories of larval dispersal (Levin 2006; Cowen and Sponaugle 2009). Bio-physical models are either general circulation models or advection-diffusion models used to quantify the effects of the physical properties of the ocean (*e.g.* general circulation patterns, tides, wind-driven circulation) on larval dispersal (Metaxas and Saunders 2009). Ideally, these studies should incorporate the best available biological parameters, such as

pelagic larval duration, mortality and vertical migration, which, are often unknown or inaccurately quantified.

Currently, most bio-physical models do not incorporate vertical migration (Metaxas and Saunders 2009) except in a handful of studies, where it affected the larval dispersal potential across a number of species (Dekshenieks et al. 1996; DiBacco et al. 2001; North et al. 2008; Banas et al. 2009). An early attempt using the shrimp *Penaus latisulcatus* did not model swimming behaviour, but rather evaluated the effect of actual vertical position on dispersal (Rothlisberg et al. 1983). In that study, an ontogenetic shift in diel vertical migration resulted in offshore dispersal of younger larvae, and onshore transport of older ones. However, the framework used by Rothlisberg (1983) fixed larvae to a certain water layer at any given time, and the lack of simulated swimming precluded any interaction with vertical advection. Similarly, Banas *et al* (2009) showed that diel and tidal vertical migration affected the larval dispersal of *Carcinus maenas*. However, the role of larval swimming was less important than seasonal differences in hydrodynamics in explaining the difference in dispersal between spring and summer spawnings. Other studies have shown that the larval dispersal of *Crassostrea virginica* can be affected by vertical distributions, which were in turn modulated by salinity gradients and temperature (Dekshenieks et al. 1996; North et al. 2008). However, in both these studies, "idealized" swimming behaviours were generated through mean swimming and sinking velocities to model vertical migration. If changes in larval vertical position can be accurately modelled based on pattern of cues such as temperature, salinity or light, behavioural outcomes of these models could be then incorporated into bio-physical models of larval transport.

Random walks are useful in numerically simulating the trajectory of an animal that makes successive random steps. Initially developed to study the irregular movements (Brownian motion) of plant pollen (Brown 1828), models based on random walks are now widely used to study movement of many organisms, such as slime moulds, insects and even large mammals (Benhamou and Bovet 1989; Bartumeus et al. 2005; Codling et al. 2008). In the ocean, such models have been used to study the aggregation of copepods in turbulence (Yamazaki 1993), encounter rates of zooplankton (Cianelli et al. 2009), and the relative importance of swimming in a turbulent medium (Porch 1998) among others. Porch (1998) suggested that horizontal diffusion of larvae was not affected by random swimming, which, however, can affect vertical diffusion since vertical turbulence is much weaker than horizontal turbulence.

In the present study, I created a random walk model that simulated larval swimming behaviour in the green sea urchin, *S. droebachiensis*, in response to thermal stratification of the water column. The modelled vertical distributions were compared with the observed vertical distributions from a previous study on the vertical distribution of real sea urchin larvae in relation to thermoclines generated in the laboratory (Daigle and Metaxas 2011). The movement of organisms can result from 2 main types of responses to a stimulus or cue. Klinokinesis refers to the sinuosity of the organism's path or the rate of change of directions, whereas orthokinesis refers to the modulation of speed (Codling et al. 2008). Since the model described here only considers the vertical dimension, klinokinesis (path sinuosity), which generally operates in 2 or more dimensions, would not be a relevant means of adjusting position; therefore, I simulated orthokinesis. To parameterize the model, I examined the effect of temperature on larval

vertical swimming speed experimentally in the laboratory. An organism can sense and react to either an absolute or a differential stimulus (Benhamou and Bovet 1989). Since the vertical scale of the thermoclines simulated in the laboratory experiments (Daigle and Metaxas 2011), and consequently those in the model domain, were exaggerated with respect to those found in nature, the use of temperature gradients (differential mode) as the sensory stimulus in the model was inappropriate. Rather, the absolute mode of stimulus, where only the temperature in the immediate area will affect the behaviour of the simulated larvae (SL), was preferred. Additionally, since bio-physical models often have gradients that are less steep than those found in nature, the absolute mode of stimulus avoids the use of non-biologically derived gradient thresholds, as was done in North et al. (2008). This allows us to use biologically derived data and apply it directly to a bio-physical model by using a modified random walk model. The physiological condition of invertebrate larvae can affect the behavioural response to a cue and consequently their vertical distribution (Metaxas and Young 1998; Chan and Grünbaum 2010). For the sand dollar *Dendraster excentricus*, diet did not affect larval swimming speed or vertical swimming velocity, but it affected the helical width of their swim path (Chan and Grünbaum 2010). In this study, I examined the role of thermal conditioning on larval swimming speed and vertical velocity. I evaluated the ability of one dimensional random walk-based models with various degrees of complexity (mean vertical swimming velocity, unbiased random walk, or the full model with the probability distribution function of vertical swimming velocities) at predicting the vertical distribution of *Strongylocentrotus droebachiensis* larvae in response to thermal stratification. Data from a previous laboratory study on the effects of thermal stratification on the vertical

distribution of *S. droebachiensis* (Daigle and Metaxas 2011) were compared to the model results to evaluate the predictive ability of the model.

I used the green sea urchin as a model species because its behaviour has been studied extensively and is well documented (Strathmann 1971; Burdett-Coutts and Metaxas 2004; Sameoto and Metaxas 2008a; b; Daigle and Metaxas 2011). Additionally, it is the dominant herbivore in the rocky subtidal habitats in my region and is also a commercially harvested species. The use of model organisms allows predictions to be made about the behaviour of other related species that may be of ecological or commercial interest, such as invasive or threatened species. The insights into larval behavior gained in this study combined with the predictive ability of my model would allow for better predictions of larval vertical distributions. Combining these distributions with a general circulation models or advection-diffusion models would ultimately produce more accurate estimates of dispersal than a bio-physical model which does not consider vertical distributions. For example, the effect of behaviour on dispersal distance is important in the design networks of Marine Protected Areas (MPA), created with the intent to conserve biodiversity. If a greater functional diversity of behaviours is considered in the MPA design phase, the MPA network could be scaled more appropriately to allow dispersal between individual MPAs and provide protection for a broader range of species.

3.3 Methods

3.3.1 Fertilization and larval rearing

Adults of *Strongylocentrotus droebachiensis* were collected from the shallow subtidal zone at Bear Cove, NS, in Mar 2009 and Mar 2010. They were maintained in ambient seawater flow-through tanks in the Aquatron facility at Dalhousie University and fed kelp (*Saccharina latissima* and *Laminaria digitata*) *ad libitum*. Spawning was induced by injecting 2-4 ml of 0.55 M KCl through the peristomial membrane. Eggs and sperm from a total of 22 parental pairs (15 in 2009 and 7 in 2010) were combined in 0.45 µm-filtered seawater. Fertilization success, determined as the proportion of eggs with elevated perivitelline membranes, ranged between 96 and 100% (n = 50).

All zygotes and larvae were transferred into 4-L culture jars containing 0.45-µm filtered seawater, which were maintained either in a temperature-controlled room at 9 ± 1 °C or in a water bath at 5 ± 1 °C. Water was gently stirred with slowly rotating paddles and was changed every other day. Larvae were kept at a maximum density of 4 larvae ml^{-1} and were fed a mixture of *Isochrysis galbana* (from Tahiti) and *Chaetoceros muelleri* at a total concentration of 5000 cells ml^{-1}. Larvae were used in the experiments once they reached the 4-arm (6-d old at 9 °C or 8-d old at 5 °C) stage. This larval stage was chosen because it represents the dominant early dispersal stage for this species.

3.3.2 Quantifying larval swimming

In the laboratory, larval swimming was recorded using a Panasonic WV-3170 camera with a 12.5-75 mm (f 1:1.4) TV Zoom Lens in order to quantify swimming speed (s), vertical swimming velocity (w), as well as the temporal covariance of the latter.

Plexiglas columns (10 x 10 x 30 cm, LxWxH) were filled with 2.95 L of 0.45-µm filtered seawater, and placed in a 55-L water bath to maintain the desired water temperatures. For larvae reared in 9 °C, swimming was measured in 3, 5, 10, 15 and 20 °C, while for those reared in 5 °C it was measured in 5, 10 and 20 °C. Larvae from 4 randomly selected parental pairs were used for each of the 3 replicates at each experimental temperature. The 3 °C treatment was done in 2010 with a different batch of larvae, but the large number of parental pairs and the random mixing of offspring used should make the results comparable between years. Larvae were introduced to within 1 cm from the bottom of the experimental tank by gently pouring 50 ml of seawater containing 8-10 larvae ml^{-1} into a funnel attached to a small tube (2-mm inner diameter), yielding a final density of ~ 0.15 larvae ml^{-1}. The camera was focused on the center of the experimental tank at 15 cm depth (field of view: 5 x 7 x 2 cm, HxWxD) for a period of 60 min.

To quantify larval swimming, still images were extracted every 2.5 s for the entire 60-min video recording, and larval positions (x, z co-ordinates) were measured using ImageJ. To obtain *w* and *s* for each replicate, all individuals in focus from 20 pairs of frames (frames in a pair were 2.5 s apart) were used, each pair being separated by 3-min intervals. Vertical velocity (*w*) and speed (*s*) were calculated as:

$$w = \frac{z_2 - z_1}{t_1 - t_2} \tag{3.1}$$

$$s = \sqrt{\left(\frac{z_2 - z_1}{t_1 - t_2}\right)^2 - \left(\frac{x_1 - x_2}{t_1 - t_2}\right)^2} \tag{3.2}$$

where z is the larva's depth, x is its horizontal position and t is the time at which the measurements were made (1 and 2 refer to the two measurements within a frame pair). A positive velocity indicated that the larva was swimming towards the surface. Kernel smoothing was used to estimate the probability distribution functions (PDF) of the vertical swimming velocities for the different temperature treatments.

To analyze the temporal covariance of vertical swimming velocities, the position of 20 randomly selected larvae (1 every 3 minutes) was recorded over time (t) for as long as possible (*i.e.* until it crossed paths with another larva, or moved out of frame or out of focus). The covariance of each larva's vertical swimming velocity was calculated for time lags from 0 to 60 s. An exponential decay curve was fit to the mean temporal covariance to determine its decay rate (λ).

3.3.3 Statistical analysis of larval swimming

I used two-way ANOVAs to determine the effects of rearing (5 and 9 °C) and experimental (5, 10 and 20 °C) temperature on vertical swimming velocity and swimming speed. For larvae reared in 9 °C, I examined the effects of experimental temperature (3, 5, 10, 15 and 20°C) on vertical swimming velocity and swimming speed with one-way ANOVAs. Post-hoc (Tukey's) tests were used to identify significant differences among treatments or treatment combinations.

3.3.4 Vertical position model

An individual-based correlated biased random walk model was developed to calculate vertical position of simulated larvae (SL) in the water column, based on larval vertical swimming velocity and its temporal covariance. The model domain was based on

previous laboratory experiments in which the vertical distributions of larvae of *S. droebachiensis* were observed in relation to the thermal structure of the water column (Daigle and Metaxas 2011). These experiments were conducted in Plexiglas chambers that were 50 cm in height and the thermocline occurred at depths of 20-30 cm. The model domain represented the same dimensions as in the chambers, and the boundaries were solid. In the model, the temperature above and below the thermocline was uniform while the temperatures in the experimental chambers were within ±1 °C of the expected temperature. The temperatures at the thermocline (20-30 cm depth) were linearly interpolated between the temperature above (19 cm depth) and below (31 cm depth), and to facilitate computation, temperatures were rounded to the nearest integer for each 1-cm bin. In the model, the SL responded to the absolute temperature in the 1-cm depth bin at which they were found at each 1-s time-step. The vertical position of an individual was calculated as:

$$z_t = z_{t-1} + (w_t + \varepsilon_T) \times \Delta t \tag{3.3}$$

where z is vertical position, w_t is the vertical swimming velocity at that time, and Δt is the time step. ε_T is random error based on a normal distribution with a null mean and standard deviation equal to the standard deviation measured in the acceleration of real larvae at that specific temperature (the standard deviations which were not directly measured were linearly interpolated). In the model, 100 replicates were run for each treatment, each with 300 SL while there were 5 empirical replicates of each treatment, each with 250-350 larvae.

3.3.5 Modelled vertical velocities

The probabilities of vertical swimming velocities from the PDFs for real larvae were used to generate the vertical swimming velocities of individual SL. Using the PDF for the appropriate temperature, SL were randomly assigned to velocity bins of 0.1 mm s^{-1}, and then distributed uniformly within that bin. If the desired temperature was not represented by an experimentally generated PDF, a PDF was linearly interpolated from adjacent PDFs. When the SL changed swimming velocity (see below), they were reassigned to adjacent velocity bins (*i.e.* ± 0.1 mm s^{-1}) and once again distributed uniformly within the new bin.

Acceleration or deceleration between time steps was based on the probability of SL making the opposite transition from the adjacent bins. These probabilities were calculated to ensure the PDF of vertical swimming velocities of SL remained stable over time. To achieve this stability, there must be an equal and opposite flux of individuals between any 2 bins. For example, at the positive or negative extremity of a PDF, the SL cannot accelerate or decelerate respectively, since the probability of observing velocities beyond those points is null (probabilities below 0.1 % were considered null for this purpose). Therefore, the direction of change is known for all SL at the extremities of the PDFs. Given the total number of SL, I can estimate the flux of SL from the extreme bins to the only adjacent bins. Since: 1) the flux of SL must be the same in either direction; and 2) I assume that the probability of changing vertical velocity is not dependent on velocity; I can estimate the flux of SL from the adjacent bins towards the center of the distribution. By repeating this process, the probability of accelerating or decelerating can be calculated for every bin within the PDF and for every temperature.

It must be noted that this method results in a slight drift in mean vertical swimming velocity of SL. To correct for this, the mean velocities over time were calculated for 300 SL from each of 100 model runs for each temperature. The means rapidly changed at first but stabilized at ~5 minutes into the model run. The slope of the relationship between mean velocity and time was calculated for the first 15 s and added as a temperature dependent constant (multiplied by Δt) to all vertical swimming velocities at each time step. These constants ranged from -0.0024 to -0.0002 mm s^{-2}.

3.3.6 Modelled temporal covariance

For the covariance in the swimming patterns of the SL to approximate the observed patterns, the SL must change velocity, based on a probability calculated as in Equation 4.4 below. Modeling the temporal covariance in vertical velocities is dependent on 2 factors: 1) the variance in acceleration; and 2) the probability of changing velocities. Since the acceleration of all SL is logistically constrained to ± 0.1 mm s^{-2}, accurate modeling of temporal covariance depends on the probability of changing velocities (p), equal to:

$$p = (1 - e^{\lambda \Delta t}) \times \frac{V_a}{\left(0.1 \text{mm s}^{-2}\right)^2} \tag{3.4}$$

where λ is the decay rate of the mean temporal covariance, Δt is the time step, V_a is the variance of the measured acceleration in the swimming experiments and 0.1 mm s^{-2} represents the value used for acceleration in the model. The right hand side of Equation 3.4 acts as a dimensionless scaling factor that increases p when V_a is larger than (0.1 mm s^{-2})^2 and vice versa.

3.3.7 Model validation

To validate the model, the predicted vertical distributions for all 12 temperature combinations were compared to the empirically derived ones. For each distribution I calculated the center of larval mass (ZCM), as:

$$ZCM = \sum p_i z_i \tag{3.5}$$

where p_i is the proportion of larvae at depth interval i and z_i is the median depth of that interval. I also calculated the proportion of larvae found in 4 functional categories of vertical position ("surface" = < 1, "above the thermocline" = 1-19, "thermocline" = 20-30 cm and "below thermocline" = 31-50 cm). For each of these two indices, I compared predicted and empirical vertical distributions with linear regression analysis. While there is error associated with measuring both the modelled and empirical variables used in the regressions, the variance in the modelled data is at least an order of magnitude smaller than that of the empirical data. Consequently, I assumed that the independent variable (modelled data) is measured with no error, which allowed us to use ordinary least squares linear regressions (McArdle 1988; Legendre and Legendre 1998). Student's t-tests (α = 0.05) were used to determine whether the slope and the intercept differed from 1 and 0, respectively.

3.3.8 Alternative Models

In addition to the full model described above, I developed 2 alternative models. In the first model ("mean vertical swimming velocity") the swimming velocity of the SL was fixed to the mean vertical swimming velocity of the temperature which the SL were experiencing. In this model, the only variability in swimming velocity was from the

random error term (ε_T). In the second model ("unbiased random walk model") the mean velocity was null, but the SL experienced variability in swimming velocities similar to those in the full model. To achieve this, instead of the real PDFs of vertical swimming velocities, I used a normal distribution with a null mean and standard deviation equal to that of the real PDFs.

3.4 Results

3.4.1 Quantifying larval swimming

The mean vertical swimming velocities ranged from 0.32 to -0.17 mm s^{-1} (Figure 3.1). Larvae reared at 5 °C had significantly greater vertical swimming velocities than those reared at 9 °C, but swimming speeds did not differ significantly between rearing temperatures (Table 3.1). Swimming velocities also varied with experimental temperature (Table 3.1), with the larvae in 20 °C being significantly slower than those at 5 and 10 °C (Table 3.2). Similarly, treatment temperature had a significant effect on vertical velocity and speed of larvae raised at 9 °C (Table 3.1), with vertical velocities peaking at 10 °C (Figure 3.1, Table 3.2). Swimming speeds appeared to increase with temperature (Figure 3.1).

The mode for all PDFs of vertical swimming velocities occurred at or very near 0 mm s^{-1}, but in most treatments the mean departed from 0 mm s^{-1} because of an extended tail or a second mode (Figure 3.2). The PDF of larvae swimming in 3 °C showed a tight distribution centered at 0 mm s^{-1}. The PDF of larvae swimming in 10 °C had a second mode at 1.5 mm s^{-1}, while that of larvae swimming in 20 °C had an extended tail of negative swimming velocities.

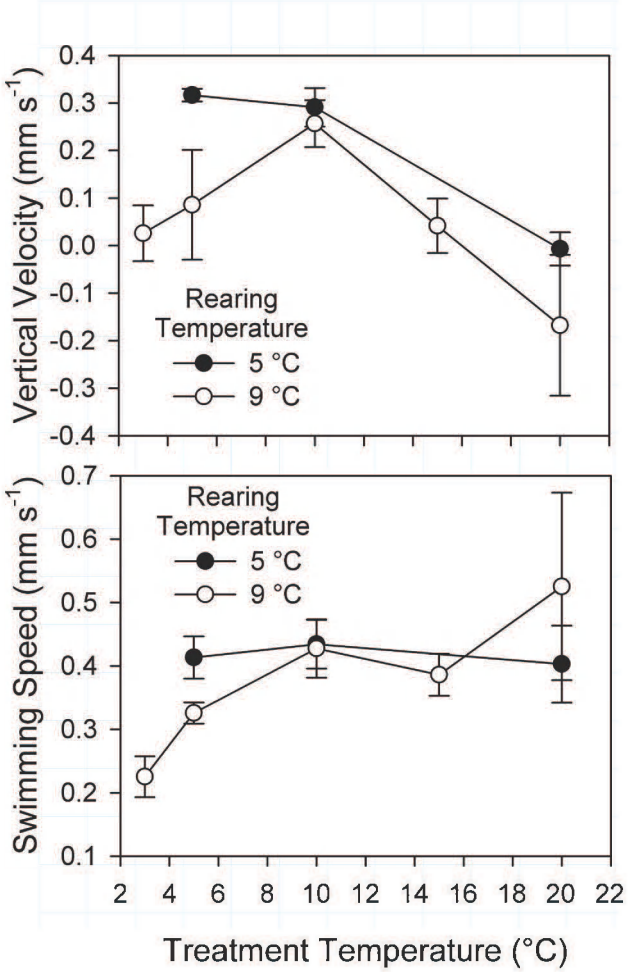

Figure 3.1: Mean (± SD, n = 3) of replicated mean vertical swimming velocity (n = 60 - 647) or swimming speed of larvae of *Strongylocentrotus droebachiensis* reared at 5 and 9 °C exposed to various experimental temperatures in experimental columns (10 x 10 x 30 cm, LxWxH) in the laboratory.

Table 3.1: Results of 2-way ANOVAs examining the effects of rearing temperature (5 or 9 °C) and experimental temperature (5, 10 or 20 °C) on mean vertical swimming velocity and mean swimming speed of larvae of *Strongylocentrotus droebachiensis*; and 1-way ANOVAs examining the effects of experimental temperature (3,5, 10, 15 or 20 °C) on mean vertical swimming velocity and mean swimming speed of larvae raised at 9 °C. Asterisks indicate significant values.

	Velocity				Speed			
2-way	**df**	**MS**	**F**	**p**	**df**	**MS**	**F**	**p**
Rearing	1	0.090	13.328	0.003*	1	0.000	0.076	0.787
Experimental	2	0.219	32.270	<0.0001*	2	0.014	2.713	0.107
R*E	2	0.015	2.193	0.154	2	0.014	3.305	0.072
Error	12	0.007			12	0.005		
1-way								
Experimental	4	0.069	7.772	0.004*	4	0.038	7.146	0.006*
Error	10	0.009			10	0.005		

Table 3.2: Post-hoc comparisons (Tukey's HSD test) for significant effects as detected in ANOVAs in Table 3.1 of mean vertical swimming velocity of larvae of *Strongylocentrotus droebachiensis* between experimental temperatures or mean swimming velocity or speed of larvae between experimental temperatures. Asterisks indicate significant values.

(°C)	p-value		
	2-way	1-way	
	Velocity	Velocity	Speed
3 vs 5		0.930	0.478
3 vs 10		0.078	0.042*
3 vs 15		1.000	0.122
3 vs 20		0.163	0.003*
5 vs 10	0.313	0.247	0.467
5 vs 15		0.976	0.842
5 vs 20	<0.001*	0.050	0.045*
10 vs 15		0.107	0.952
10 vs 20	<0.001*	0.002*	0.502
15 vs 20		0.120	0.207

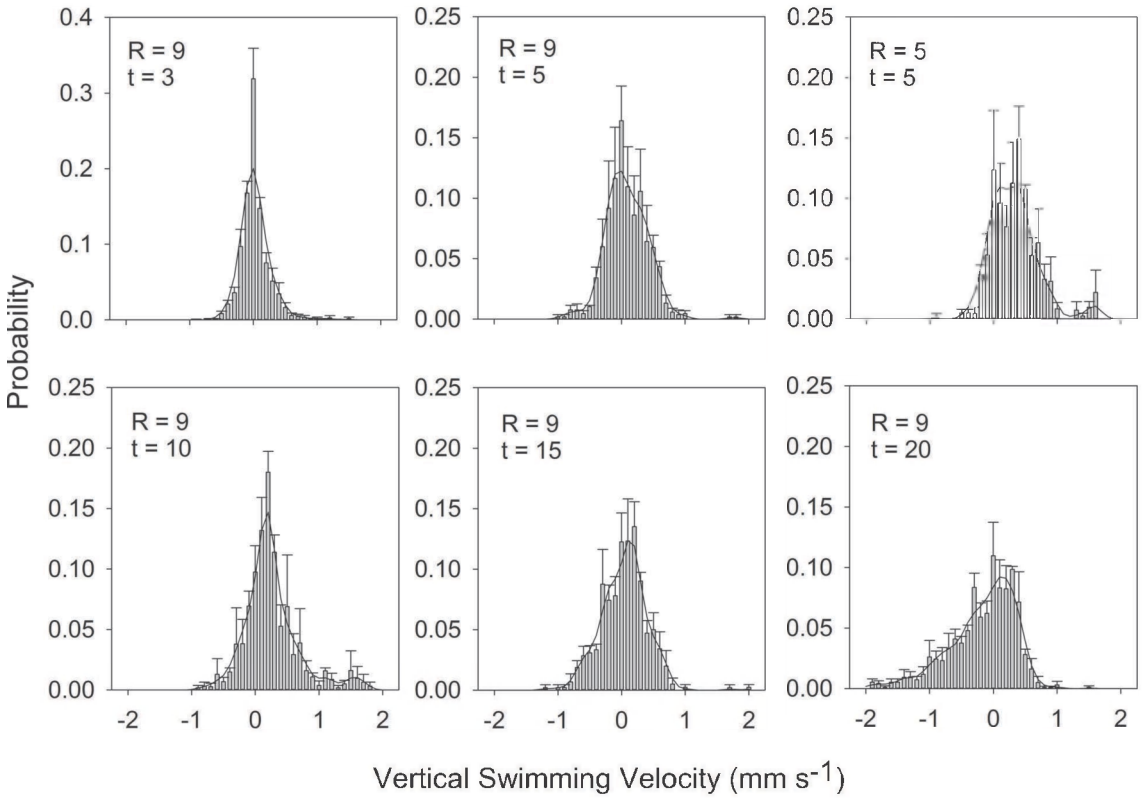

Figure 3.2: Mean (± SD, n = 3) probability distributions of vertical swimming velocity of larvae reared at 5 and 9 °C (R5 or R9, respectively) exposed to various experimental temperatures (t3-20). Solid line indicates the kernel smoothed probability distribution function used in the model

3.4.2 Temporal covariance

The similarity between the temporal covariance of the vertical swimming velocities in the full model and that measured empirically (Figure 3.3) was achieved by using probabilities of a change in velocity of 6, 5, 13, 18 and 100% (Equation 3) for 3, 5, 10, 15 and 20 °C, respectively. For all temperatures, empirical temporal covariance reached an asymptote near zero at a time lag of 30 s, but the initial variance (covariance at 0 time lag) increased with temperature. Pearson's correlation coefficients between the empirical and modelled temporal covariance ranged between 0.89 and 0.95, indicating that the pattern observed in the empirical temporal covariance was well reproduced in the model.

3.4.3 Model validation

Qualitatively, the modelled vertical distributions of larvae were very similar to the empirical distributions (Figure 3.4). For example, the large surface aggregations observed in 10 °C were reproduced and these aggregations were less pronounced in the treatments with either higher (*e.g.* 20 °C) or lower (*e.g.* 3 °C) temperatures. Aggregations at the thermocline, such as those in treatments where the surface layer was 20 °C and the bottom layer 9 °C, were accurately predicted. However, there was some dissimilarity between the empirical and modelled data. For most treatments, there was an aggregation of larvae in the bottom layer between 40 and 50 cm depth that was not reproduced in the model (Figure 3.5). Similarly, above the thermocline, there was an aggregation of SL between 1 and 10 cm depth in the model that was not observed empirically (Figure 3.5).

The relationship between empirical ZCM and modelled ZCM fell near the 1:1 line, but there were some distinct biases (Figure 3.6). There was a cluster of treatments

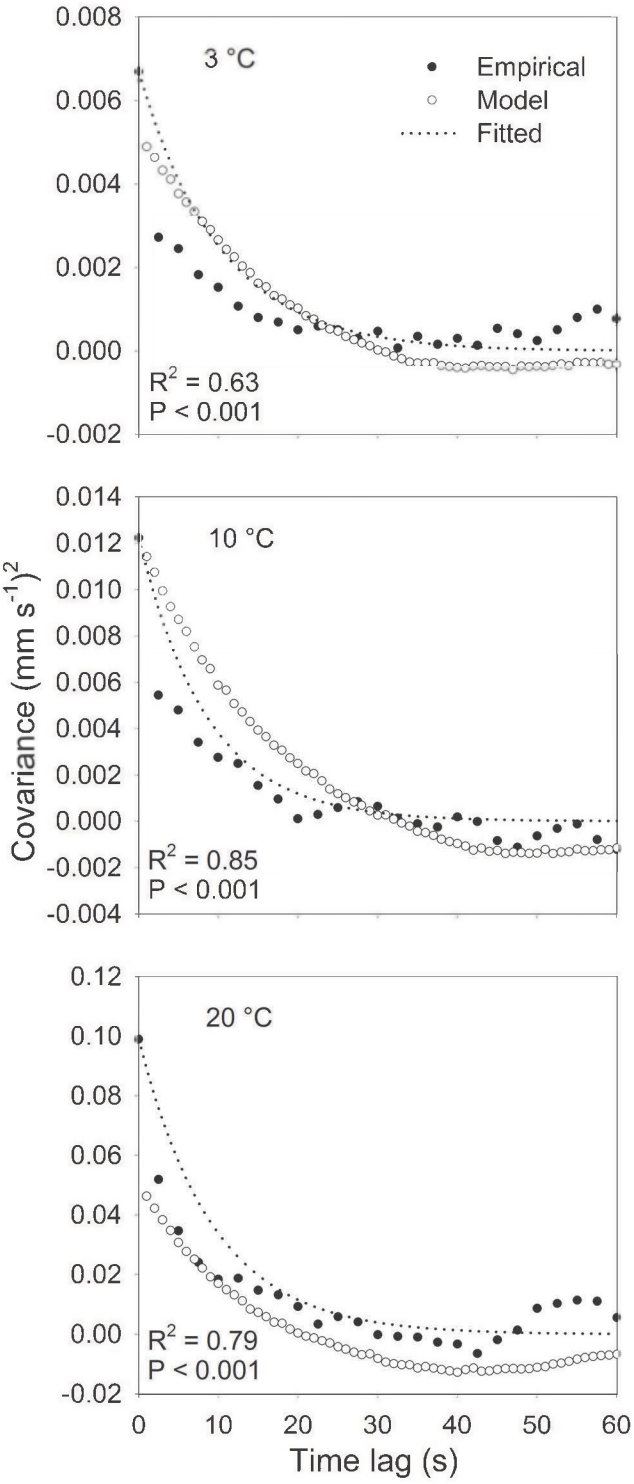

Figure 3.3: Change in the covariance of vertical swimming velocities with time lag for 3 different temperatures measured in the laboratory as well as calculated from model data. An exponential decay line fitted to the empirical data which was used to parameterize the model is also shown.

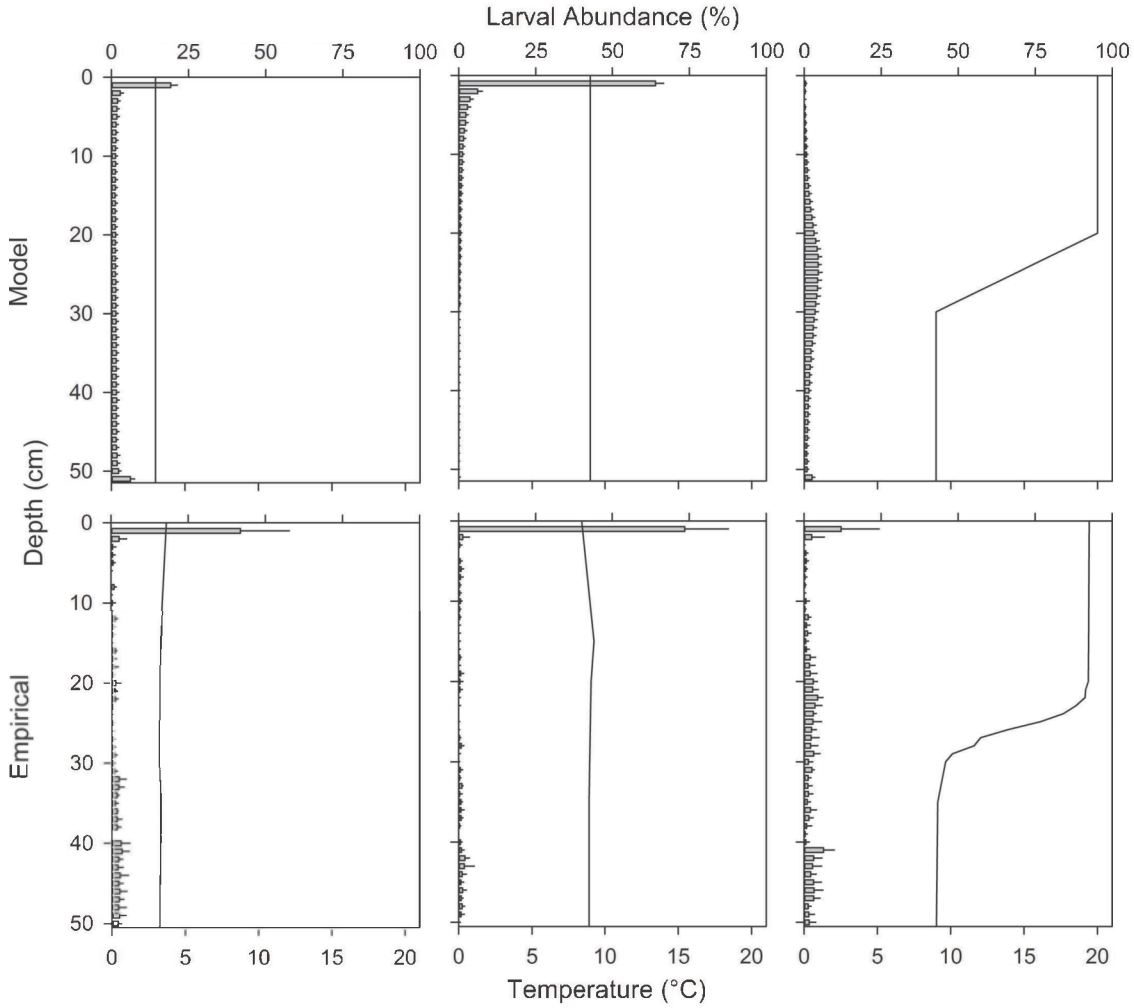

Figure 3.4: Examples of modelled and empirical vertical larval distributions of the sea urchin *Strongylocentrotus droebachiensis* in thermocline chambers after 60 min. Shown is mean abundance (± SD, n=100 and n=5, respectively) at each 1-cm interval. Superimposed line plots show temperature profiles.

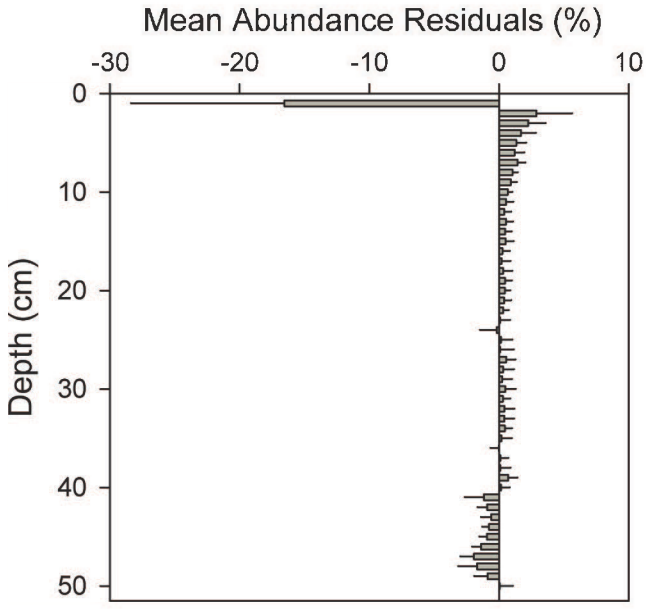

Figure 3.5: Mean (± SD, n = 12) abundance residuals between modelled and empirical vertical larval distributions of *Strongylocentrotus droebachiensis* in thermocline chambers after 60 min. Calculated as the difference between modelled and empirical abundance at each 1-cm interval, averaged over all 12 temperature combinations. Errors are the standard deviations among temperature combinations.

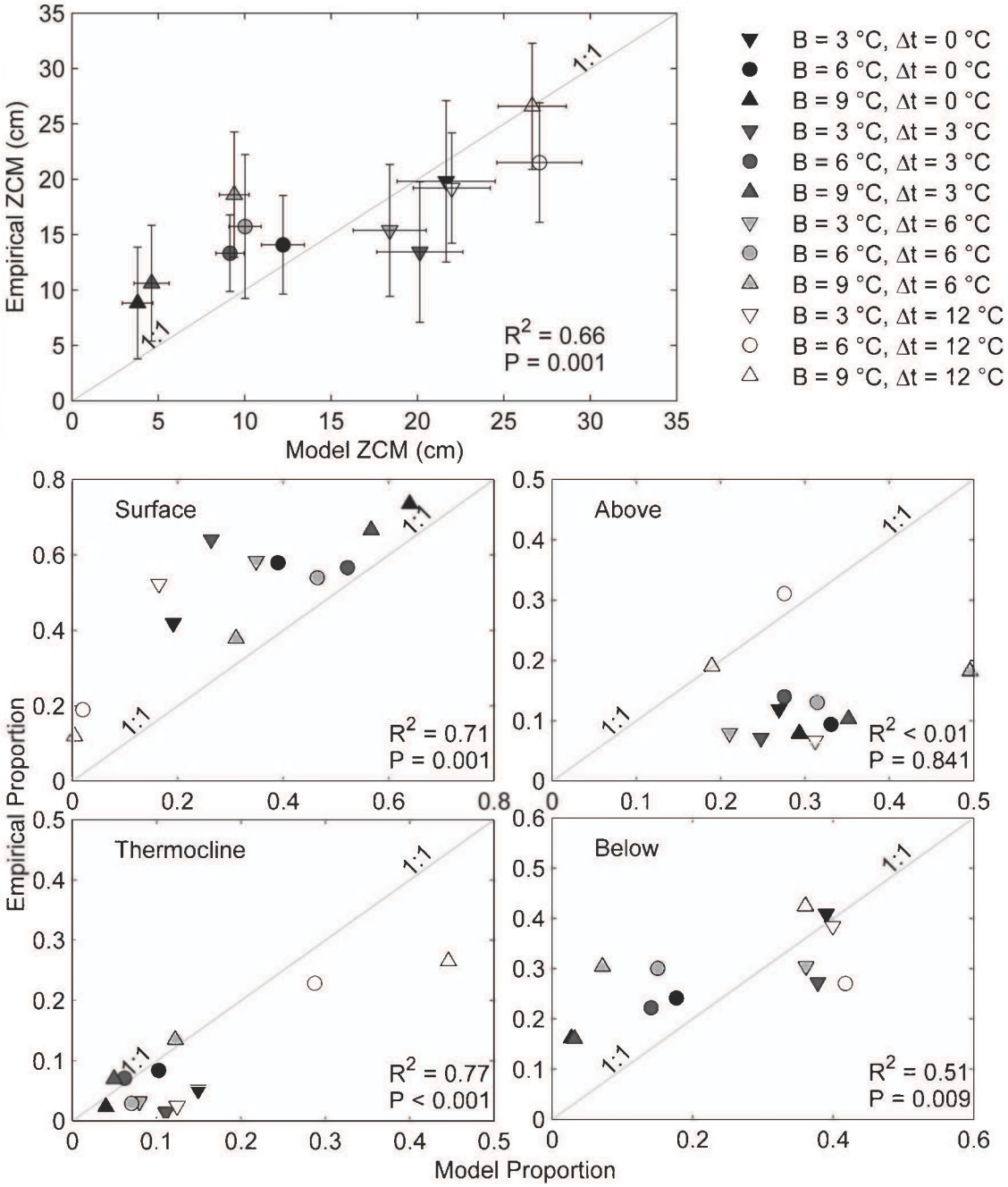

Figure 3.6: Relationship between empirical and modelled (full model) variables representing vertical larval distributions of *Strongylocentrotus droebachiensis* in thermocline chambers after 60 min. Shown is the mean (± SD, n = 12) center of larval mass (ZCM), and the mean proportion of larvae at the surface, above the thermocline, at the thermocline and below the thermocline. The error bars for the proportions have been omitted for legibility.

that had a ZCM above the 1:1 line, suggesting that the model produced values that were shallower than expected, and another below the 1:1 line, suggesting that the model produced values that were deeper than expected. While there was a strong relationship between the modelled and the empirical ZCMs ($r^2 = 0.66$, $p = 0.001$), the slope and intercept were significantly different from 1 ($t_{10} = 4.6$, $p = 0.001$) and 0 ($t_{10} = 4.6$, $p = 0.001$) respectively.

When individual components of the distribution were examined separately, there was a significant relationship between empirical and modelled distributions at the surface ($r^2 = 0.71$, $p = 0.001$), at the thermocline ($r^2 = 0.77$, $p < 0.001$) and below the thermocline ($r^2 = 0.51$, $p = 0.009$), but not above the thermocline ($r^2 < 0.01$, $p = 0.841$). At the surface, all treatments were above the 1:1 line, suggesting that the model underestimated the proportion of larvae at that location. The slope of this relationship was not significantly different from 1 ($t_{10} = 1.5$, $p = 0.163$), but the intercept was significantly higher than 0 ($t_{10} = 4.2$, $p = 0.002$). Conversely, the model overestimated the proportion of larvae above the thermocline and at the thermocline, for all treatments. The intercept for either of these relationships was not significantly different from 0 ($t_{10} = 1.3$, $p = 0.214$ and $t_{10} = 0.1$, $p = 0.959$, respectively), but the slopes were significantly smaller than 1 ($t_{10} = 3.3$, $p = 0.007$ and $t_{10} = 3.6$, $p = 0.005$, respectively). Below the thermocline, some of the treatments were clustered around the 1:1 line, but for the treatments which fell closer to the intercept, the model underestimated the proportion of larvae at that depth. The slope and intercept of this relationship were significantly different from 1 ($t_{10} = 4.9$, $p < 0.001$) and 0 ($t_{10} = 5.5$, $p < 0.001$), respectively.

3.4.4 Alternative Models

The relationship between empirical ZCM and modelled ZCM for the alternative models is relatively far from the 1:1 line (Figure 3.7) compared to that of the full model, and there was no significant relationship between the modelled and the empirical ZCMs. While the "mean swimming velocity" model was successful at producing ZCMs that spanned most of the domain similar to the empirical observations, all SL were found within 6 cm of one another since variability is restricted. The "unbiased random walk" model failed to get any SL above the thermocline within 60 min since it does not use directed movement.

3.5 Discussion

I found that both thermal conditioning and experimental temperature significantly affected vertical swimming velocities, but only experimental temperature affected swimming speed. The larvae reared in different temperatures were of different ages but morphologically similar (*i.e.* same length and width), and had similar swimming abilities since there was no difference in swimming speeds. This suggests previous thermal conditioning affected swimming behaviour only by altering vertical swimming velocities, i.e. direction of travel. Since larvae raised in 5 °C had higher mean vertical swimming velocity, these larvae had a higher probability of swimming upward. Because echinoid larvae are negatively buoyant (Pennington and Strathmann 1990; Sameoto and Metaxas 2008b), upward swimming requires active expenditure of energy suggesting that the larvae raised at 5 °C were in better physiological condition. It is also possible that thermal conditioning and dietary conditioning are intrinsically linked since rearing temperature also affects feeding rates (Podolsky 1994). However, the effect of

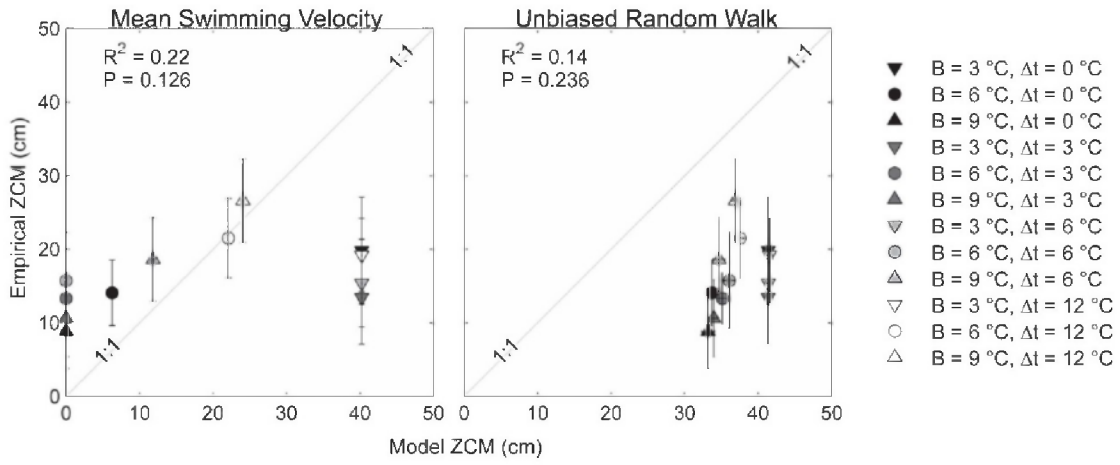

Figure 3.7: Relationship between empirical and modelled ("mean vertical swimming velocity", and "unbiased random walk" models) centers of larval mass (ZCM) representing vertical larval distributions of *Strongylocentrotus droebachiensis* in thermocline chambers after 60 min. Shown is the mean (± SD, n = 12)

experimental temperature on vertical swimming velocities was greater than that of thermal conditioning.

Increases in swimming speed with increasing experimental temperature could result from effects on the rate of physiological processes, such as the ciliary beat rate (Jørgensen et al. 1990; Larsen et al. 2008). Additionally, dynamic viscosity is inversely related to temperature, and the positive relationship between swimming speeds and temperature are not surprising since drag is reduced in higher temperatures (Podolsky and Emlet 1993). Temperature appeared to have no effect on the speed of larvae that were raised in 5 °C, likely due to interactions between thermal stress and the effects of viscosity. At lower temperatures (high viscosity), the larvae were slowed by drag while at higher temperatures they might have been physiologically stressed (more so for larvae raised in 5 °C). However, apparent differences between the swimming speeds of larvae reared at different temperature were not statistically significant because of high individual variability.

The differences in vertical swimming velocity among experimental temperatures can affect depth regulation in these larvae. The proportion of time a larva spent swimming upwards or downwards in combination with its speed, determined its depth, but also changed over time. While SL had enough time to swim to the surface in the full model runs, the dynamic nature of a larva's depth indicates that the shape of the PDF of vertical swimming velocities affected the likelihood of an SL being found at the surface at a given time. The parabolic pattern in mean vertical swimming velocity was not surprising given previous observations of vertical distribution (Daigle and Metaxas, 2011). The lower mean vertical swimming velocities (*i.e.* larvae are more likely to be

swimming downwards) at the temperature extremes (3 and 20 °C) correspond to those in the experimental treatments 3/3 and 21/9 in Daigle and Metaxas (2011), in which few larvae were found at the surface and ZCM was deep. Conversely, the highest vertical velocities (10 °C) correspond to those in the treatment 9/9 °C where most larvae were found at the surface and had the shallowest ZCM. As discussed in Daigle and Metaxas (2011), this response to experimental temperature was likely to maximize growth rate and minimize mortality related to temperature stress.

The alternative models did not reproduce either realistic larval vertical distributions or accurate ZCMs. This suggests that both the directed swimming and the variability in swimming velocity are important in simulating larval behaviour. Directed swimming was important because the rate of diffusion in the unbiased random walk is not sufficient to get any larvae above the thermocline in the 60 min model runs. The variability and temporal covariance of swimming velocities are important in the model because it reflects the natural variability in larval swimming and is critical in reproducing realistic distributions of larvae.

I believe that the full model realistically simulates larval response to temperature, by utilizing temperature dependent PDFs of vertical swimming velocity. Both the range in ZCMs and the proportions of larvae at a particular depth category were similar between empirical and modelled distributions and there was a significant relationship between the two types of distributions for 4 out of 5 variables (*i.e.* ZCM or proportion of larvae in a depth category). The model was also successful in terms of reproducing surface aggregations and varying depth positions for larvae (*i.e.* there was larval exchange between layers even once the vertical distribution had stabilized).

A few attempts at incorporating behavioural components that simulate vertical migration into biophysical models of larval dispersal have been made recently (Dekshenieks et al. 1996; DiBacco et al. 2001; North et al. 2008; Banas et al. 2009). However, these attempts utilized mean swimming velocity for a particular ontogenetic stage and/or stimulus intensity (*i.e.* "idealized behaviours"), rather than observations of probability distributions of swimming velocities. In contrast, the model used a mechanistic approach with representative swimming velocities. It is difficult to ascertain whether the model simulates the vertical distribution of larvae more accurately than these other attempts since the latter do not include a formal validation of the model results. However, since themodel uses realistic swimming patterns instead of an idealized swimming behaviour, I expect that it would perform better. If I had used mean velocities instead of PDFs the results would be substantially less accurate since all the SL would simply have swam towards the surface (or the bottom at 20 °C).

While the model was only developed for use with 1 species and 1 stimulus, the mechanism by which stimulus intensity modulates the probability distribution of the vertical swimming velocities is broadly applicable. The vertical position of any larva that responds to an absolute stimulus could be simulated with this type of model by modifying its vertical swimming velocity. Additionally, this type of model does not assume that larvae remain at a fixed depth for a specific period and it allows SL to swim independently of one another (*e.g.* not all larvae are swimming upwards during ebb tide).

Random walk models are among the simplest numerical representations of individual organism movement. Simple modifications (*e.g.* bias, auto-correlation) can transform a random walk model into a powerful tool to predict movement (Benhamou

and Bovet 1989; Codling et al. 2008). These models allow the incorporation of additional levels of complexity, such as turbulence by adding a random term representing turbulent diffusion (Jonsson 1989; Yamazaki 1993; Porch 1998). The simplicity, flexibility and predictive nature of random walk models make them ideal for generating predictions of larval vertical distributions to be used in biophysical models. Running the random walk model as a sub-model to a general circulation model at appropriate time intervals would allow the incorporation of larval vertical migration in response to changing biological and physical cues as they are being advected horizontally.

The effect of many other cues such as salinity, turbulence, predators and food on larval behavior and distribution can be quantified in the laboratory, as I have done for temperature, and a similar approach used to study diel and tidal vertical migration by quantifying larval swimming parameters over time. Larval response (and its associated variability) to the presence of a cue can take several forms of modifications in mean swimming velocity such as: 1) random swimming (null mean, high variability), 2) maintaining position (null mean, low variability), 3) directed swimming (biased mean, low variability), 4) biased random swimming (biased mean, high variability) or intermediate forms. In this study, the larvae display mostly biased random swimming and nearly random swimming at some temperatures; however, a study by Sameoto and Metaxas (2008) suggests that larval *S. droebachiensis* and *Asterias rubens* also display directed downward swimming in response to low salinities since the larvae are absent from the low salinity layer at the surface in some treatments. The structure of the temporal covariance in vertical swimming velocities can also change the time scale and the nature of the response. Very high temporal covariance would result in larvae that

maintain the same velocity for long periods of time and could lead to accumulations of larvae at the boundaries, while larvae with low temporal covariance would be changing velocity very frequently and would effectively be swimming at the mean velocity if observed on longer time scales. The random walk approach can be adapted to accommodate any of these behavioural combinations, as well as different covariance schemes.

While, in general, there was good agreement between empirical and modelled data, the model did have some biases. In almost all cases, there were too many SL above the thermocline (particularly in the top 10 cm) but not enough at the surface. However, if the positions "surface" and "above the thermocline" are combined, the observed proportions of larvae converge much closer to a 1:1 relationship with those of the SL. This suggests that the larvae in the top 10 cm interact with and are likely attracted to the surface. While this behaviour was not directly quantified, larvae might react to being near the surface by detecting pressure. I have observed larvae swimming down from the surface layer and almost immediately return (i.e. "bouncing off" the surface), usually remaining in the top 2-3 cm. Similarly, there was an empirically observed aggregation in the bottom 10 cm that was not reproduced in the model. This could be caused by a subset of the population that has distinct swim patterns. Such slow swimmers, likely of poor condition or shocked during the introduction into the experimental chamber, would not have been captured by the field of view of the camera, and therefore, would not be reproduced in the model. Despite these shortcomings, I believe that the model illustrates the mechanism (*i.e.* temperature dependent vertical velocity PDF) by which temperature stratification affects the vertical distribution of larvae.

My model could be scaled to predict vertical distributions of larval *S. droebachiensis* in the field by simply changing the limits to the model domain, if the differences between modelled and empirical values were indeed caused by processes that were limited to the boundaries (top and bottom 10 cm). Additionally, since the swimming velocity is known for each larva, first order interactions (advective transport) with vertical advection and turbulence could be modelled by adding an advective term and turbulent diffusion to the model (Jonsson 1989), respectively. However, larvae likely react to multiple interacting stimuli such as food availability, salinity or sheared flow (Burdett-Coutts and Metaxas 2004; Sameoto and Metaxas 2008b; Metaxas et al. 2009) they encounter in the ocean. My model could incorporate responses to these other stimuli by expanding the range of factors that modulate swimming velocities measured in additional laboratory experiments, *in situ* or possibly even deducing velocities from vertical distributions in the field.

In conclusion, I believe that my behavioural model successfully reproduces the mechanism by which larval vertical distribution in response to thermal structure is regulated. The thermal conditioning of the larvae affected their vertical swimming velocity, but the effect of treatment temperature accounted for a greater proportion of the variability in vertical swimming velocity. While the modelled vertical distributions resemble the empirical distributions, the model does have some biases. The model's performance was poor near the boundaries (top and bottom 10 cm), but these issues would likely be minimized if the model domain was scaled to dimensions in the natural habitat (10s m vs cm). This model and its mechanistic framework improve my understanding of larval behaviour and my ability to predict vertical distributions. These

improvements lead to better predictions of dispersal and connectivity which are important for the design of MPAs, fisheries management areas or invasive species monitoring.

CHAPTER 4: FINE-SCALE DISTRIBUTION AND SPATIAL VARIABILITY OF BENTHIC INVERTEBRATE LARVAE[3]

4.1 Abstract

This study quantified the spatial scale of variability in the horizontal distributions of benthic invertebrate larvae and related this variability to that in physical and biological variables, such as density, temperature, salinity, fluorescence and current velocity. Larvae were sampled continuously (one sample every ~ 500 m) along two perpendicular 10-km transects with a 200-μm plankton ring net (0.75-m diameter) in St. George's Bay, Nova Scotia, Canada, in Aug 2009. Temperature, conductivity, pressure and fluorescence were measured with a CTD cast at each station, and currents were quantified with an ADCP moored at the intersection of the 2 transects. Gastropod, bivalve and, to a lesser extent, bryozoan larvae had very similar spatial distributions, but the distribution of decapod larvae had a different pattern. These findings suggest that taxonomic groups that have functionally similar larvae (i.e. similar swimming ability; *e.g.* bivalves and gastropods) have similar dispersion properties (distribution and spatial variability), while the opposite is true for groups with functionally dissimilar larvae (*e.g.* bivalves and decapods). The spatial variability in larval distributions was anisotropic and matched the temporal/spatial variability in the current velocity. my study suggests that in a system with no strong oceanographic features, the scale of spatially coherent physical forcing (*e.g.* tidal

---

[3] Daigle, R. M., and A. Metaxas. Submitted to Marine Ecology Progress Series in May 2013.
My coauthor Dr. Anna Metaxas supervised the study design and analyses, and edited the manuscript.

periodicity) can regulate the formation or maintenance of larval patches; however, swimming ability may modulate it.

4.2 Introduction

The dynamics and persistence of populations of marine benthic invertebrates are affected by connectivity, which is in turn regulated by dispersal during the planktonic larval phase (Levin, 2006; Cowen and Sponaugle, 2009). For example, spatial and temporal variability in larval supply and settlement influences the patterns of recruitment of new individuals to adult populations (Underwood and Fairweather 1989b; Shanks and Brink 2005). The scale of temporal variability in larval abundance can range from decadal climatic variations (Menge et al. 2009) to diel or tidal vertical migrations (Tamaki et al. 2010). Spatially, variability in larval abundance can result from the variation in water properties at regional scales (Jillett 1976) to small scale features of the water column that may aggregate and transport invertebrate larvae, such as up- or downwelling flow (Poulin et al. 2002; DiBacco et al. 2011), internal tidal bores (Pineda 1991), or frontal systems and Langmuir cells (Omori and Hamner 1982). Many different physical processes can influence the spatial or temporal pattern of larval dispersal and connectivity. At large spatial or temporal scales, the variability in larval abundance leads to spatially dependant variability in recruitment, and consequently, spatially dependant species assemblages. At smaller scales, physical processes aggregate larvae and alter larval transport, ultimately affecting larval dispersal. Additionally, patchiness or spatial heterogeneity generated by variability in larval abundance, affects the perceived patterns in the distribution of planktonic larvae, and may contribute to the detection of erroneous

patterns through spatial aliasing or masking of the true pattern by high sampling variability (Omori and Hamner 1982).

Quantifying larval dispersal and connectivity is difficult (Levin, 2006; Cowen and Sponaugle, 2009). Geochemical tracers and genetic markers have been used to quantify realized dispersal, but bio-physical modelling remains the only method currently used to predict trajectories of larval dispersal for all species. There are examples where the dispersal of relatively large, short-lived tunicate larvae has been visually tracked (Olson 1985), but this technique is not practical for very small or long lived larvae. Biophysical models are mostly either general circulation models or advection-diffusion models used to quantify the effects of the physical properties of the ocean on larval dispersal (Metaxas and Saunders, 2009). The validity of the bio-physical model is limited by the model's ability to resolve relevant physical features of the water column with which larvae could interact behaviourally, such as up- or downwelling, as well as by the incorporation of this behaviour into the "bio" component of the bio-physical model.

By comparing the spatial scale in larval patchiness with that of the physical variables of the water column (temperature, salinity etc), I can determine the relative contribution of different physical features (upwelling, internal tidal bore etc) in generating patterns in larval abundance. For example, if larval patch size is similar in scale to that of the variability in temperature, but not salinity, I can conclude that temperature is more important in determining the larval pattern. Both a correlation in space between larval abundance and physical variables of the water column, and a similarity in the scale of spatial variability for biological and physical variables can be used as indicators of the physical features that regulate larval abundance (Sokal 1978). In

this study, I determined the patch size through spatial autocorrelation in larval abundance of different taxonomic groups (bryozoans, bivalves, gastropods, bivalves, decapods) and in the physical variables of the water column (temperature, salinity, fluorescence, density, depth of the fluorescence maximum and depth of the mixed layer), and identified relevant physical or biological processes that may regulate larval distributions.

4.3 Methods

4.3.1 Field sampling

Larval abundance and biological and physical variables were sampled in St. Georges Bay, Nova Scotia, on 15 Aug 2009. Two 10-km transects (Figure 4.1) were sampled continuously (contiguous samples) every ~ 500 m for 5 min each at 3 m depth with a 200-μm plankton ring net (0.75-m diameter). The net was towed at ~1.7 m s^{-1} for 5 min and the volume of filtered water was quantified using a flowmeter. Temperature, conductivity, pressure and fluorescence were measured through the entire water column by doing vertical casts with a Seabird 25 Conductivity-Temperature-Depth (CTD) recorder, and an attached SCUFA fluorometer. CTD casts were done between plankton tows and at both extremities of the transects. Each transect consisted of 20 plankton samples to quantify larval abundance, and 21 CTD casts. The CTD was recording at 1 Hz, but the data from 1-5 m depth (which was always in the surface mixed layer at all sites) were averaged to provide a representative estimate of the physical variables at 3 m. The depth of the mixed layer was calculated by determining the shallowest depth at which the density differences between consecutive measurements exceeded 2 standard deviations of all density differences between consecutive measurements of the entire density profile

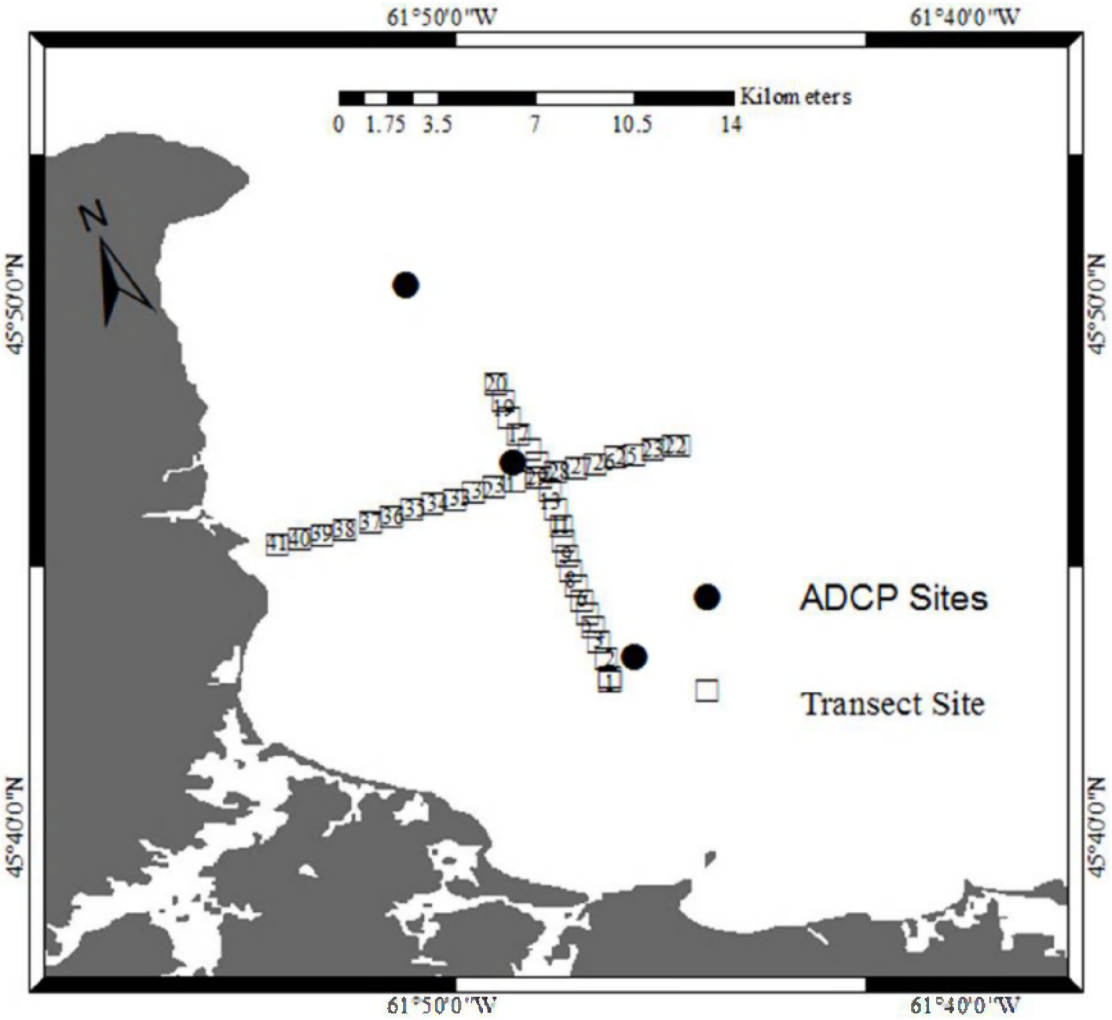

Figure 4.1: Map of St. George's Bay, Nova Scotia, Canada indicating sites along 2 perpendicular ~10-km transects which were sampled continuously (one larval sample every ~ 500 m for 5 min) at 3 m depth, with a 200-µm plankton ring net (0.75 m diameter). The entire water column was profiled with a CTD between larval samples. The site of the ADCP mooring is also shown.

between 1-5 m. Each transect took 6 h to complete and was timed so that high tide (which coincided with high noon) would occur between transects. By ensuring that transects were sampled during a single phase of the tidal cycle (and light cycle), any effect of tidal or diel vertical migration would be of the scale of the entire transect (10 km). The first transect was sampled from South to North (low to high tide) and the second transect was sampled from East to West (high to low tide). All plankton samples were preserved in 95% ethanol and larvae were identified and enumerated under a Nikon SMZ 1500 as described in Lloyd *et al.* (2012). Samples were split into subsamples using a Folsom plankton splitter. For n = 8, samples were split to 1/64 of the original volume and all subsamples were processed. Based on those samples, I determined that at least 20 individuals of each species needed to be counted to get an estimate of abundance that was within 5% of the true sample abundance. The remainder of the samples were split to between 1/128 and 1 to ensure that ≥20 individuals of the most abundant species (*Margarites spp.*, *Astyris lunata*, *Mytilus* spp., *Electra pilosa*, and *Cancer irroratus*) were counted. Individual larval species have also been combined into broader taxonomic groupings to generalize the interpretation of results.

Three 600 kHz Teledyne RDI Workhorse Sentinel Acoustic Doppler Current Profilers (ADCP) were deployed on the seafloor, sampling the full water column in 1-m depth bins every 20 min from11 July to 22 Aug 2009 (Figure 4.1). I only included the horizontal velocities in the bin centered at 3 m in my analyses. The reliability of the current velocities at 3 m was assessed by plotting the variance in current velocities for each 1-m depth bin for the entire water column; the variance in the 2.5-3.5 m bin was not greater than that in the mixed layer below it (~ 4 -12 m). Cross-correlation and

coherence-squared analyses were applied to current data collected by the 3 ADCP in Aug 2009 to examine the structure of the flow regime. For the spatial/temporal analyses, the data record was truncated to 4 days (12-15 Aug) to reflect recent hydrodynamic conditions that may have affected larval distributions at the time scale of my study. The mean horizontal speed over the week preceding the study was 28.6 mm s^{-1} (0.1 km h^{-1}), and spatial scales of 10 km correspond to approximately 4 days.

4.3.1 Data analyses

I examined the relationship among abundances of different larval groups or species, as well as the relationship between the abundance of each larval group or species and each physical variable (temperature, salinity, fluorescence, density, depth of the fluorescence maximum and depth of the mixed layer) using Pearson correlations. The logarithm (base 10) of larval abundance data was used for all statistical tests because it improved the normality of count data (Zar 1999).

Since this study is designed to look specifically at small scale patterns, I removed large scale trends in larval abundance by linearly regressing larval abundance through space and using the residuals for the spatial analyses. The smaller scale variability was still within the residuals, but the large scale variability (possibly related to vertical migration, sampling design, etc) was removed. To quantify spatial and temporal autocorrelation, the residuals of larval abundances (to remove large scale variables) and the physical variables were analysed using Moran's I calculated as:

$$I(d) = \frac{\frac{1}{W}\sum_{h=1}^{n}\sum_{i=1}^{n} w_{hi}(y_h - \bar{y})(y_h - \bar{y})}{\frac{1}{n}\sum_{i=1}^{n}(y_i - \bar{y})^2} \quad for\ h \neq i \tag{4.1}$$

In this equation, y_h and y_i are the values of the variable of interest (abundance or physical parameter) at sites *h* and *i*, *d* is the distance class, w_{hi} are the weights which take the value of 1 when sites *h* and *i* are at distance *d* or are equal to 0 otherwise, and *W* is the sum of those weights (Legendre and Legendre 1998). Moran's I is a spatial autocorrelation statistic that takes on a null value when no autocorrelation is detected and varies from 1 to -1, indicating positive and negative spatial autocorrelation, respectively. Spatial lags were binned in 12 bins with equal numbers of site pairs in each bin (n = 15-16 and 17-18, for larval abundances and physical variables, respectively) to allow bins to have the same statistical power. For the velocity data from the ADCP, temporal lags were binned into 15 bins (n = 2755) to maintain a resolution similar to that of the spatial autocorrelation. To allow comparisons between the two, the temporal autocorrelation was converted to spatial autocorrelation by multiplying the time lag with the mean speed measured by the ADCP from 12-15 Aug (32.9 and 22.5 mm s^{-1}, in the S-N and W-E directions, respectively). All autocorrelation analyses were done in SAM v4.0 (Rangel et al. 2010).

For consistency and comparability, I chose to analyse all spatial and temporal patterns using Moran's I. This metric was chosen because all data series except current velocity are relatively short, making conventional spectral analysis difficult (very coarse resolution). Additionally, with Moran's I, the width of the distance or time bins can be customized to allow the use of the same number of variable pairs for each data point.

Patterns in the differences in physical variables among sites were explored using Nonmetric Multidimensional Scaling (nMDS). The nMDS plot was created using the "metaMDS" function in the "vegan" package (Oksanen et al. 2012) in R 2.14.1 (R Core Team 2012). The nMDS plot was then rotated in order for the first dimension (NMDS1) to be parallel to the abundance of each larval group, using "MDSrotate". This function rotates the nMDS plot so that the dispersion of points of the abundance of a particular larval group is highest along NMDS1. This rotation allowed the visualization of the relationship among sites that were physically similar (a single water mass) or dissimilar (different water masses), and larval abundance.

4.4 Results

4.4.1 Larval distributions

Collected larvae were categorized as bryozoans, bivalves, gastropods or decapods (Table 4.1). The bryozoans consisted almost entirely of *Electra pilosa*, whereas the bivalves were largely un-identifiable to species, but the most abundant identifiable genus was *Mytilus* spp. The gastropods consisted of *Margarites* spp. and *Astyris lunata*, and the decapods were mostly *Cancer irroratus*. In the S-N transect, the most striking feature in larval distribution of taxonomic groups was a peak in abundance at 5.8 km for both the bivalves and gastropods, and at the same location, an increase in abundance of bryozoan larvae (Figure 4.2). At the species level, the pattern similar except that the peak at 5.8 km was not as pronounced for the 'other bivalves' (Figure 4.3). In the W-E transect, peaks in the abundance of bivalves, gastropods and decapods occurred at 0 km (closest to shore) and 7.8 km (Figure 4.2). At the species level, the pattern was similar, but the peak at 7.8

Table 4.1: Mean, minimum and maximum abundance (individuals m^{-3}) of larval taxonomic groups, during plankton sampling in St. George's Bay, Nova Scotia, Canada, in Aug 2009. Proportional species composition for each group is also shown.

A) Abundance

Bryozoans		Bivalves		Gastropods		Decapods	
Mean	4.80		20.6		26.0		0.30
Minimum	0.32		0.46		1.92		0.04
Maximum	10.6		114		119		0.87

B) Composition

Species	%	Species	%	Species	%	Species	%
Electra pilosa	99.9	*Mytilus* spp.	34.6	*Margarites* spp.	49	*Cancer irroratus*	71.7
Membranipora membranacea	0.1	*Modiolus modiolus*	14.6	*Astyris lunata*	32.5	*Crangon septemspinosa*	16.4
		Anomia simplex	5.4	*Diaphana minuta*	6.2	*Neopanopeus sayi*	8
		other	45.4	*Crepidula spp.*	4.6	*Carcinus maenas*	3.9
				Arrhoges occidentalis	4.1		
				Bittiolum alternatum	3.1		
				other	0.5		

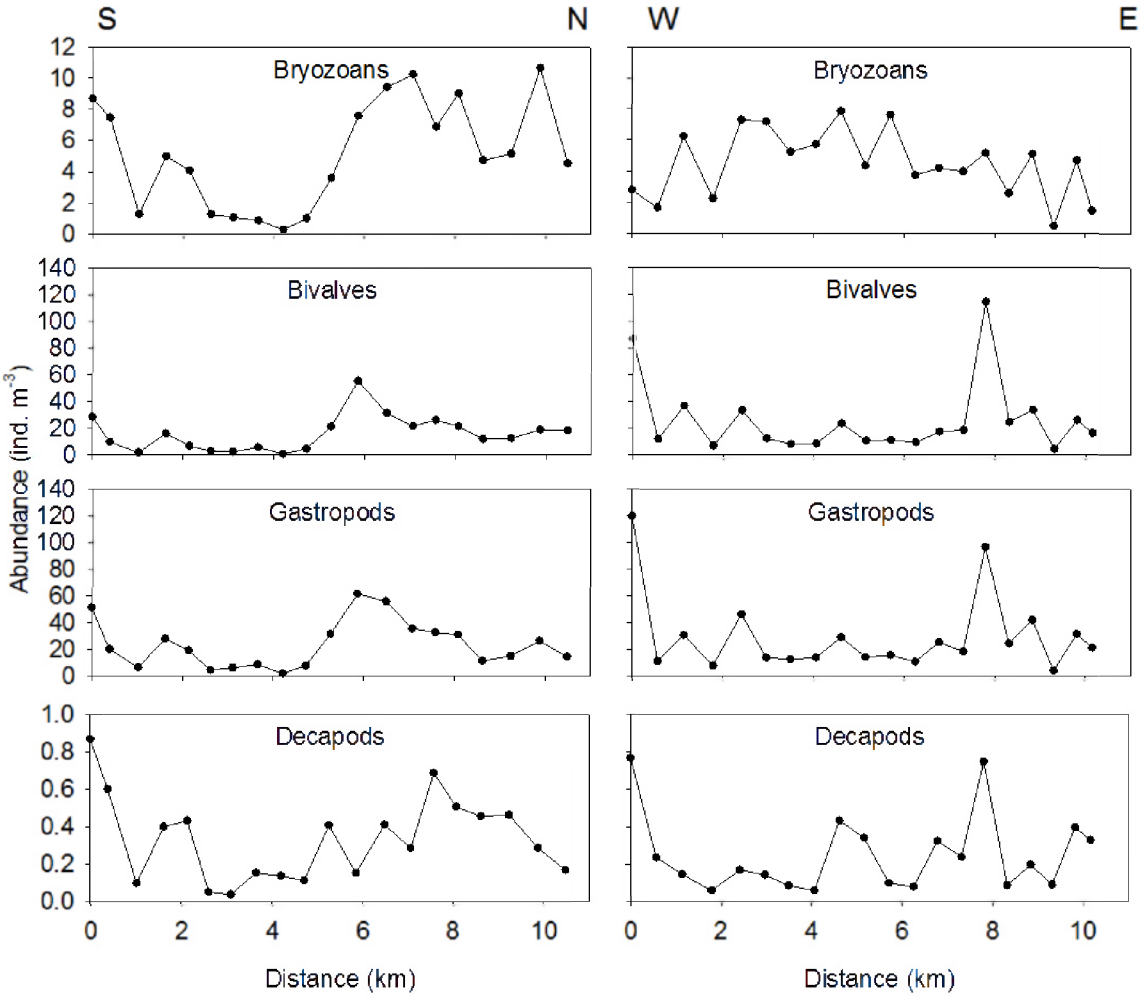

Figure 4.2: Larval abundance from North to South and West to East transects in St. George's Bay, Nova Scotia, Canada, which were sampled continuously (one sample every ~ 500 m for 5 minutes) at 3 m depth with a 200-µm plankton ring net (0.75 m diameter).

Figure 4.3: Larval abundance from North to South and West to East transects in St. George's Bay, Nova Scotia, Canada, which were sampled continuously (one sample every ~ 500 m for 5 minutes) at 3 m depth with a 200-µm plankton ring net (0.75 m diameter).

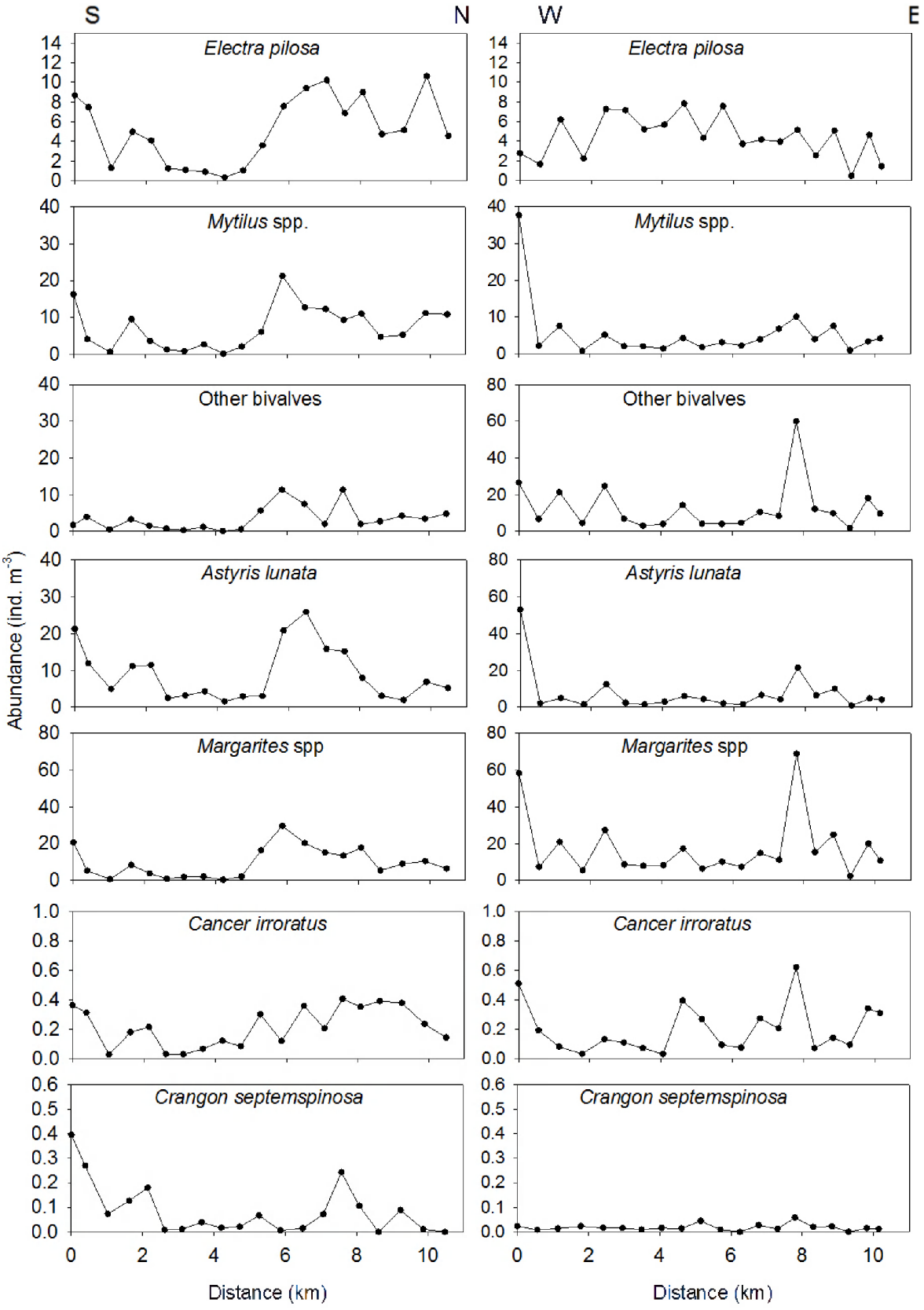
S
N
W
E
Electra pilosa
Mytilus spp.
Other bivalves
Astyris lunata
Margarites spp
Cancer irroratus
Crangon septemspinosa
Abundance (ind. m-3)
Distance (km)

km was less pronounced for *Mytilus* sp. and *A. lunata*, and there are no large peaks in the distribution of *Crangon septemspinosa* (Figure 4.3).

The abundances of bivalves and gastropods were highly correlated with one another, while the correlation between the abundance of bryozoans and decapods was much weaker (Table 4.2). Intermediate correlation coefficients were obtained for the remaining pairs of taxonomic groups (Table 4.2). The abundances of bivalves and gastropods were also highly correlated at the species level, except for *A. lunata* (Table 4.3). Additionally, the abundance of *C. irroratus* was significantly correlated with that of all other species whereas that of *C. septemspinosa* was only correlated with *E. pilosa* and *A. lunata.* In general, there were more correlations between the physical variables and the abundance of bryozoans, gastropods and bivalves than for decapods (Table 4.4). Interestingly, all species were negatively correlated with fluorescence (in most cases significantly) and positively correlated with salinity (not always significantly) except *C. septemspinosa,* which was significantly negatively correlated with the depth of the fluorescence maximum. Bryozoan and bivalve abundance was significantly correlated with both fluorescence and salinity. Overall, fluorescence and salinity had the highest number of significant correlations with the abundance of all groups and species (Table 4.4).

When large scale spatial gradients were removed from the abundances of larvae and from the physical variables through spatial regression, the patterns were similar, but the relationship with fluorescence was stronger (Table 4.5). The abundance of *E. pilosa* and *A. lunata* was significantly correlated with fluorescence, and that for all other species abundance was also significantly negatively correlated with fluorescence except 'other

Table 4.2: Pearson correlation examining the relationship in abundance for pairs of taxa: bryozoans (Bz), bivalves (Bv), gastropods (Gp) and decapods (Dp). Relationships were assessed for both the logarithm (base 10) of the abundances and the physical variables (A) and the residuals of the abundances and residuals of the physical variables from the large scale spatial regression (B). The upper half of the matrix indicates the correlation coefficients for $\log_{10}(x+1)$ where x is larval abundance, lower half indicates the p-value. Statistically significant correlations are indicated in bold.

A)	**Bz**	**Bv**	**Gp**	**Dp**
Bz	**1**	**0.646**	**0.684**	**0.429**
Bv	**<0.001**	**1**	**0.943**	**0.567**
Gp	**<0.001**	**<0.001**	**1**	**0.654**
Dp	**0.006**	**<0.001**	**<0.001**	**1**
B)	**Bz**	**Bv**	**Gp**	**Dp**
Bz	**1**	0.231	**0.317**	**0.402**
Bv	0.151	**1**	**0.929**	**0.556**
Gp	**0.046**	**<0.001**	**1**	**0.649**
Dp	**0.010**	**<0.001**	**<0.001**	**1**

Table 4.3: Pearson correlation examining the relationship in abundance for pairs of species: *Electra pilosa* (Bz1), *Mytilus* spp. (Bv1), Other bivalves (Bv2), *Astyris lunata* (Gp1), *Margarites* spp. (Gp2), *Cancer irroratus* (Dp1), *Crangon septemspinosa* (Dp2). Relationships were assessed for both the logarithm (base 10) of the abundances and the physical variables (A) and the residuals of the abundances and residuals of the physical variables from the large scale spatial regression (B). The upper half of the matrix indicates the correlation coefficients for $\log_{10}(x+1)$ where x is larval abundance, lower half indicates the p-value. Statistically significant correlations are indicated in bold.

A)	Bz1	Bv1	Bv2	Gp1	Gp2	Dp1	Dp2
Bz1	**1**	**0.631**	**0.419**	**0.491**	**0.668**	**0.405**	0.302
Bv1	**<0.001**	**1**	**0.506**	**0.811**	**0.779**	**0.602**	0.279
Bv2	**0.007**	**0.001**	**1**	**0.435**	**0.853**	**0.480**	-0.142
Gp1	**0.001**	**<0.001**	**0.005**	**1**	**0.636**	**0.557**	**0.432**
Gp2	**<0.001**	**<0.001**	**<0.001**	**<0.001**	**1**	**0.592**	0.073
Dp1	**0.009**	**<0.001**	**0.002**	**<0.001**	**<0.001**	**1**	**0.365**
Dp2	0.058	0.081	0.381	**0.005**	0.655	**0.021**	**1**
B)	Bz1	Bv1	Bv2	Gp1	Gp2	Dp1	Dp2
Bz1	**1**	0.300	0.105	0.240	0.257	**0.359**	**0.391**
Bv1	0.060	**1**	**0.341**	**0.905**	**0.692**	**0.479**	0.311
Bv2	0.519	**0.031**	**1**	**0.445**	**0.881**	**0.523**	-0.084
Gp1	0.135	**<0.001**	**0.004**	**1**	**0.731**	**0.480**	**0.372**
Gp2	0.109	**<0.001**	**<0.001**	**<0.001**	**1**	**0.609**	0.065
Dp1	**0.023**	**0.002**	**0.001**	**0.002**	**<0.001**	**1**	**0.315**
Dp2	**0.013**	0.051	0.607	**0.018**	0.688	**0.048**	**1**

Table 4.4: Pearson correlation coefficients examining the relationship among physical variables of the water column and abundance of A) taxonomic groups [bryozoans (Bz), bivalves (Bv), gastropods (Gp) and decapods (Dp)] and B) species [Electra pilosa (Bz1), Mytilus spp. (Bv1), Other bivalves (Bv2), Astyris lunata (Gp1), Margarites spp. (Gp2), Cancer irroratus (Dp1), Crangon septemspinosa (Dp2)] from 15 Aug 2009 for sampling depths of 3 m (n = 20). Relationships were assessed for the logarithm (base 10) of the abundances and the physical variables. The value in brackets indicates the p-value. Statistically significant correlations are indicated in bold.

	Physical variables and logarithm (base 10) of abundance				
A)	**Temperature**	**Salinity**	**Fluorescence**	**Fluo. Max.**	**Mixed Layer**
Bz	-0.267	**0.637**	**-0.662**	0.096	**-0.445**
	(0.255)	**(0.003)**	**(0.001)**	(0.687)	**(0.049)**
Bv	-0.194	**0.479**	**-0.593**	0.237	-0.281
	(0.412)	**(0.033)**	**(0.006)**	(0.313)	(0.229)
Gp	-0.053	0.381	-0.431	0.125	-0.120
	(0.823)	(0.097)	(0.058)	(0.599)	(0.615)
Dp	0.160	0.274	-0.414	-0.267	-0.076
	(0.501)	(0.243)	(0.069)	(0.256)	(0.749)
B)	**Temperature**	**Salinity**	**Fluorescence**	**Fluo. Max.**	**Mixed Layer**
Bz1	-0.266	**0.637**	**-0.662**	0.095	-0.444
	(0.257)	**(0.003)**	**(0.001)**	(0.689)	(0.050)
Bv1	-0.224	**0.508**	**-0.600**	0.186	-0.310
	(0.343)	**(0.022)**	**(0.005)**	(0.432)	(0.184)
Bv2	-0.300	**0.491**	**-0.532**	0.235	-0.300
	(0.199)	**(0.028)**	**(0.016)**	(0.319)	(0.199)
Gp1	0.110	0.557	-0.223	-0.041	0.098
	(0.646)	(0.274)	(0.345)	(0.864)	(0.680)
Gp2	-0.119	0.427	**-0.573**	0.268	-0.245
	(0.618)	(0.060)	**(0.008)**	(0.254)	(0.297)
Dp1	-0.056	**0.461**	**-0.651**	0.032	-0.352
	(0.814)	**(0.041)**	**(0.002)**	(0.893)	(0.128)
Dp2	0.429	-0.093	0.022	**-0.615**	0.318
	(0.059)	(0.695)	(0.928)	**(0.004)**	(0.172)

Table 4.5: Pearson correlation coefficients examining the relationship among physical variables of the water column and abundance of A) taxonomic groups [bryozoans (Bz), bivalves (Bv), gastropods (Gp) and decapods (Dp)] and B) species [Electra pilosa (Bz1), Mytilus spp. (Bv1), Other bivalves (Bv2), Astyris lunata (Gp1), Margarites spp. (Gp2), Cancer irroratus (Dp1), Crangon septemspinosa (Dp2)] from 15 Aug 2009 for sampling depths of 3 m (n = 20). Relationships were assessed for the residuals of the abundances and residuals of the physical variables from the large scale spatial regression. The value in brackets indicates the p-value. Statistically significant correlations are indicated in bold.

	Residuals of physical variables and residuals of abundance				
A)	**Temperature**	**Salinity**	**Fluorescence**	**Fluo. Max.**	**Mixed Layer**
Bz	-0.151	**0.601**	**-0.708**	-0.139	-0.331
	(0.525)	**(0.005)**	**(0.001)**	(0.560)	(0.154)
Bv	0.254	0.273	**-0.510**	0.202	0.010
	(0.279)	(0.224)	**(0.022)**	(0.392)	(0.968)
Gp	0.209	0.360	**-0.581**	0.110	-0.030
	(0.377)	(0.119)	**(0.007)**	(0.645)	(0.900)
Dp	-0.243	0.331	**-0.645**	-0.270	-0.235
	(0.302)	(0.155)	**(0.002)**	(0.250)	(0.320)
B)	**Temperature**	**Salinity**	**Fluorescence**	**Fluo. Max.**	**Mixed Layer**
Bz1	-0.151	**0.601**	**-0.708**	-0.140	-0.329
	(0.526)	**(0.005)**	**(0.001)**	(0.555)	(0.157)
Bv1	0.135	0.328	**-0.559**	0.009	-0.071
	(0.570)	(0.159)	**(0.010)**	(0.971)	(0.768)
Bv2	0.101	0.257	-0.430	0.202	0.033
	(0.671)	(0.274)	(0.059)	(0.393)	(0.891)
Gp1	0.203	**0.520**	**-0.705**	-0.009	-0.075
	(0.390)	**(0.019)**	**(0.001)**	(0.970)	(0.755)
Gp2	0.269	0.277	**-0.528**	0.178	0.015
	(0.252)	(0.238)	**(0.017)**	(0.463)	(0.951)
Dp1	-0.192	0.327	**-0.608**	-0.108	-0.302
	(0.416)	(0.160)	**(0.004)**	(0.649)	(0.195)
Dp2	-0.306	0.319	**-0.627**	**-0.488**	-0.090
	(0.189)	(0.171)	**(0.003)**	**(0.029)**	(0.706)

bivalves' (Table 4.5). Lower fluorescence corresponded to a high larval abundance at the local scale (< 10 km).

In the S-N transect, significant positive spatial autocorrelation of larval abundance was observed at the smallest observable scale of 0.5 km for bryozoans, and at 7.2 km for the gastropods and bivalves (Figure 4.4). Significant negative autocorrelation of abundance was observed at 2.5 km for bryozoans, 2.5 and 3.0 km for bivalves and gastropods, and 3.0 and 4.3 km for decapods. In the W-E transect, no statistically significant spatial autocorrelation of larval abundance was observed for any taxonomic group, except gastropods at 9.2 km. Unsurprisingly, a similar pattern is present at the species level (Figure 4.5). In the S-N transect, all species except 'other bivalves' and *C. irroratus* had significant negative spatial autocorrelation between 2.5 and 4.3 km and positive spatial autocorrelation between 6 and 7.2 km.

4.4.2 Distribution of physical variables

In the S-N transect, there was a large increase in salinity (front) at ~6 km, with a corresponding decrease in fluorescence (Figure 4.6). In the W-E transect, the most identifiable feature was the low temperature and salinity combined with high fluorescence, density and depth of fluorescence maximum at 0 km, which was closest to shore. Significant positive spatial autocorrelation was observed in temperature, density and fluorescence at the smallest observable scale of 0.4 km on both transects, and in the depth of the fluorescence maxima and mixed layer in the S-N transect (Figure 4.7). Additionally, in the S-N transect, 3 out of 6 of the variables were significantly negatively autocorrelated at 3.2, 3.9 and 5.5 km. In the W-E transect, more than one of the physical variables were significantly negatively autocorrelated at 3.2, 5.3 and 6.3 km. Salinity was

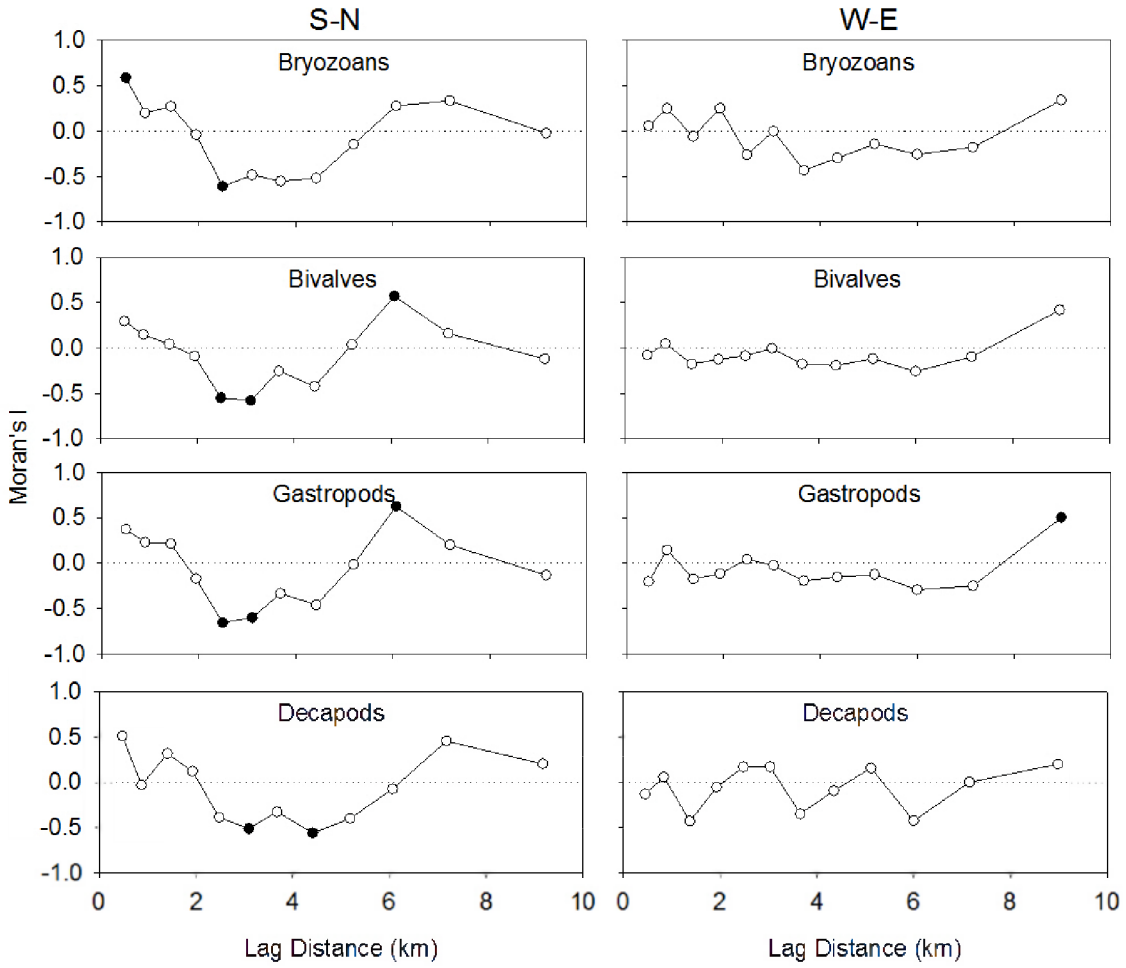

Figure 4.4: Spatial analysis of the abundance for each of 4 larval groups (*Electra pilosa*, *Mytilus* spp., Other bivalves, *Astyris lunata*, *Margarites* spp., *Cancer irroratus*, *Crangon septemspinosa*) using Moran's I. Positive and negative values of Moran's I indicate positive and negative spatial autocorrelation, respectively. Filled circles indicate significant spatial autocorrelation at that scale..

Figure 4.5: Spatial analysis of the abundance for each of 7 larval species (gastropods, bivalves, bryozoans, and decapods) using Moran's I. Positive and negative values of Moran's I indicate positive and negative spatial autocorrelation, respectively. Filled circles indicate significant spatial autocorrelation at that scale.

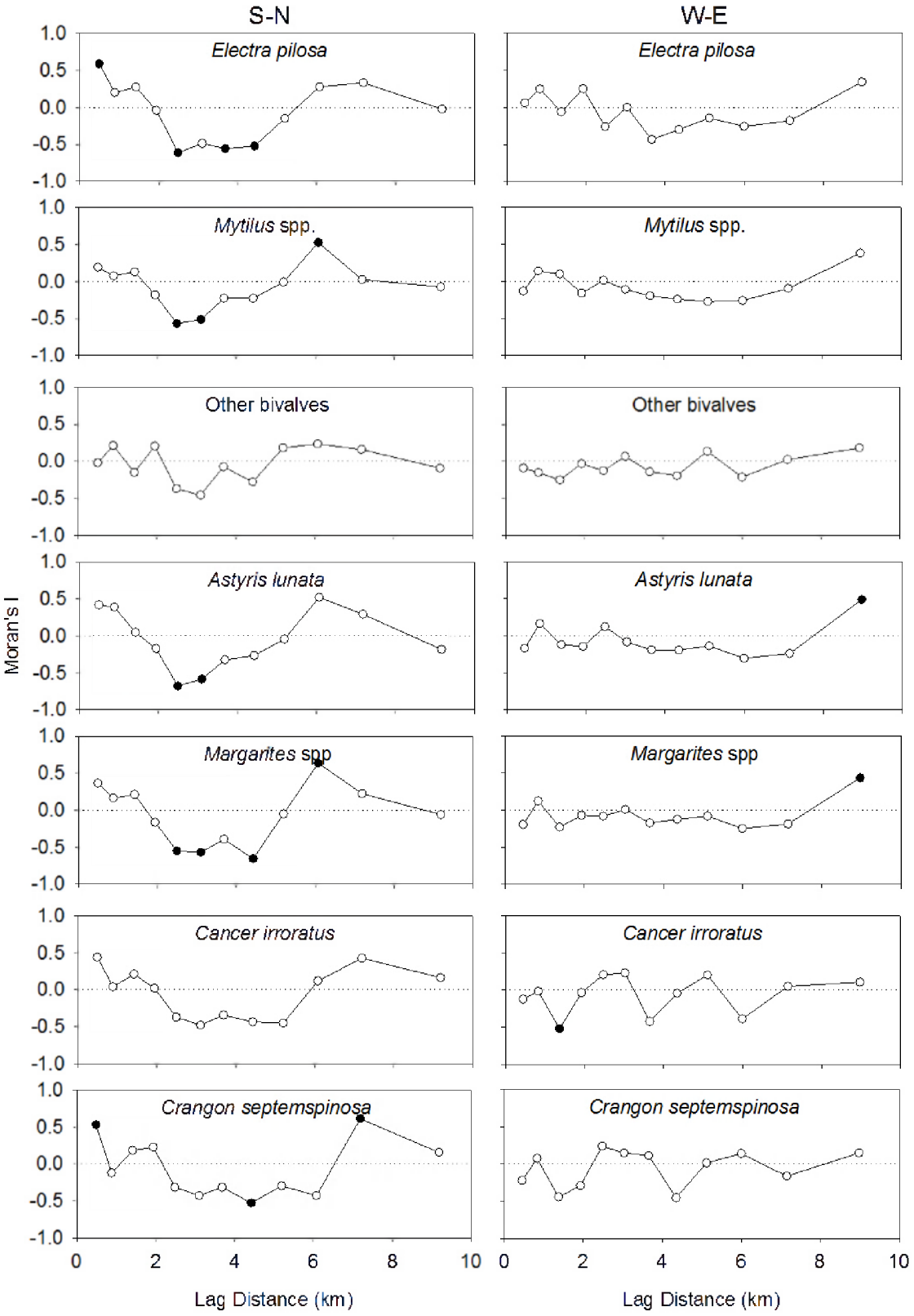
S-N
W-E
Electra pilosa
Mytilus spp.
Other bivalves
Astyris lunata
Margarites spp
Cancer irroratus
Crangon septemspinosa
Moran's I
1.0
0.5
0.0
-0.5
-1.0
0
2
4
6
8
10
Lag Distance (km)

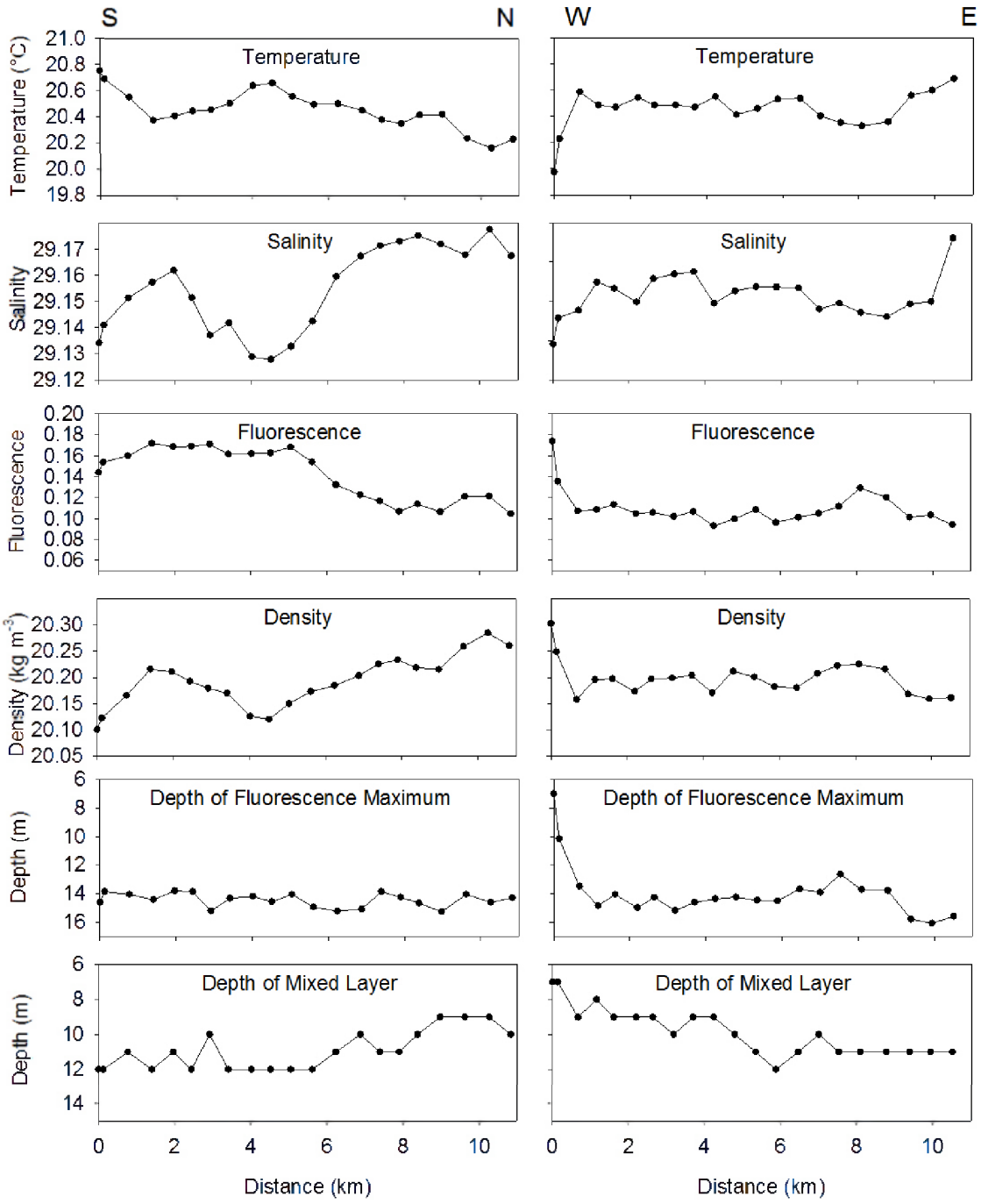

Figure 4.6: Physical variables in the water column of North to South and East to West transects in St. George's Bay, Nova Scotia, Canada which were sampled once every ~ 500 m. Data represents the average for the water column from 1-5 m depth.

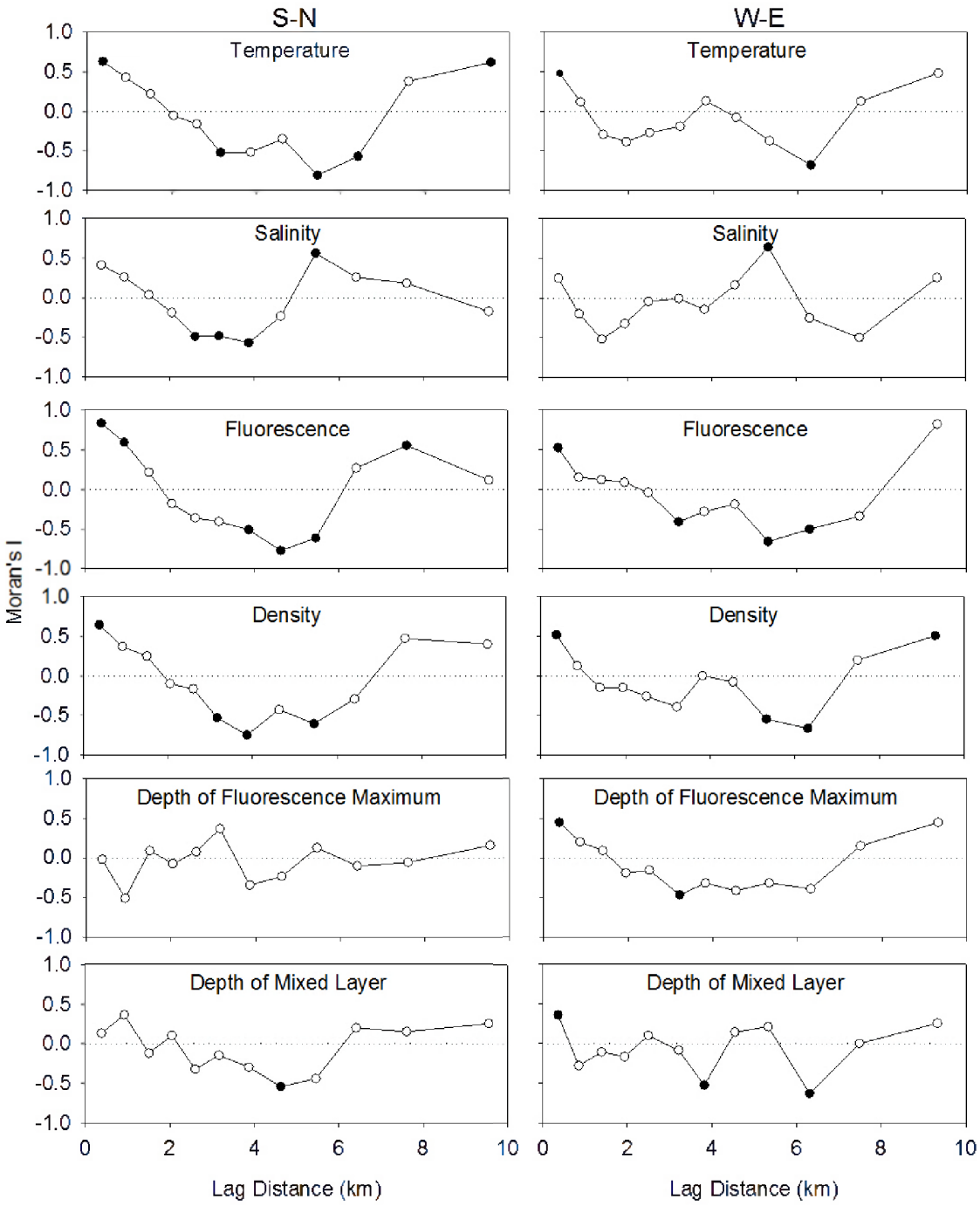

Figure 4.7: Spatial analyses of the physical variables using Moran's I. Positive and negative values of Moran's I indicate positive and negative spatial autocorrelation, respectively. Filled circles indicate significant spatial autocorrelation at that scale.

significantly positively autocorrelated at 5.5 km in the S-N transect, and at 5.3 km in the W-E transect.

The cross-correlation in current velocity among the ADCP moorings was just under 0.6 for moorings separated by 3-4 km, and 0.2-0.3 for moorings separated by 5-6 km. Only at tidal periods was coherence squared greater than the significance threshold of 0.3 (just below 0.6 for neighbouring moorings). The current velocity data showed significant temporal autocorrelation at most time lags because of the large sample size (Figure 4.8). An important difference in the pattern of autocorrelation between directions is that the peak at 8.5 h is positive in the S-N direction; therefore, the first negative peak in autocorrelation is at 33 h in the S-N direction and 8.5 h in the W-E direction. After being converted to distance by multiplying by the mean speed, these time lags correspond to 3.9 and 0.7 km, in the S-N and W-E direction, respectively. Spectral analysis (Daigle, unpublished data) also indicated that the dominant peak in the periodogram for the S-N transect is at a lower frequency than in W-E transect. This suggests that the oscillations along the S-N transect occur over a longer time period, translating into larger spatial scales, than in the W-E direction.

4.4.3 Biophysical interactions

The dispersion of sites classified by their physical variables in the rotated nMDS plots was relatively parallel to NMDS1 for bryozoans, bivalves and gastropods compared to NMDS1 for the decapods (Figure 4.9). The loadings for the physical variables were oriented perpendicular to the gradient of larval abundance for the decapods. For the other taxonomic groups, the loadings of the physical variables varied in parallel to the larval

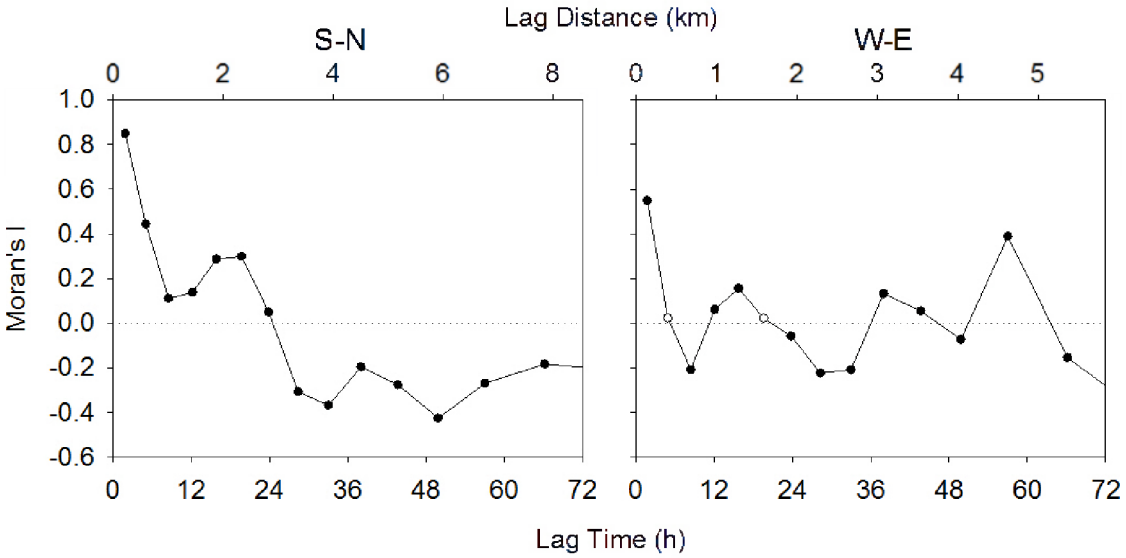

Figure 4.8: Temporal analyses of horizontal current velocities using Moran's I. Positive values of Moran's I indicate positive spatial autocorrelation and vice versa. Filled circles indicate significant spatial autocorrelation at that scale. Equivalent lag distances were calculated by multiplying the time lag by the mean speed (see Methods).

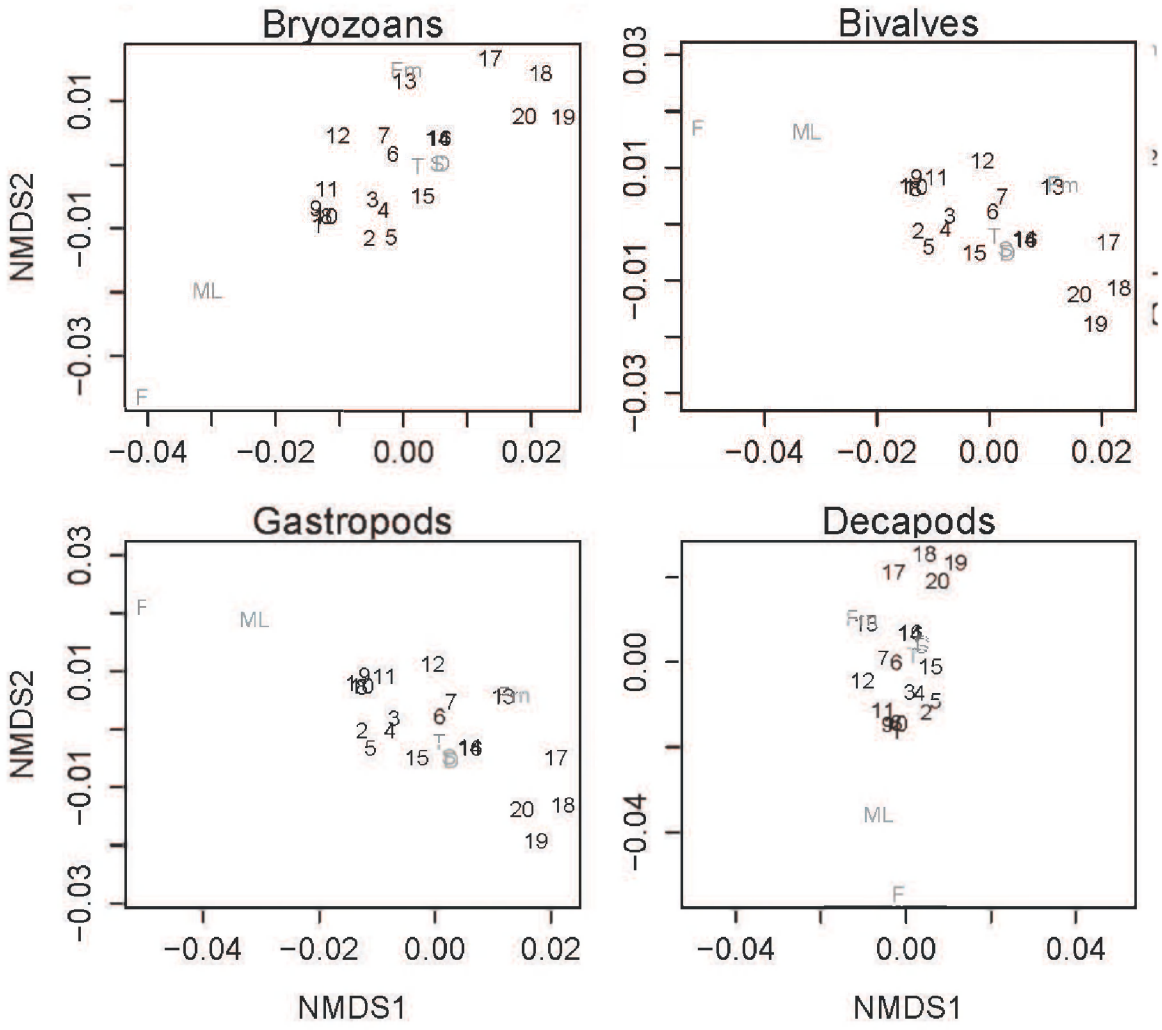

Figure 4.9: Ordination from nonmetric multidimensional scaling of the sampling sites based on physical variables. The ordinations were rotated so that NMDS1 is parallel to an external variable (abundances of bryozoans, bivalves, gastropods and decapods). Larval abundance increases from left to right. Numbers indicate the location of the site in nMDS ordination space and the letters represent the physical variables of the water column [temperature (T), salinity (S), fluorescence (F), density (D), depth of the fluorescence maximum (Fm) and depth of the mixed layer (ML)]. The letter's distance from the origin represents the weight of that factor in the ordination space and the values for the physical variables increase from the origin to the letters indicating that variable.. Stress=0.0486

gradient. Fluorescence and the depth of the mixed layer had the largest influence on the separation of the sites indicated by their letter symbols being furthest from the origin.

4.5 Discussion

The distributions of gastropods and bivalves were most similar to one another, and those of bryozoans and decapods were most different from one another. Gastropods and bivalves are similar morphologically (*i.e.* calcareous shells), have similar swimming ability, and both groups display vertical migration (Chia et al. 1984; Lloyd et al. 2012a). These biological similarities are the likely cause of similarity in distributions. If different types of larvae behave similarly or have similar early life history strategies, then they will likely aggregate in the same types of oceanographic features (Pineda 1991; Folt and Burns 1999; Shanks et al. 2000). Conversely, contrasting life strategies result in very different dispersal properties, and consequently, different larval distributions. Bryozoans are among the slowest swimmers (Ryland 1977; Chia et al. 1984), and decapods are among the fastest of the invertebrate larvae (Young 1995; Shanks 1995). Additionally, while bryozoans in St. George's bay display no vertical migration, decapods show evidence of both diel and tidal vertical migration both at my study site and elsewhere (Tamaki et al. 2010; Lloyd et al. 2012a). The weak correlation between the abundance of bryozoans and decapods is consistent with the hypothesis that swimming ability can affect horizontal distribution on the scale of kilometers. It is well established that larval behaviour can be species- and even stage-specific, which can lead to differences in patterns of horizontal distribution (DiBacco et al. 2001; Tapia and Pineda 2007; Lloyd et al. 2012a). In this study, species specific behaviour may be observed in *C. septemspinosa*.

However, the similarity in larval distribution among most species in my study is suggestive of common mechanisms of pattern formation.

The consistent relationship between bryozoan abundance and salinity suggests that bryozoans were being advected like a passive tracer such as salinity. I found that the abundance of bryozoans was negatively correlated with fluorescence although others have found that the peak in the vertical bryozoan abundance was associated with the fluorescence maximum (Lloyd et al. 2012a). Similarly, for all species, lower fluorescence corresponded to a high larval abundance at the local scale (< 10 km). Given the relatively small horizontal differences in fluorescence compared to vertical ones, the association with lower fluorescence likely reflects an association with a particular water mass with low fluorescence rather than with food availability. Additionally, I found that the abundance of bryozoans, gastropods and bivalves had a stronger relationship than the decapods with the physical variables in multivariate space. While the abundance of *C. irroratus* had generally weaker relationship with physical variables than that of bryozoan, bivalve and gastropod species, the pattern differed for *C. septemspinosa*. The negative relationship between the abundance of *C. septemspinosa* and the depth of the fluorescence maximum combined with the relatively weak relationship with the other physical variables, suggests that: either 1) larvae aggregated in areas where the fluorescence maximum is relatively shallower (*i.e.* available to them during the deep phase of their vertical migration); or 2) larval mortality was lower in these regions. However, the horizontal distribution for this species suggests that the larvae are largely retained in the southern portion of the bay.

For both the larvae (all groups, most species) and all the physical properties of the water column, except the fluorescence maximum, there was significant negative autocorrelation at distance lags between 2.5 and 5 km in the S-N direction. The first peak in negative autocorrelation of current velocity at time lags of 28.3 or 33 h corresponded to spatial lags of 3.3 to 3.9 km. While the peaks in autocorrelation of current velocity didn't quite correspond with the M2 tidal cycle period (12.42 h), the offset in periodicity likely reflects an interaction between the tidal cycle and the diel cycle (24 h) of wind driven circulation. In the W-E direction, the first peak (at 8.5 h) in negative autocorrelation of the ADCP current velocities was as large as all other peaks. This indicates that the data were dominated by the signal that corresponds to that peak. Since this peak corresponds to a distance lag of 1 km, any spatial autocorrelation along the W-E transect would not have been properly resolved by the larval sampling at a frequency of 500 m. The method used to convert temporal to spatial autocorrelation in current velocity (multiplying the time lag with the mean speed), has similar assumptions to a progressive vector method which converts Eulerian observations into Lagrangian data. In both cases, it is assumed that the current is spatially uniform and only varies in time. This method is justified since there was stronger autocorrelation in the current velocities among the ADCPs that were closer together (3-4 km), indicating some spatial uniformity of current velocities at this scale.

I suggest that the scale of cyclical periodicity of coherent structures in current velocity (*i.e.* tidal period in this case) affects not only the physical properties of the water column, but also larval distributions. This effect of cyclical periodicity in current velocities should be particularly noticeable in the autocorrelation patterns of the poor

swimmers, since their distribution is most related to the physical properties of the water column. Indeed, the peak in negative autocorrelation is lower for bryozoans than for decapods. The difference in patterns between the 2 transects suggests that the scale of cyclical periodicity in current velocities may play a directionally dependent role in the scaling of larval patchiness. Consequently, to properly resolve larval patchiness, biophysical models used to predict larval dispersal should at the very least resolve to the scale of the tidal excursion or the scale of the wind driven circulation, whichever is smallest.

While it is well known that the distribution of larvae can be affected by salinity, temperature, density or food availability (Tremblay and Sinclair 1990; Gallager et al. 1996; Daigle and Metaxas 2011), the magnitude of the observed variance in these variables in my study is biologically irrelevant. For example, a change in temperature of 0.075 °C over a 500-m distance (which was the average thermal gradient) should not elicit a larval behavioural response. Such a gradient also should not have any direct consequences for growth or mortality. It is also possible that the larval patches are the result of predator-prey diffusive instabilities, where predator and prey disperse at different rates (possibly due to swimming ability) and the resulting predator-prey interactions can cause spatial heterogeneity in larval abundance (Steele 1976). In this case, larvae could be either the predator or the prey. However, diffusive instabilities are thought to occur at larger scales (10 - 100 km), and those instabilities do not explain the relationships among physical variables of the water column and the larval distributions.

I propose that the observed relationships between the abundance of larval groups and physical variables are the result of the non-uniform mixing of water masses. Given

the weak mean currents (~0.02 m s^{-1}) it is clear that the residence time for larvae in St. George's Bay can be quite long, in the order of days to tens of days, O(40 km / 0.02 m s^{-1} ≈ 20 days), a result supported by results from a numerical simulation (B. deYoung, unpublished data). This residence time is very similar to the estimate of 15 d based on current meter observations in 1974-1975 (Petrie and Drinkwater, 1978). The relatively low cross-correlation in velocity among moorings suggests that large scale, coherent flow features in St. George's Bay are relatively weak. The persistent tide (M_2 tide is dominant, with a period of 12.42 hours) and the weak mean circulation generate an ideal dispersive environment. The long residence time and the weak spatial coherence in the velocity field at long periods and large spatial scales, combined with the regular tidal dispersion, twice daily at short spatial scales (km's) will lead to significant dispersion in larval patterns (Okubo and Levin 2002). By definition, flow structures with low coherence act to enhance mixing within a water-mass and coherent flow structures act to transport a water mass. I argue that the significant spatial coherence in the tidal period reduced advective diffusion at that scale, and the low coherence at smaller scales enhances advective diffusion; spatial structures at those smaller scales will be erased while structure at the scale of the tidal period will be preserved.

My observations provide a snapshot of the conditions in the bay on that particular day, since sampling was conducted over a single 12-h period, and may not be representative of average conditions. However, observations from 3 different sampling periods also suggested that distributions of gastropods and bivalves were most similar to, and those of bryozoans and decapods were most different from one another (Daigle and Metaxas, Chapter 5). Additionally, the negative relationship between fluorescence and

larval abundance was remarkably consistent across taxa. I contend that the most parsimonious explanation for the similarity in scales of the spatial coherence in the tidal period, the larval distributions and the physical variables is that they are related due to the reduced advective diffusion at that scale and/or the advective-diffusive history of the water masses. In either case, the scale of the coherent structure (tides) is important in determining the patterns in larval distribution. Furthermore, I suggest that the scale of coherent structure in current velocities may be important in forming larval distribution patterns in other systems, which similarly to ours are not dominated by strong oceanographic features (e.g. estuarine plumes, upwelling events, or markedly different water masses).

The effects of the spatial distribution of the adult habitat and the influence of large scale hydrographic conditions (i.e. estuarine plume, eddies) on larval distributions (Mackas 1984; Shanks et al. 2002; Vázquez et al. 2007) or small scale aggregating processes (Pineda 1991; Shanks et al. 2000) have been identified previously. However, these effects influence larval distributions at very large scales (> 100 km), in locations with very different water masses, or at scales below the resolution of my study. My study shows that small scale larval patchiness (< 10 km) can exist even in areas of relatively homogenous physical properties. It is well established that the distribution of phytoplankton and holoplankton are affected by a variety of processes with multiple and overlapping scales (Steele 1976; Okubo 1977; Martin 2003), but the relative importance of all these processes on meroplankton is poorly known at present (Pineda 1991; Manuel and O'Dor 1997; Fuchs et al. 2007). These studies have shown that larvae are not passive particles randomly drifting in the ocean. Their active interactions with the water column

can affect their horizontal distribution at multiple scales from small-scale aggregations at fronts, to medium scale patches such as those observed, to large scale oceanographic features (DiBacco et al. 2001; Levin 2006; Cowen and Sponaugle 2009); ultimately these larval behaviours affect larval dispersal.

Unlike holoplankton, the larvae of benthic invertebrates settle on the seafloor before taking their adult form, and the patchiness of larval distributions can affect the distributions of adults (Grosberg and Levitan 1992; Hughes et al. 2000; Fuchs et al. 2007). This effect can result from direct settlement of "patches", but also indirectly by affecting larval dispersal through aggregations at fronts, advection along with water masses or vertical migration. I have shown that larval groups with similar life strategies (*e.g.* swimming ability) can have similar distributions. I have also shown that the weaker swimming larvae have a demonstrably tighter relationship with the physical properties of the water column, suggesting that they have dispersal properties similar to that of a passive tracer. Therefore, incorporating larval behaviour in biophysical models of larval transport would be more important in larvae with strong swimming abilities, whereas it may not be as important for weak swimmers. Additionally, I have shown that the scale of larval patchiness corresponds with that of both the physical variables of the water column and the tidal/diel periodicity in the current velocities. Factors such as larval swimming ability and the scale of coherent structures (*e.g.* tidal period), which determine larval distribution and patch size, will affect larval dispersal and ultimately the recruitment of benthic adults.

CHAPTER 5: BAY-SCALE PATTERNS IN THE DISTRIBUTION, AGGREGATION AND SPATIAL VARIABILITY OF LARVAE OF BENTHIC INVERTEBRATES[4]

5.1 Abstract

This study aimed to investigate mechanisms of pattern formation in the larval distributions of benthic invertebrates by relating the spatial and temporal variability in the larval distributions to that in physical and biological variables, such as temperature, salinity, fluorescence and current velocity. Larvae were sampled at 11 sites on 7-8, and 11-12 Aug 2008 and at 16 sites on Aug 2-4, 2009, with a 200-μm plankton ring net (0.75-m diameter) towed for 5 min at each of 3 m and 12 m depth in St. George's Bay, Nova Scotia, Canada. Density, temperature, salinity, and fluorescence were measured with a CTD cast at each station, and currents were quantified with an ADCP moored at 5 locations throughout the bay in 2009. Gastropod, bivalve and, to a lesser extent, bryozoan larvae had very similar spatial distributions, but the distribution of decapod larvae followed a different pattern. These findings suggest that taxonomic groups that have functionally (*i.e.* swimming ability) similar larvae (*e.g.* bivalves and gastropods) also show similar dispersion properties (distribution and spatial variability), while the opposite is true for groups with functionally dissimilar larvae (*e.g.* bivalves and decapods). I also found that larval distributions of all taxa were significantly aggregated, although the degree of aggregation varied among taxa. Using an aggregation-diffusion

---

[4] Daigle, R. M., and A. Metaxas. Submitted to Marine Ecology Progress Series in May, 2013.
My coauthor Dr. Anna Metaxas supervised the study design and analyses, and edited the manuscript.

model, I demonstrated that horizontal swimming was not an effective means of forming aggregations even at modest levels of diffusion. I propose that events occurring after the gamete/larval release determined the observed horizontal patterns. I also suggest that dispersal by currents may have a smaller effect on these distributions than mortality due to predation and food availability. I hypothesize that the influences of mortality due to predators, food availability, or directly related to adult distributions (larval source) on these aggregations likely are minimal.

5.2 Introduction

Larval dispersal is a key factor regulating the persistence of populations of marine benthic invertebrates and population dynamics of adults (Levin, 2006; Cowen and Sponaugle, 2009). Adult populations can be affected by spatio-temporal variations in the supply of settling larvae (Gaines and Roughgarden 1985; Underwood and Fairweather 1989b). In turn, larval supply of settling larvae depends on a host of factors such as reproductive output, larval transport, larval behaviour, rates of mortality, and settlement behaviours in response to various cues (Rumrill 1990; Grosberg and Levitan 1992; Shanks and Brink 2005; Fuchs et al. 2007; DiBacco et al. 2011). Since adult biogeography affects larval distributions, water masses with markedly different temperature and/or salinity are often associated with larvae of different species assemblages (Jillett 1976; Shanks et al. 2002). This interdependence of life stages is the mechanism that connects disjunct populations both demographically and genetically (Levin, 2006; Cowen and Sponaugle, 2009).

It is well established that the vertical distribution of larvae will affect their dispersal distance and direction (North et al. 2008; Tapia et al. 2010; Lloyd et al. 2012a;

b). Larvae can alter their vertical distribution by sinking, floating or swimming in response to cues such as light, tidal cycle, temperature, salinity, and food availability (Tremblay and Sinclair 1990; Kingsford et al. 2002; Sameoto and Metaxas 2008b; Daigle and Metaxas 2011). Larvae that occupy different layers of the water column are exposed to different current patterns and have different resulting dispersal trajectories.

Different mechanisms for cross shelf larval migration have been documented, such as tidal stream transport (DiBacco et al. 2001; Forward Jr et al. 2003), and the upwelling-relaxation paradigm (Wing et al. 1995; Miller and Emlet 1997). In selective tidal stream transport, larvae exploit the vertical shear in current velocity by vertically migrating over a tidal cycle. For example, larvae that are in the surface layer during flood tide and migrate to the bottom layer (with lower current velocities) during ebb tide will experience net transport towards the mouth of an estuary. Along the western margins of continents where major upwelling occurs, larvae can exploit cross shelf currents to disperse offshore during upwelling periods and return to a coastal habitat to settle during a period of relaxation. There are also mechanisms that occur at smaller scales and can affect larval transport and aggregation, such as internal tidal bores (Pineda 1991), or frontal systems and Langmuir cells (Omori and Hamner 1982). These mechanisms operate by aggregating larvae in up- or downwelling areas since larvae can float, sink or swim in response to vertical current velocities. However, all these behaviours appear to be species- or developmental stage- specific and can also vary among populations (Forward Jr et al. 2003; Shanks and Brink 2005; Tapia et al. 2010).

Horizontal swimming is not generally considered an important factor regulating larval transport or patch formation since invertebrate larvae are relatively poor swimmers

(Chia et al. 1984). However, it is feasible that orientated swimming may assist shoreward transport for the stronger swimmers, such as crab megalopae (Shanks 1995). Despite their poor swimming ability, larval aggregations, or patches, do occur on horizontal scales (Olson and Olson 1989; Folt and Burns 1999). These patches can form because of spatially heterogeneous mortality due to predation, lack of food availability, or other environmental variables, such as low salinity or extreme temperatures (Rumrill 1990). Patches can also form due to the interaction between vertical swimming and physical features of the water column (internal tidal bores, vertical currents, etc).

By comparing patterns of larval distribution and the physical properties of the water column (temperature, salinity, fluorescence, current velocities), I can identify potentially important larval transport mechanisms. I conducted this study in a bay with no strong oceanographic features (e.g. estuarine plumes, upwelling events, or markedly different water masses) to identify mechanisms that affect larval dispersal that are not dependent on these strong features. Such mechanisms have the potential to be more broadly applicable, in coastal embayments throughout the world. I have also constructed an aggregation-diffusion model to explore the potential role of horizontal swimming in the formation of larval aggregations.

5.3 Methods

5.3.1 Field sampling

The study site was located at St. George's Bay, Nova Scotia, Canada (Figure 5.1), a bay without strong oceanographic features and with a flushing time on the order of a month (Petrie and Drinkwater 1978). The depth at the sampling locations ranged from

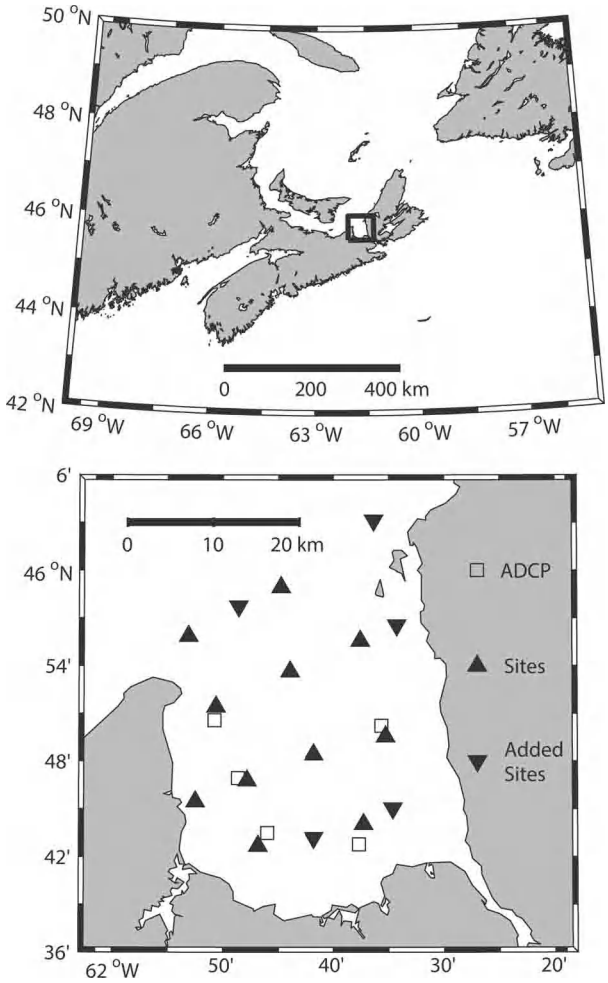

Figure 5.1: Regional map showing the location of study site and bay-scale map showing the location of the ADCP moorings deployed in Jul/Aug 2009 (open squares), as well as the larval sampling locations for 2008 and 2009. In 2008, larvae were collected from 11 sites (triangles), while 5 additional sites (inverted triangles) were sampled in 2009 for a total of 16 sites.

18 to 36 m. Larval abundance was sampled at 11 sites on 7-8, and 11-12 Aug 2008 and at 16 sites on Aug 2-4, 2009, with a 200-μm plankton ring net (0.75-m diameter) towed for 5 min at each of 3 m and 12 m depth. These depths were designed to sample: 1) the surface mixed layer and 2) the thermocline, at or near the fluorescence maximum. The net was towed at ~1.7 m s^{-1} and the volume of filtered water was quantified using a General Oceanics flow meter. All plankton samples were preserved in 95% ethanol and larvae were identified and enumerated under a Nikon SMZ 1500 as described in Lloyd et al. (2012). Samples were split into subsamples using a Folsom plankton splitter. For n = 8, samples were split to 1/64 of the original volume and all subsamples were processed. Based on those samples, I determined that at least 20 individuals of each species needed to be counted to get an estimate of abundance that was within 5% of the true sample abundance. The remainder of the samples were split to between 1/128 and 1 to ensure that ≥20 individuals of the most abundant species (*Margarites* spp., *Astyris lunata*, *Mytilus* spp., *Electra pilosa*. and *Cancer irroratus*) were counted.

In 2009, temperature, conductivity, pressure and fluorescence were measured with a conductivity-temperature-density (CTD) profiler immediately before and after larval sampling. Data from the two down-casts were averaged into 1-m bins. Since no large site-specific differences were detected (e.g. at 3 m, differences were less than 1.5 °C, 0.4 relative salinity and 0.08 relative fluorescence), data from all sites were averaged over the entire bay (Figure 5.2). No such data are available for 2008 because of a mechanical failure of the CTD. To measure circulation patterns throughout the bay, five 600 kHz Teledyne RDI Workhorse Sentinel Acoustic Doppler Current Profilers (ADCP) were

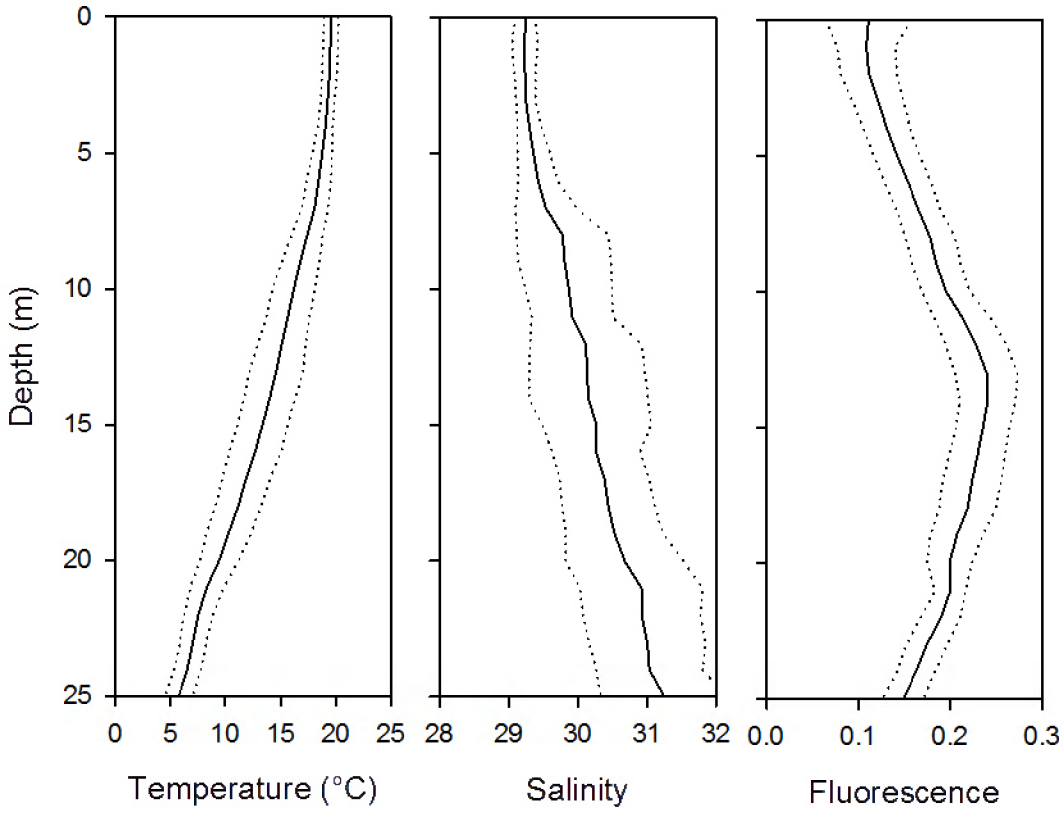

Figure 5.2: Average (± 1 S.D., n = 32) vertical profiles of temperature, salinity and fluorescence in St. George's Bay, Nova Scotia, Canada, from 2-4 Aug 2009.

deployed on the seafloor, sampling the full water column in 1-m depth bins every 20 min from 11 Jul to 22 Aug 2009 (Figure 5.1). The ADCP in the south-east corner of the bay malfunctioned and only recorded data from 11 to 14 Jul 2009. For each profile, I only included the horizontal velocities in the bin centered at 3 m and 12 m in my analyses of mean current velocities.

5.3.2 Data analyses

The logarithm (base 10) of larval abundance (no. m^{-3} for each station by depth combination) was used for all statistical tests because it improved the normality of count data (Zar 1999). For some analyses, species were combined into 4 taxonomic groups (bryozoans, gastropods, bivalves and decapods) to allow taxonomic generalizations of the results. I used 2-way ANOVA to examine the effects of depth (fixed factor; 2 levels) and sampling period (random factor; 3 levels) on the larval abundance of each species, and also of each taxonomic group, using different sites as replicates. In cases where the p-value for the interaction term was ≥ 0.250, I pooled the mean squares and degrees of freedom from the interaction with those of the error term, and used the pooled error term to calculate a new F-statistic for depth (Underwood 1997). I also used a non-metric multidimensional scaling (nMDS) plots to visualize: (1) the similarity in distribution of sites among species for each depth (combined for all sampling periods); and (2) the similarity of species assemblages among sampling sites (combined for all sampling periods). Species with more than 1/3 null abundance were not used in the nMDS analysis.

I examined the relationship among larval abundances of the most abundant species and of the 4 taxonomic groups within a sampling period, as well as among abundances at different sampling periods using Pearson's correlations. The former was

performed on: 1) the entire data set to identify overall patterns (n = 79), and 2) on each of the first 2 sampling periods (7-8 and 10-11 Aug) separately to compare the relative significance of cross-group relationships within a sampling period and among sampling periods, with similar statistical power (n = 22). I also examined the relationship between the physical variables of the water column (temperature, salinity and fluorescence) and larval abundance using Pearson's correlations. I used only the 2 most abundant species from each taxonomic group (except bryozoans for which I used 1 species) for these analyses because the estimates for the less abundant species were highly variable and less accurate. I calculated the index of dispersion (I_D) for each taxonomic group given by:

$$I_D = \frac{\sigma}{\mu} \tag{5.1}$$

where μ is the mean of larval abundance, σ is its variance, and I_D follows a χ^2 distribution with n-1 degrees of freedom (Cox and Lewis 1966). I also calculated a Morisita's index of dispersion (I_M) given by:

$$I_M = \frac{n\sum_i x_i^2 - x_i}{n\bar{x}^2 - n\bar{x}} \tag{5.2}$$

where x_i is the larval abundance at site i, and n is the number of sites. I calculated the statistic:

$$I_M\left(\sum_i x_i - 1\right) + n - \sum_i x_i \tag{5.3}$$

which follows a χ^2 distribution with n-1 degrees of freedom test for departures from randomness (Morisita 1959).

5.3.3 Aggregation-Diffusion Model

An individual-based aggregation-diffusion model was developed to examine the effect of the interaction between diffusion and aggregative horizontal swimming on the larval distribution as detected by a sampling design comparable to the one I used in St. George's Bay. All simulations were initiated with a 40-km 1-dimensional transect with reflective boundaries, representing the width of the bay. The transect was randomly seeded with 3.3×10^4 to 7.78×10^5 individual simulated larvae (SL) to approximate the mean larval densities of 4 taxonomic groups in St-George's Bay (Table 5.1). Aggregative swimming behaviour was simulated by SL swimming towards the nearest "point of attraction". These stationary points in space could represent any hypothetical point to which a larva may swim towards (e.g. food patch, ideal settling location, etc). This simulation was not intended to represent a specific scenario, but it was designed to assess the feasibility of aggregation formation through horizontal swimming. I placed points of attraction every 3 km, to reflect an estimated larval patch size in St. George's Bay (Daigle et al. Chapter 4). The horizontal position (x_t) of each larva at time t after a time interval (Δt) was given by:

$$x_t = x_{t-1} + (u_t + d_t) \times \Delta t \qquad (5.4)$$

where u_t is the larval swimming speed, set to 0.75 mm s^{-1} for bryozoans, 1.35 mm s^{-1} for bivalves, 1.3 mm s^{-1} for gastropods, and 13 mm s^{-1} for decapods reflecting mid-range values from the literature (Ryland 1977; Chia et al. 1984; Young 1995; Shanks 1995). I varied the diffusion index (D) from 0 to 50 m^2 s^{-1}, by adding random movement

Table 5.1: Summary statistics of larval abundance (individuals m-3), during plankton sampling in St. George's Bay, Nova Scotia, Canada, in Aug 2008 at 11 sites, and in Aug 2009 at 16 sites. Proportional species composition for each group is also shown.

A) Basic Statistics

Bryozoans		Bivalves		Gastropods		Decapods	
Mean	14.1		32.5		44.0		2.38
Median	10.8		10.7		20.9		1.27
Minimum	0.01		0.05		0.06		0
Maximum	54.7		436		709		13.1

B) Composition

Species	%	Species	%	Species	%	Species	%
Electra pilosa	99.2	*Mytilus spp.*	61.9	*Margarites spp.*	39.4	*Cancer irroratus*	71.5
Membranipora membranacea	0.8	*Modiolus modiolus*	3.4	*Astyris lunata*	31.5	*Crangon septemspinosa*	24.1
		Anomia simplex	8.0	*Diaphana minuta*	8.2	*Neopanopeus sayi*	0.5
		other	26.7	*Crepidula spp.*	11.6	*Carcinus maenas*	3.9
				Arrhoges occidentalis	1.8		
				Bittiolum alternatum	3.9		
				other	3.6		

(d_t) based on a normal distribution with a null mean and a standard deviation (SD) given by

$$SD = \sqrt{q_i D \Delta t} \tag{5.5}$$

where q_i is a numerical constant that depends on dimensionality (in this case q_i = 2) and Δt is the time interval (Δt = 1 h) (Einstein 1956). To ensure that aggregations were given sufficient time to form, I chose to run the simulation for 30 days which reflects realistic planktonic larval durations for these species. I_M and I_D were calculated based on larval abundance on day 30, which was sampled with 11 randomly-located, 500-m long simulated tows along the transect (reflecting the empirical sampling design).

5.4 Results

In St. George's Bay, there was a surface mixed layer in the top ~10 m that is warm and slightly fresher than the water below (Figure 5.2). Below the mixed layer, temperature decreases and salinity increases gradually to the seafloor. The fluorescence maximum was at ~13 m. In 2009, mean (± S.D., n = 241-3100) vertical current speed ranged from 0.07 (± 2.3) mm s^{-1} to 0.83 (± 5.0) mm s^{-1} while horizontal current speed ranged from 0.002 (± 0.081) m s^{-1} to 0.038 (± 0.068) m s^{-1} at 3 m, and from 0.006 (± 0.081) m s^{-1} to 0.071 (± 0.084) m s^{-1} at 12 m (Figure 5.3). The highest mean velocities were recorded by the ADCP in the south-east corner of the bay, and only represent a few days of data because it malfunctioned. Mean current velocities in either N-S or E-W directions at all sites were generally ~ ½ the magnitude of the standard deviation. The orientations of the current velocity vectors suggested a counter-clockwise gyre, but the

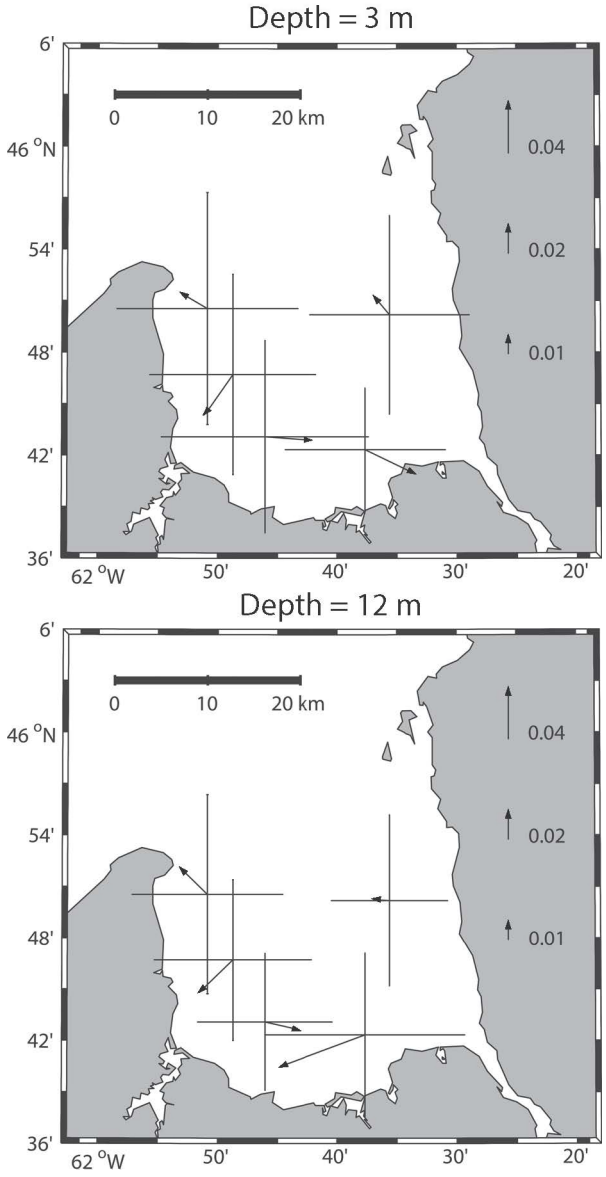

Figure 5.3: Mean current velocities (m s^{-1}) from 11 Jul to 22 Aug 2009 at 3 and 12 m. Error bars indicate one standard deviation (n = 3081, 3085, 3088, 241, 3100, respectively counter-clockwise from N-E) in both the N-S and E-W directions.

relative size of the standard deviation error bars compared to the mean current velocity indicate an absence of a well-defined circulation pattern.

Each taxonomic group consisted mostly of a few species (Table 5.1). The bryozoans consisted almost entirely of *Electra pilosa*, whereas the bivalves were mostly *Mytilus* spp. The gastropods consisted of *Margarites* spp. and *Astyris lunata*, and the decapods were mostly *Cancer irroratus*. For each species, there was little variability in abundance among sampling periods (Figure 5.4, Table 5.2). Only the larval abundance of *E. pilosa*, *Anomia simplex*, *Bittiolum alternatum, Crangon septemspinosa* and *Neopanopeus sayi* varied significantly with depth (Figure 5.4, Table 5.2). Additionally, there was a significant interaction between period and depth for *Modiolus modiolus, Margarites spp.* and *Diaphana minuta* indicating that their depth distribution varied over time. When combined into taxonomic groups (Figure 5.5), larval abundance did not vary with sampling period and only bryozoan abundance varied significantly with depth (Table 5.3). In contrast, the ordination of species based on sites (i.e. horizontal distribution) revealed that several gastropod and bivalve species were clustered in the center of the plot, while the bryozans, all decapods and a few gastropod and bivalve species were on the periphery (Figure 5.6). These results suggest that the horizontal distributions vary with species and this may be the result of vertical gradients (e.g. *A. simplex, B. alternatum, C. septemspinosa*) or not (e.g. *C. irroratus, M modiolus*). The relationship between species assemblages and depth is unclear (Figure 5.7), since the species assemblages seems to vary among depths on 11-12 Aug 2008, but not on Aug 2-4 2009, with a weak pattern on Aug 7-8 2008.

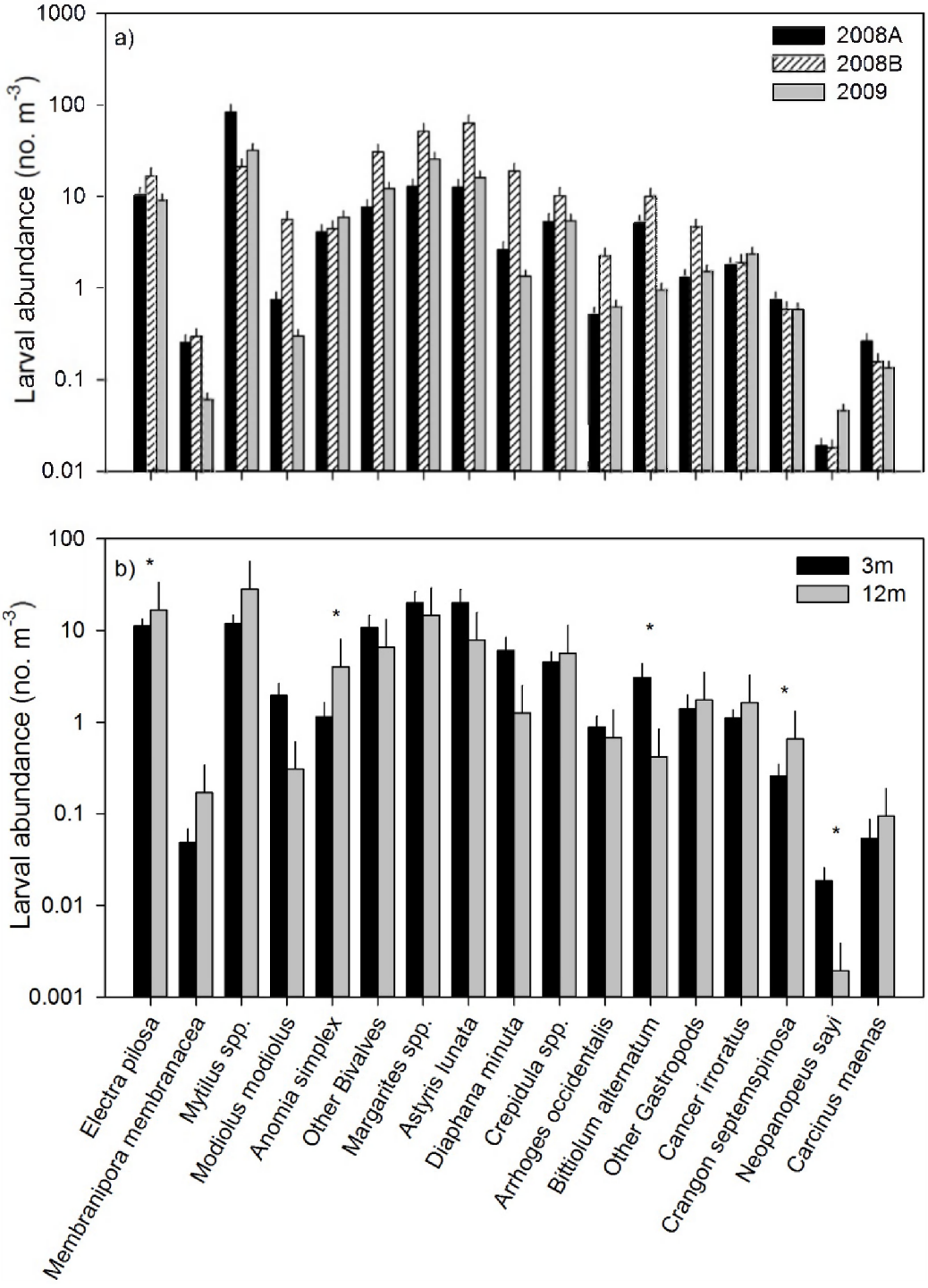

Figure 5.4: Average larval abundance of species in St. George's Bay, Nova Scotia, Canada, at different a) sampling dates, and b) depths. Larvae were sampled at 3 and 12 m depth with a 200-µm plankton ring net (0.75-m diameter) on 7-8 Aug 2008 (2008A), 11-12 Aug 2008 (2008B), and 2-4 Aug 2009. Error bars indicate standard errors (n = 79) and asterisks indicate significant differences as detected by ANOVA (see Table 5.2 for details).

Table 5.2: Results of ANOVAs examining the random effect of sampling period (P) and fixed effect of depth (D) on the logarithm (base 10) of larval abundance by species. Asterisks indicate significant differences. Bold values indicate where the sums of squares and d.f. from error term and for P*D have been pooled (when $p \geq 0.250$ for P*D), and F and p values for D (d.f. = 1,75) have been recalculated.

Taxon	P (d.f. = 2,73)		D (d.f. = 1,2)		P*D (d.f. = 2,73)	
Bryozoans	**F**	**p**	**F**	**p**	**F**	**p**
Electra pilosa	0.902	0.526	**8.953**	**0.004***	1.411	0.250
Membranipora membranacea	2.318	0.301	4.455	0.167	2.230	0.115
Bivalves						
Mytilus spp.	0.175	0.851	1.027	0.416	1.898	0.157
Modiolus modiolus	2.032	0.330	5.512	0.142	3.671	0.030*
Anomia simplex	1.969	0.337	**11.397**	**0.001***	1.333	0.270
Other Bivalves	0.734	0.577	0.328	0.624	1.616	0.206
Gastropods						
Margarites spp.	1.100	0.476	0.071	0.815	3.841	0.026*
Astyris lunata	0.545	0.647	**2.144**	**0.147**	0.797	0.455
Diaphana minuta	3.417	0.226	2.881	0.231	3.520	0.035*
Crepidula spp.	1.885	0.347	**1.895**	**0.173**	0.471	0.626
Arrhoges occidentalis	2.828	0.261	**0.015**	**0.901**	1.303	0.278
Bittiolum alternatum	1.236	0.447	**15.199**	**<0.001***	1.302	0.278
Other Gastropods	0.811	0.552	2.255	0.270	1.897	0.157
Decapods						
Cancer irroratus	5.245	0.160	**0.685**	**0.41**	0.362	0.698
Crangon septemspinosa	5.759	0.148	**13.554**	**<0.001***	0.560	0.574
Neopanopeus sayi	20.261	0.047*	**5.034**	**0.028***	0.012	0.988
Carcinus maenas	0.083	0.923	0.368	0.605	3.082	0.052

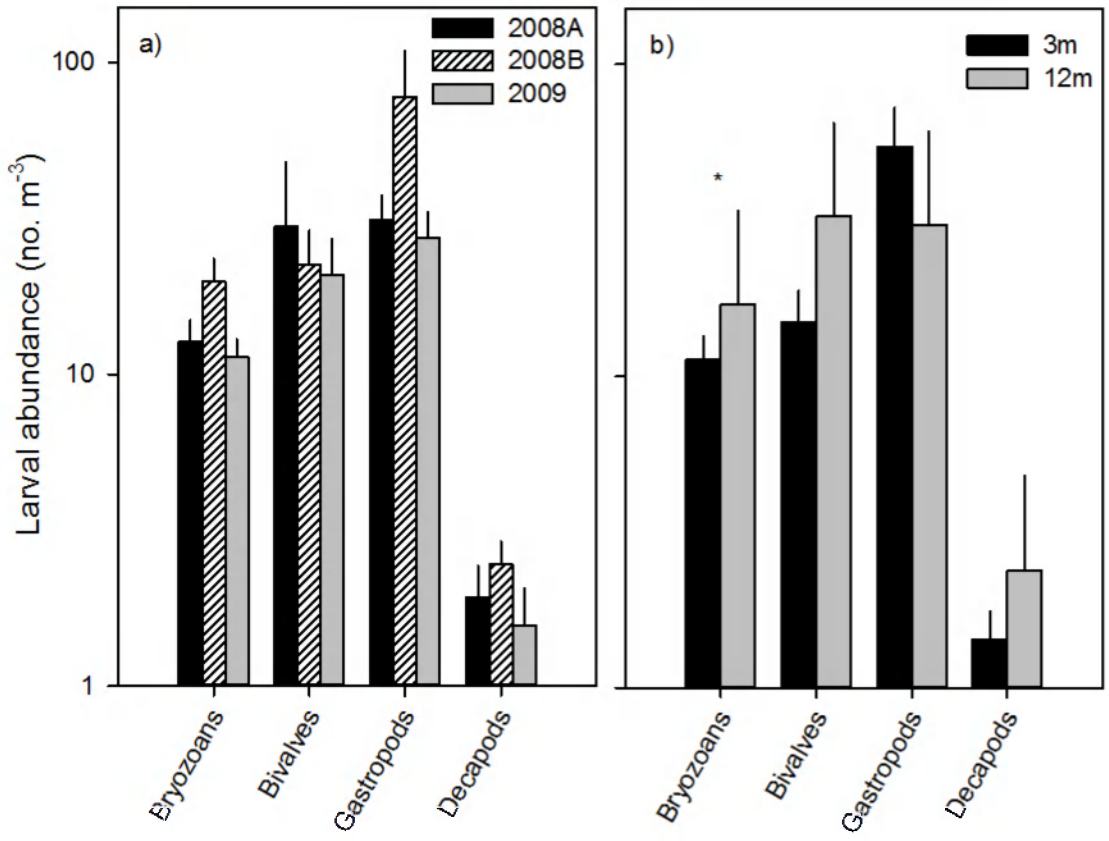

Figure 5.5: Average larval abundance of taxonomic groups in St. George's Bay, Nova Scotia, Canada, at different a) sampling dates, and b) depths. Larvae were sampled at 3 and 12 m depth with a 200-µm plankton ring net (0.75-m diameter) on 7-8 Aug 2008 (2008A), 11-12 Aug 2008 (2008B), and 2-4 Aug 2009. Error bars indicate standard errors (n = 79) and asterisks indicate significant differences as detected by ANOVA (see Table 5.3 for details).

Table 5.3: Results of ANOVAs examining the random effect of sampling period (P) and fixed effect of depth (D) on the logarithm (base 10) of larval abundance by taxonomic group (error d.f. = 73). Asterisks indicate significant differences. Bold values indicate where the sums of squares and d.f. from error term and for P*D have been pooled (since $p \geq 0.250$ for P*D), and F and p values for D (d.f. = 1,75) have been recalculated.

Taxon	P (d.f. = 2,73)		D (d.f. = 1,2)		P*D (d.f. = 2,73)	
	F	p	F	p	F	p
Bryozoans	0.938	0.516	**9.0251**	**0.004***	1.396	0.254
Bivalves	0.232	0.812	0.362	0.608	1.171	0.188
Gastropods	0.288	0.776	0.079	0.805	2.573	0.083
Decapods	16.711	0.057	**3.403**	**0.069**	0.169	0.844

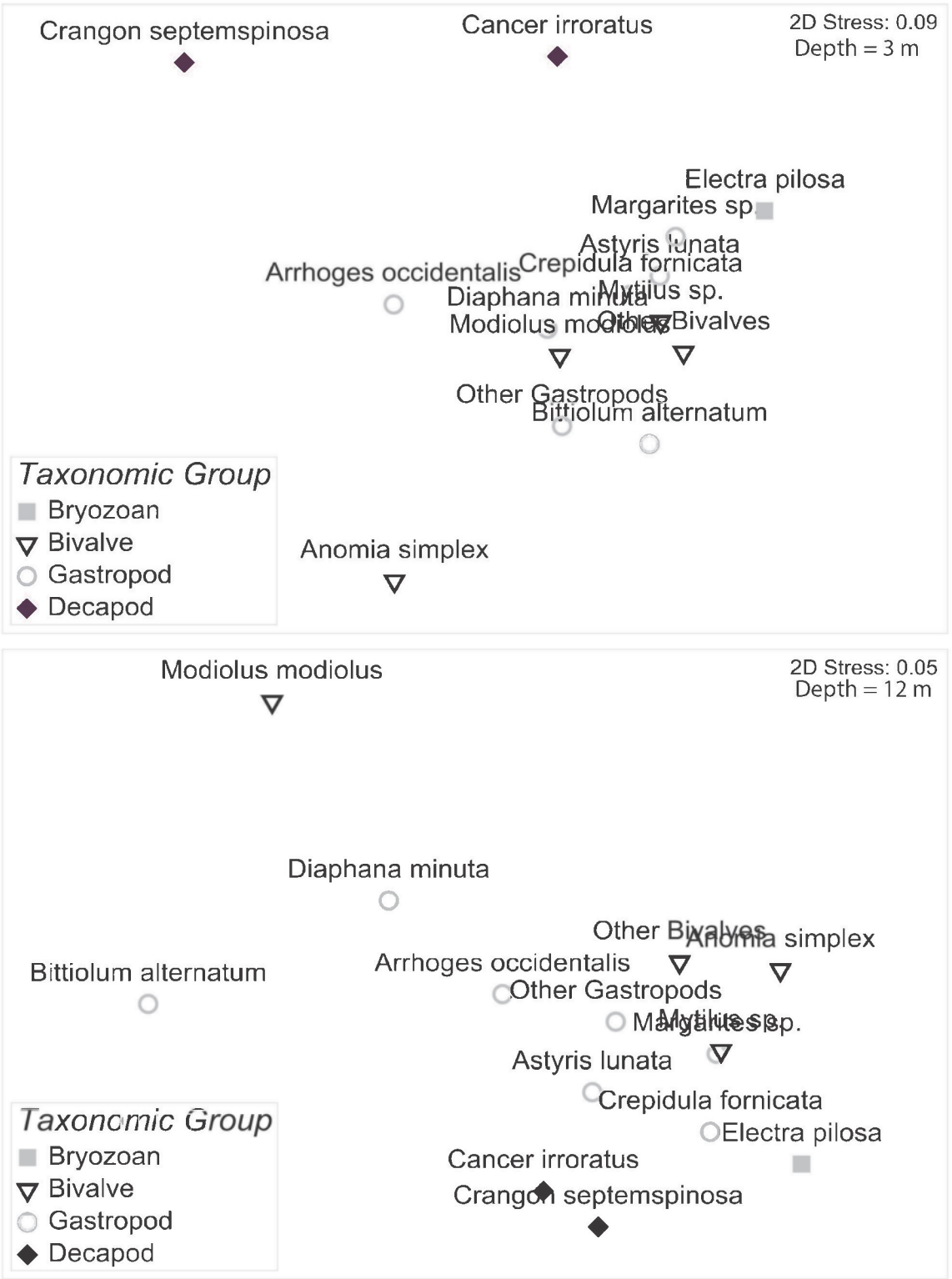

Figure 5.6: Ordination from nonmetric multidimensional scaling of the species based on the similarity of their larval abundance at each site and time

Figure 5.7: Ordination from nonmetric multidimensional scaling of the sites and depth combinations based on the similarity in abundance of larval assemblages.

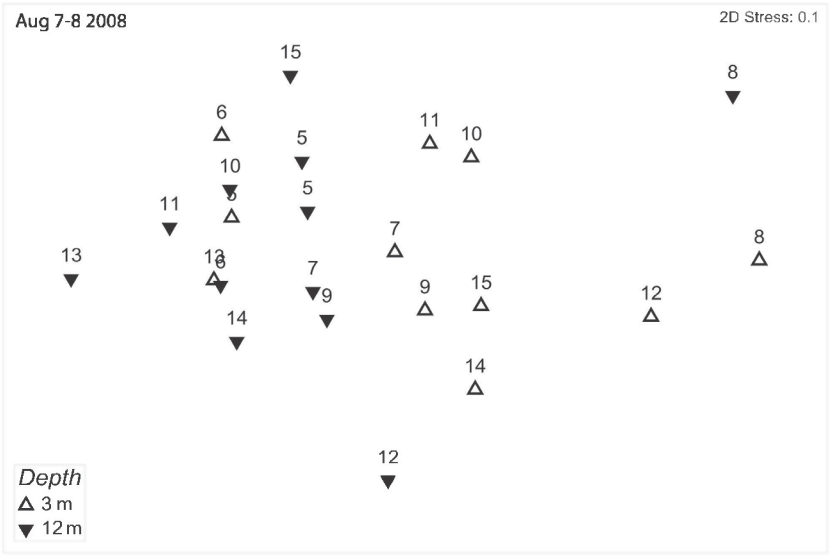
Aug 7-8 2008
2D Stress: 0.1
Depth
3 m
12 m

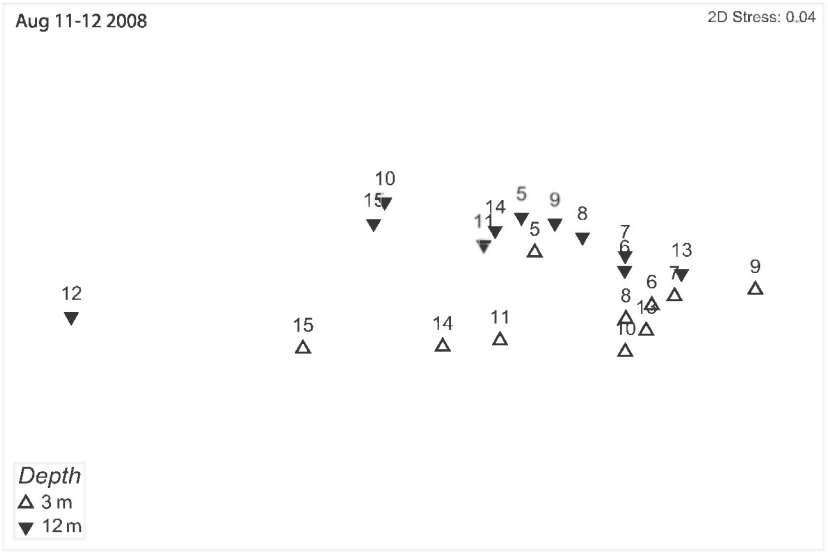
Aug 11-12 2008
2D Stress: 0.04
Depth
3 m
12 m

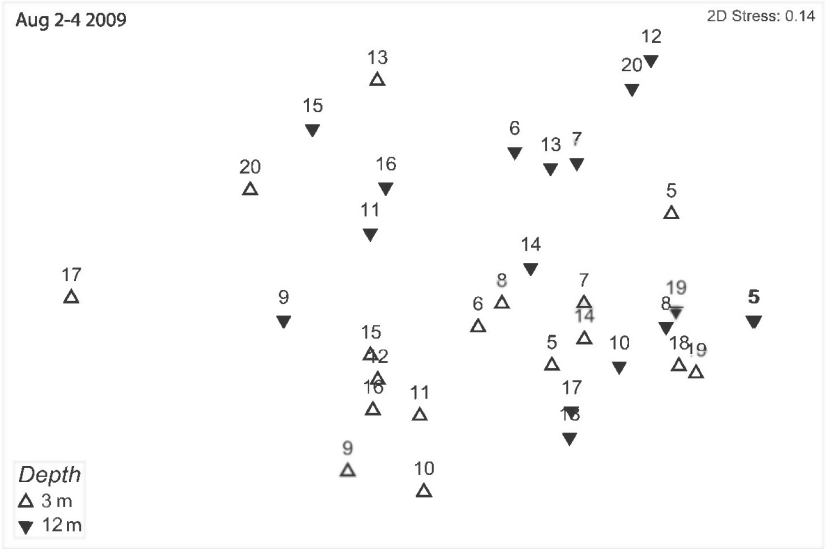
Aug 2-4 2009
2D Stress: 0.14
Depth
3 m
12 m

Larval distribution of all taxonomic groups showed significant departures from randomness (Table 5.4), exhibiting aggregation. For gastropods and bivalves, I_D was more than an order of magnitude higher, and the overall I_M was more than double that of bryozoans and decapods. Therefore, the distributions of gastropods and bivalves consistently showed the highest degree of aggregation. This trend is fairly consistent over time and depth as there are only 2 instances where decapod distributions were more aggregated than that of gastropods (August 7-8, 2008 at 3 m and August 2-4, 2009 at 12 m), and only 2 instances where decapod distributions were more aggregated than that of bivalves (August 7-8, 2008 and August 2-4, 2009 at 3 m). The I_M for decapods was highly variable and ranged from 1.08 ($p = 0.071$), corresponding to a random distribution, to 3.3 ($p < 0.001$), which is higher than that of gastropods at that time and depth. Conversely, the I_M for bryozoans at all depths and times was consistently close to 1, but still high enough to depart from randomness.

Geographically, there was no consistent pattern of larval abundance over time. For 7-8 Aug 2008, there was a fairly even distribution of larvae of all taxonomic groups throughout the bay except at the northernmost site and near the southeast corner of the bay which had higher and lower abundances, respectively (Figure 5.8). For 11-12 Aug 2008, sites in the southern half of the bay generally had higher larval abundance than sites in the northern half across all taxa (Figure 5.9). For 2-4 Aug 2009, sites along the eastern and southern shores of the bay generally had higher abundance of bryozoans, bivalves and gastropods. Decapods were more abundant in the northwest corner of the bay (Figure 5.10).

Table 5.4: Index of dispersion (σ/μ) and Morisita's Index for larval abundance (individuals m-3) of each taxonomic group, during plankton sampling in St. George's Bay, Nova Scotia, Canada, in Aug 2008 at 11 sites, and in Aug 2009 at 16 sites. Morisita's index was calculated for the overall distribution, and for distributions for each depth and sampling period. Asterisks indicate significantly aggregative dispersal indices.

	Bryozoans		**Bivalves**		**Gastropods**		**Decapods**	
Index of dispersion								
	σ/μ	p	σ/μ	p	σ/μ	p	σ/μ	p
Overall	11.02	<0.001*	126.07	<0.001*	164.43	<0.001*	3.46	<0.001*
Morisita's Index								
	I_M	p	I_M	p	I_M	p	I_M	p
Overall	1.77	<0.001*	6.22	<0.001*	4.83	<0.001*	2.78	<0.001*
3 m								
2008A	1.73	<0.001*	2.34	<0.001*	2.23	<0.001*	3.59	<0.001*
2008B	1.83	<0.001*	3.06	<0.001*	3.13	<0.001*	1.54	<0.001*
2009	1.90	<0.001*	3.06	<0.001*	2.42	<0.001*	3.14	<0.001*
12 m								
2008A	1.37	<0.001*	5.83	<0.001*	1.48	<0.001*	1.79	<0.001*
2008B	1.48	<0.001*	1.71	<0.001*	2.02	<0.001*	1.74	<0.001*
2009	1.32	<0.001*	4.09	<0.001*	2.37	<0.001*	3.65	<0.001*

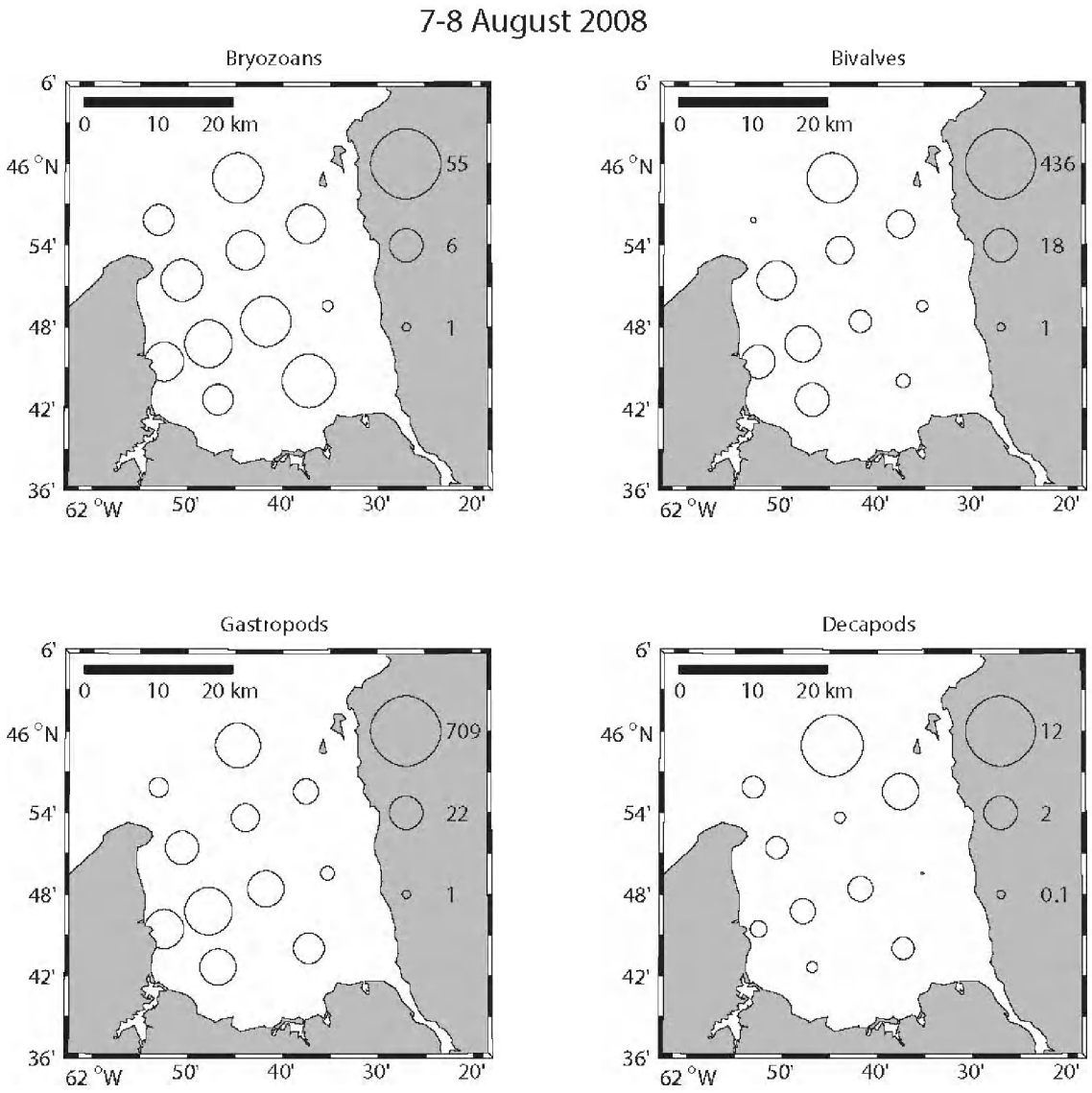

Figure 5.8: Larval abundance (no. m^{-3}; averaged across depth) of taxonomic groups in St. George's Bay, Nova Scotia, Canada, at 11 different sampling sites. Larvae were sampled with a 200-µm plankton ring net (0.75-m diameter) on Aug 7-8, 2008. The size of the bubble is proportional to abundance.

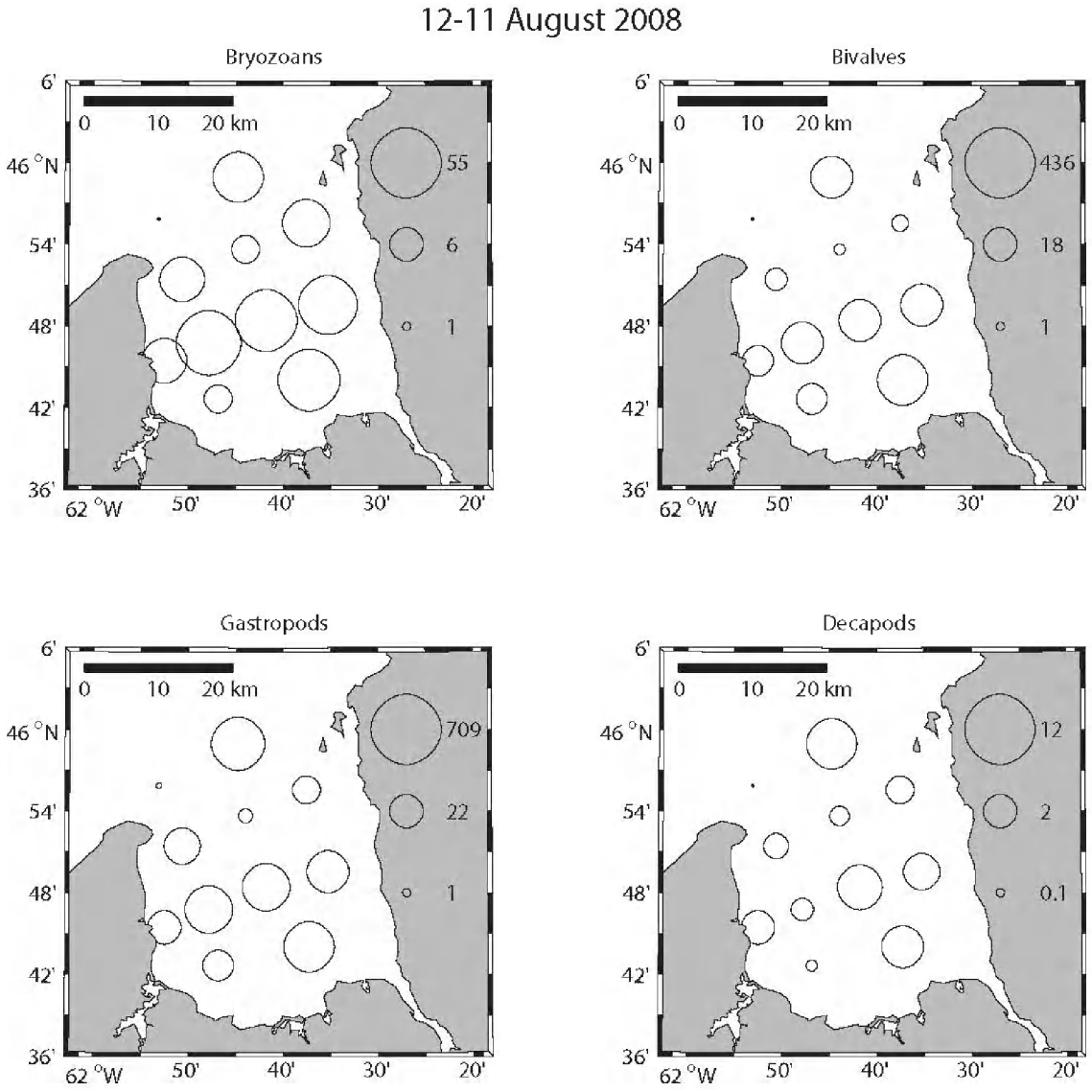

Figure 5.9: Larval abundance (no. m^{-3}; averaged across depth) of taxonomic groups in St. George's Bay, Nova Scotia, Canada, at 11 different sampling sites. Larvae were sampled with a 200-µm plankton ring net (0.75-m diameter) on Aug 11-12, 2008. The size of the bubble is proportional to abundance.

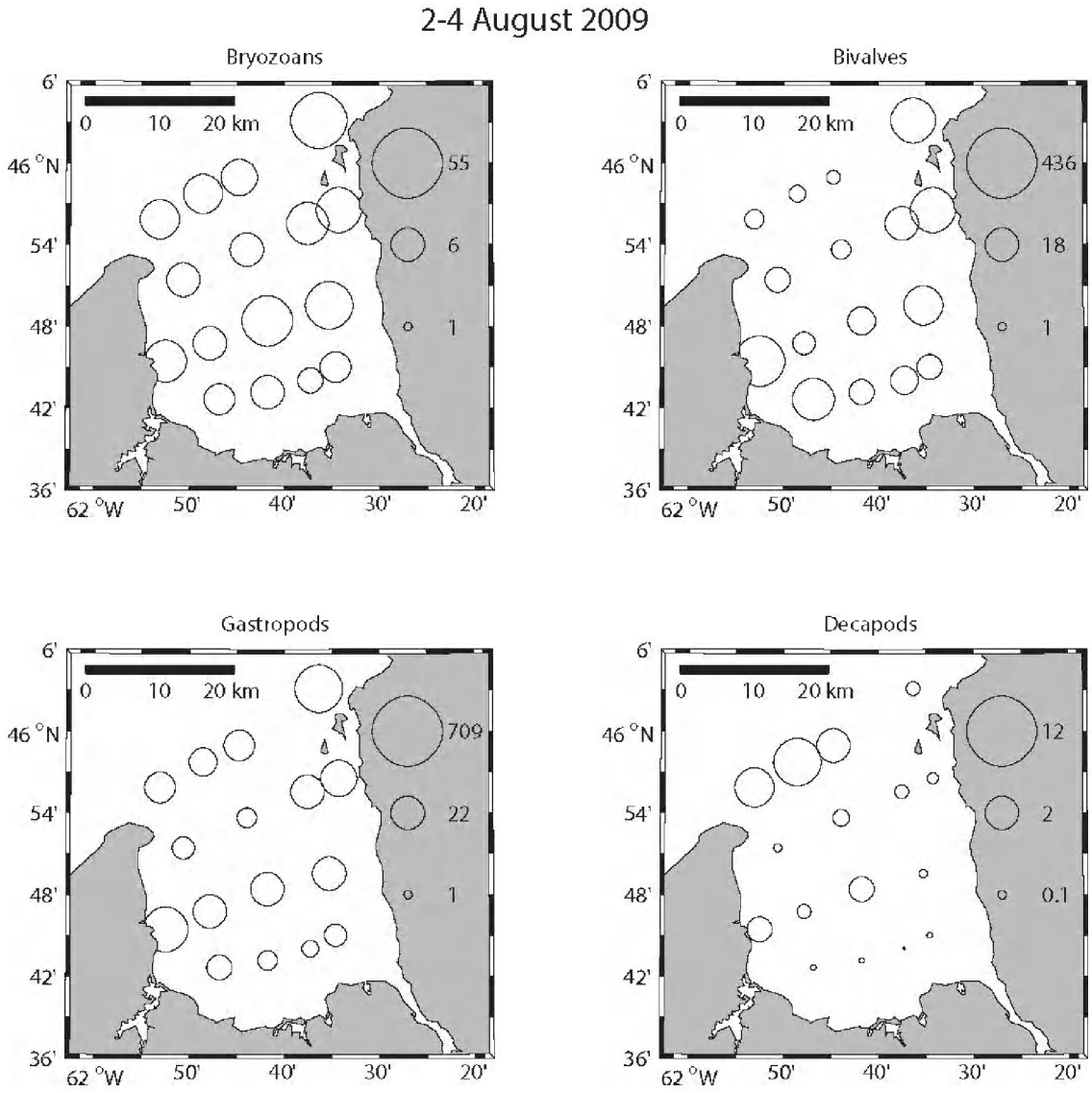

Figure 5.10: Larval abundance (no. m^{-3}; averaged across depth) of taxonomic groups in St. George's Bay, Nova Scotia, Canada, at 16 different sampling sites. Larvae were sampled with a 200-µm plankton ring net (0.75-m diameter) on Aug 2-4, 2009. The size of the bubble is proportional to abundance.

Larval abundance (combined for both depths) was correlated for most pairs of taxonomic groups both when sampling period were combined, and within each sampling period. When considering the entire data set, the highest correlation was between the larval abundances of gastropods and bivalves (Table 5.5a), and the only non-significant correlation was between decapods and bivalves. When considering only specific sampling dates, the highest correlation was also between the larval abundances of gastropods and bivalves (Table 5.5b). On 11-12 Aug, correlations among all pairs were significant, while only 4 of 6 pairs were significantly correlated on 7-8 Aug. In general, the correlations among the larval abundance of decapods and other taxa were relatively weak, and most often occurred with bryozoans. A similar pattern was observed in the correlation of pairs of species (Table 5.6). The abundances of gastropod and bivalve species were highly correlated with one another, whereas decapod species were not significantly correlated with species of either bivalves or gastropods. Additionally, significant correlations were recorded among species within the same taxonomic group. However, when comparing abundances from 7-8 Aug to those from 11-12 Aug, there were no significant correlations for any pair of taxa or species (Tables 5.5&5.6). This suggests that the spatial relationship among taxonomic groups at any one time is stronger than the temporal relationship within a single taxonomic group.

Overall, fluorescence and salinity had the highest correlations with larval abundance (Table 5.7)Fluorescence was significantly positively correlated with both gastropods species and *M. edulis* at 3 m, and with *C. septemspinosa* at 12 m. Overall, fluorescence was positively correlated with 6 of 7 species at 3 m and all species at 12 m. At 3m, salinity was significantly negatively correlated with both bivalve species and

Table 5.5: Pearson correlation examining the relationship in logarithm (base 10) abundance (all sampling depths combined) for pairs of taxa: bryozoans (Bz), bivalves (Bv), gastropods (Gp) and decapods (Dp) calculated for: A) all 3 sampling dates combined (n = 79), B) specific sampling dates (n=22) C) within and among taxa at different sampling dates where the rows represent abundances from 7-8 Aug, 2008 while the columns represent that from 11-12 Aug, 2008 (n=22). In A) and B) the upper half of the matrix indicates the correlation coefficients for larval abundance for while the lower half indicates the p-value. In C) The number in brackets is the p-value. Statistically significant correlations are indicated in bold.

A)	All Dates			
	Bz	Bv	Gp	Dp
Bz	1	**0.532**	**0.708**	**0.584**
Bv	**<0.001**	1	**0.739**	0.163
Gp	**<0.001**	**<0.001**	1	**0.437**
Dp	**<0.001**	0.152	**<0.001**	1
B)	7-8 Aug, 2008			
	Bz	Bv	Gp	Dp
Bz	1	0.414	**0.584**	**0.655**
Bv	0.050	1	**0.683**	0.290
Gp	**0.003**	**<0.001**	1	**0.438**
Dp	**0.001**	0.180	**0.037**	1
	11-12 Aug, 2008			
	Bz	Bv	Gp	Dp
Bz	1	**0.771**	**0.763**	**0.710**
Bv	**<0.001**	1	**0.902**	**0.646**
Gp	**<0.001**	**<0.001**	1	**0.564**
Dp	**<0.001**	**0.001**	**0.006**	1
	2-4 Aug, 2009			
	Bz	Bv	Gp	Dp
Bz	1	**0.421**	**0.734**	**0.406**
Bv	**0.013**	1	**0.675**	-0.234
Gp	**<0.001**	**<0.001**	1	0.303
Dp	**0.017**	0.183	0.082	1
C)	7-8 Aug VS 11-12 Aug, 2008			
	Bz	Bv	Gp	Dp
Bz	0.319 (0.148)	0.194 (0.388)	0.143 (0.525)	0.410 (0.058)
Bv	0.344 (0.117)	0.115 (0.612)	0.114 (0.615)	0.287 (0.196)
Gp	0.330 (0.134)	0.222 (0.321)	0.223 (0.318)	0.250 (0.262)
Dp	0.125 (0.578)	0.061 (0.788)	0.181 (0.420)	0.395 (0.069)

Table 5.6: Pearson correlation examining the relationship in logarithm (base 10) abundance (all sampling depths combined) for pairs of taxa: *Electra pilosa* (Bz1), *Mytilus* spp. (Bv1), *Other bivalves* (Bv2), *Margarites* spp. (Gp1), *Astyris lunata* (Gp2), *Cancer irroratus* (Dp1), *Crangon septemspinosa* (Dp2) calculated for A) all 3 sampling dates combined (n = 79), B) specific sampling dates (n=22) C) within and among taxa at different sampling dates where the rows represent abundances from 7-8 Aug, 2008 while the columns represent that from 11-12 Aug, 2008 (n=22). In A) and B) the upper half of the matrix indicates the correlation coefficients for larval abundance for while the lower half indicates the Bonferroni corrected p-value. In C) . In C) The number in brackets is the p-value. Statistically significant correlations are indicated in bold.

A)	All Dates						
	Bz1	Bv1	Bv2	Gp1	Gp2	Dp1	Dp2
Bz1	**1**	**0.547**	**0.393**	**0.583**	**0.548**	**0.529**	**0.442**
Bv1	**<0.001**	**1**	**0.831**	**0.776**	**0.397**	0.124	0.302
Bv2	**<0.001**	**<0.001**	**1**	**0.696**	**0.471**	-0.056	0.121
Gp1	**<0.001**	**<0.001**	**<0.001**	**1**	**0.560**	**0.241**	**0.288**
Gp2	**<0.001**	**<0.001**	**<0.001**	**<0.001**	**1**	**0.367**	0.301
Dp1	**<0.001**	0.278	0.625	**0.033**	0.001	**1**	**0.574**
Dp2	**<0.001**	0.007	0.288	**0.010**	0.007	**<0.001**	**1**
B)	7-8 Aug, 2008						
	Bz1	Bv1	Bv2	Gp1	Gp2	Dp1	Dp2
Bz1	**1**	**0.424**	0.297	**0.431**	0.381	**0.547**	**0.671**
Bv1	**0.044**	**1**	**0.792**	**0.842**	0.018	0.203	**0.595**
Bv2	0.169	**<0.001**	**1**	**0.849**	0.316	-0.018	0.309
Gp1	**0.040**	**<0.001**	**<0.001**	**1**	0.395	0.218	**0.495**
Gp2	0.073	0.935	0.142	0.062	**1**	0.227	0.250
Dp1	**0.007**	0.354	0.935	0.319	0.299	**1**	**0.666**
Dp2	**<0.001**	**0.003**	0.151	**0.016**	0.25	**0.001**	**1**
	11-12 Aug, 2008						
	Bz1	Bv1	Bv2	Gp1	Gp2	Dp1	Dp2
Bz1	**1**	**0.764**	**0.640**	**0.660**	**0.678**	**0.675**	0.349
Bv1	**<0.001**	**1**	**0.854**	**0.815**	**0.784**	**0.572**	**0.473**
Bv2	**0.001**	**<0.001**	**1**	**0.874**	**0.859**	**0.440**	0.393
Gp1	**0.001**	**<0.001**	**<0.001**	**1**	**0.858**	**0.451**	0.262
Gp2	**0.001**	**<0.001**	**<0.001**	**<0.001**	**1**	**0.504**	0.300
Dp1	**0.001**	**0.005**	**0.040**	**0.035**	**0.017**	**1**	0.278
Dp2	0.111	**0.026**	0.070	0.238	0.176	0.210	**1**
	2-4 Aug, 2009						
	Bz1	Bv1	Bv2	Gp1	Gp2	Dp1	Dp2
Bz1	**1**	**0.473**	0.331	**0.591**	**0.525**	0.366	0.277
Bv1	**0.005**	**1**	**0.888**	**0.840**	**0.407**	-0.245	-0.084
Bv2	0.056	**<0.001**	**1**	**0.712**	0.328	-0.314	-0.073
Gp1	**<0.001**	**<0.001**	**<0.001**	**1**	0.317	-0.050	-0.001
Gp2	**0.001**	**0.017**	0.058	0.068	**1**	0.330	0.310
Dp1	0.033	0.162	0.071	0.779	0.057	**1**	**0.6535**
Dp2	0.113	0.635	0.681	0.995	0.074	**<0.001**	**1**

C) 7-8 Aug VS 11-12 Aug, 2008

	Bz1	Bv1	Bv2	Gp1	Gp2	Dp1	Dp2
Bz1	0.320	0.212	0.098	0.004	0.199	0.332	0.322
	(0.147)	(0.344)	(0.664)	(0.986)	(0.375)	(0.131)	(0.144)
Bv1	0.336	0.142	-0.085	-0.038	0.043	0.272	-0.042
	(0.126)	(0.529)	(0.706)	(0.865)	(0.850)	(0.221)	(0.852)
Bv2	0.219	0.050	-0.168	-0.061	-0.012	-0.025	-0.033
	(0.328)	(0.826)	(0.456)	(0.787)	(0.957)	(0.914)	(0.886)
Gp1	0.352	0.210	0.003	0.100	0.158	0.164	0.101
	(0.109)	(0.349)	(0.988)	(0.657)	(0.484)	(0.466)	(0.654)
Gp2	0.197	0.278	0.103	0.214	0.138	0.023	0.329
	(0.381)	(0.211)	(0.649)	(0.339)	(0.541)	(0.919)	(135)
Dp1	0.068	-0.023	0.031	0.174	0.212	0.349	0.136
	(0.765)	(0.921)	(0.892)	(0.440)	(0.344)	(0.111)	(0.546)
Dp2	0.240	0.175	-0.046	-0.001	0.083	0.391	0.132
	(0.283)	(0.437)	(0.840)	(0.995)	(0.715)	(0.072)	(0.558)

Table 5.7: Pearson correlation coefficients examining the relationship between physical variables of the water column and the logarithm (base 10) of abundance of *Electra pilosa* (Bz1), *Mytilus* spp. (Bv1), Other bivalves (Bv2), *Margarites* spp. (Gp1), *Astyris lunata* (Gp2), *Cancer irroratus* (Dp1), *Crangon septemspinosa* (Dp2) from 2-4 Aug 2009 for sampling depths of A) 3 m (n = 16) and B) 12 m (n = 15). The number in brackets is the p-value. Asterisks indicate statistically significant correlations.

A)	**Temperature (°C)**	**Salinity**	**Fluorescence**
Bz1	-0.111 (0.682)	-0.226 (0.400)	0.201 (0.455)
Bv1	0.355 (0.177)	**-0.601 (0.014)**	**0.579 (0.019)**
Bv2	0.172 (0.524)	**-0.509 (0.044)**	0.456 (0.076)
Gp1	0.050 (0.853)	-0.248 (0.355)	**0.531 (0.034)**
Gp2	0.354 (0.178)	-0.174 (0.520)	**0.678 (0.004)**
Dp1	**-0.547 (0.028)**	**0.557 (0.025)**	-0.111 (0.683)
Dp2	-0.073 (0.787)	0.221 (0.410)	0.447 (0.082)
B)	**Temperature (°C)**	**Salinity**	**Fluorescence**
Bz1	-0.299 (0.278)	0.476 (0.073)	0.249 (0.371)
Bv1	-0.210 (0.453)	0.490 (0.064)	0.185 (0.510)
Bv2	-0.105 (0.710)	0.303 (0.273)	0.153 (0.586)
Gp1	-0.263 (0.344)	0.392 (0.149)	0.250 (0.370)
Gp2	-0.268 (0.335)	0.481 (0.069)	0.305 (0.269)
Dp1	-0.370 (0.175)	0.110 (0.696)	0.466 (0.080)
Dp2	-0.420 (0.119)	0.089 (0.753)	**0.561 (0.030)**

significantly positively correlated with *C. irroratus*. Overall, salinity was negatively correlated with 5 of 7 species at 3 m and positively correlated with all species at 12 m. Temperature was only significantly negatively correlated with *C. irroratus* at 3 m, but was positively correlated with 4 of 7 species at 3 m and negatively correlated with all species at 12 m. The aggregation-diffusion model showed that horizontal swimming does not reproduce the level of aggregation observed in the field when larvae were exposed to diffusion (Figure 5.11). Only at a diffusion index of 0 $m^2 s^{-1}$ were the I_M and I_D for bryozoans, bivalves and gastropods comparable to that from the field observations (Table 5.4). For the decapods, the I_M and I_D were similar to the values obtained from the field observations for diffusion indices 8-9 $m^2 s^{-1}$. Any evidence ($I_M > 1.1$) of aggregations was removed when diffusion indices reached 2 $m^2 s^{-1}$ for bryozoans, 3 $m^2 s^{-1}$ for bivalves, 3 $m^2 s^{-1}$ for gastropods and 30 $m^2 s^{-1}$ decapods.

5.5 Discussion

Mean larval abundance of all 17 species and 4 taxonomic groups did not change significantly over the three sampling periods. However, my sampling was limited to the first two weeks in Aug 2008 and 2009 to maximize larval abundance of most species, and would not have captured seasonal effects. In the same region, Lloyd et al (2012a, b) showed that the vertical distributions of invertebrate larvae vary with depth. In my study, three species (*E. pilosa*, *A. simplex*, and *C. septemspinosa*) were significantly more abundant at 12 m, while *B. alternatum* and *N. sayi* were significantly more abundant at 3 m. Lloyd et al. (2012b) also found that *B. alternatum* was more abundant above the thermocline in St. George's Bay, NS, over shorter time scales. The highest concentrations of bryozoans occurred at 18 m, and showed a positive relationship with fluorescence

Figure 5.11: Relationship between mean Morisita's index (± 1 S.E., n =5) and the diffusion index for 4 taxonomic groups. Morisita's index was calculated from 11 simulated 500-m net tows at randomly selected sites along a modelled 1-dimensional 40 km larval distribution.

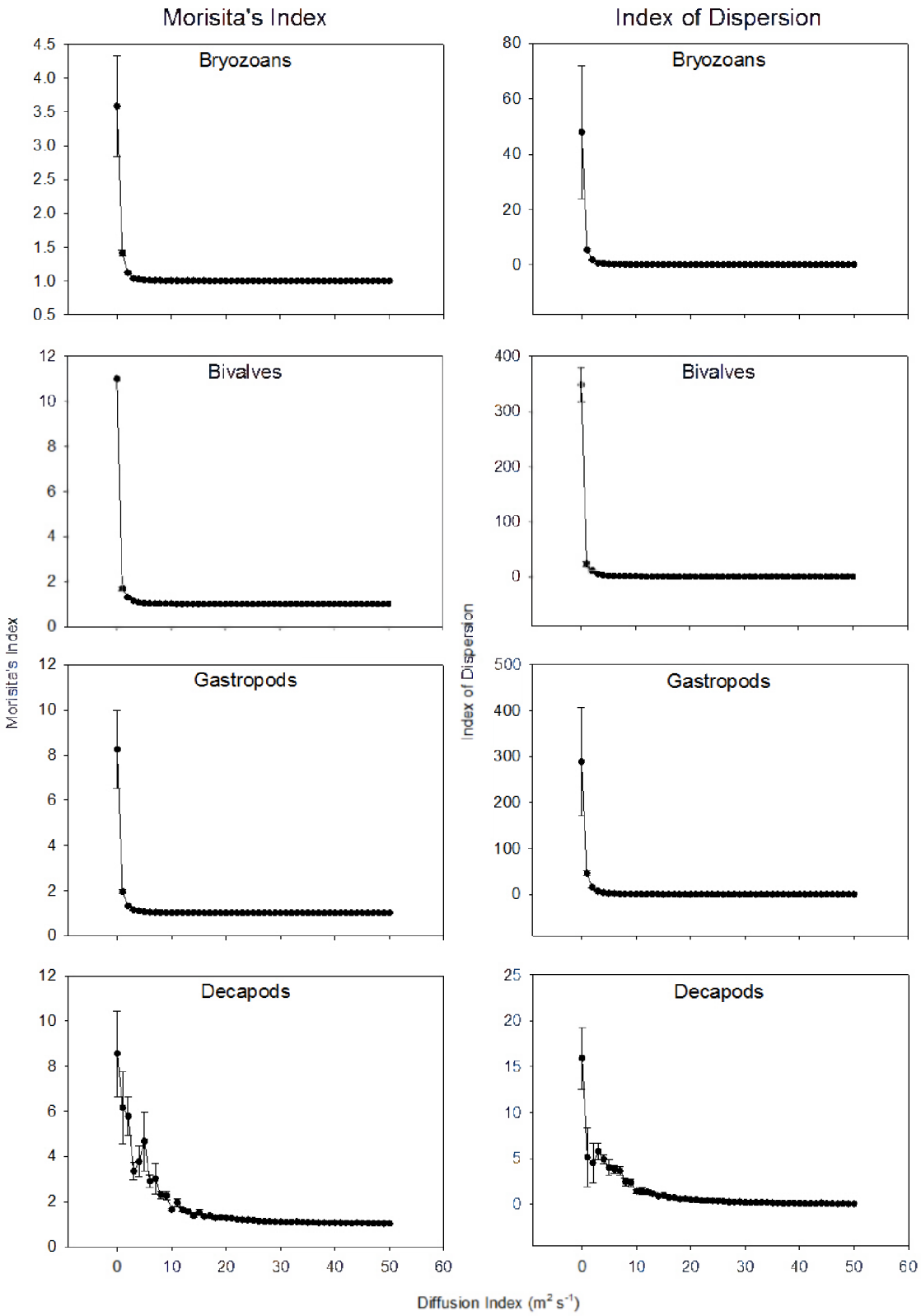
Morisita's Index
Index of Dispersion
Bryozoans
Bivalves
Gastropods
Decapods
Morisita's Index
Index of Dispersion
Diffusion Index (m² s⁻¹)

Lloyd et al. (2012a). In contrast, bryozoan abundance in St. Margarets Bay, NS, was higher at 4 m than at 12 m (Saunders and Metaxas 2010). However, the salinity and temperature at 4 m depth in St. Margarets Bay was more similar to that at 12 m in St. George's Bay. This pattern suggests that bryozoan larvae may prefer ~15 °C and salinity of ~30. *A. simplex* was most abundant at 12 m in my study which is in the thermocline, and was also concentrated around the thermocline off Tuckerton, New Jersey, USA (Ma et al. 2006). My sampling detected no significant difference in vertical distributions for bivalve larvae, but other studies with more rigorous sampling of depth distributions have found that they are most abundant below the thermocline (Lloyd et al. 2012a). Similarly, I found higher abundance of *C. septemspinosa* at 12 m which is my deepest sampling point and in Chesapeake Bay, USA, larvae of *C. septemspinosa* were found to be most abundant in the lower water column with higher salinities (Wehrtmann 1994).

Overall, the variability in larval abundance between depths was in most cases smaller than the spatial variability in larval abundance among sites. The similarity in species distributions appears to be affected by the vertical distribution of those larval populations with a vertical skew indicated by the fact that species with the largest differences in depth distribution were at the periphery of the nMDS plot. However, *C. irroratus* and *M. modiolus* had no detected vertical skew in larval population, and were also located at the periphery of the nMDS plot.

The distributions of all taxonomic groups were found to be significantly aggregated horizontally according to both indices used (I_D and I_M). Generally, larval bivalves and gastropods, with intermediate swimming abilities to the other groups, showed the strongest aggregation, whereas larval bryozoans, which are the weakest

swimmers, were the least aggregated. The magnitude of aggregation for decapod distributions was highly variable. While I_M is density independent (Hurlbert 1990), I suggest that this apparent variability in aggregation is related to the low abundance of decapods which could affect my ability to accurately estimate abundance. In fish, smaller larvae showed weaker aggregation than larger ones presumably because their swimming is dominated by viscous forces (Stanley et al. 2012). Conversely, the swimming of large larvae is dominated by inertial forces and they showed a higher degree of aggregation in the same study. However, the swimming of invertebrate larvae is mostly dominated by viscous forces because of their small size (Chia et al. 1984). It is likely that vertical swimming interacts with physical features of the water column to result in the formation of aggregations (Queiroga and Blanton 2005; DiBacco et al. 2011). While my study does not identify a mechanism for the formation of aggregations (e.g. aggregations caused by larvae swimming upwards in a downwelling current), it does appear that swimming ability is related to the degree of aggregation.

A well-defined circulation pattern, as determined by current velocity, was lacking at my study site. There was no evidence of a clockwise gyre, as suggested by Petrie & Drinkwater (1978), but the relatively low mean (±SD) current velocities (0.001 ± 0.073 to 0.071 ± 0.084 m s^{-1}) are indicative of long residence times (~30 d). The bay is a semi-enclosed system that will retain larvae longer than would occur in regions of the open ocean. There is no major upwelling/downwelling or estuarine circulation, therefore, the upwelling-relaxation (Wing et al. 1995; Miller and Emlet 1997) and tidal-stream transport (DiBacco et al. 2001; Forward Jr et al. 2003) paradigms do not apply in my system. The aggregation diffusion model illustrated that horizontal swimming of

invertebrate larvae (0.0008-0.013 m s^{-1}) is not an effective means of forming aggregations even at modest levels of diffusion. Even though the larval swimming speeds are similar to the mean current velocities, the variability (both as detected by the ADCP and at the diffusion time/length scale of the larvae) likely overwhelms the larval ability to form patterns by swimming horizontally. Interestingly, the level at which aggregations were no longer detectable was directly proportional to larval swimming ability. For example, bryozoans which swim at 0.75 mm s^{-1} did not form noticeable aggregations beyond diffusion indices of 2 m^2 s^{-1} (SD = 120 m h^{-1} or 33 mm s^{-1}), while decapods which swim at 13 mm s^{-1} did not form noticeable aggregations beyond 30 m^2 s^{-1} (SD = 436 m h^{-1} or 129 mm s^{-1}). Also, representative levels of aggregations were achieved in a realistic time scale (30 d), but only at very low levels of diffusion.

I observed that larval horizontal spatial distribution is similar among taxonomic groups and that these spatial patterns change over time. Spatial patterns in larval distributions are affected by larval supply, survival and mortality (*e.g.* predation increases mortality while food availability increases survival) (Grosberg and Levitan 1992; Morgan 1995), as well as by interaction with physical features in the water column, such as internal waves, downwelling fronts, the presence of different water masses or the scale of spatially coherent physical forcing (Pineda 1991, DiBacco et al. 2011, Thompson et al. 2012, Daigle et al. unpublished data). It is unlikely that the similarity in spatial distributions of taxonomic groups in my study were caused by predation, since the most abundant predators in St. George's Bay, scyphozoans (*Cyanea capillata*) and planktivorous fish, were found to differentially select for or against particular species or broader taxonomic groups of meroplanktonic prey (Short et al. 2012). For example, *C.*

capillata was found to select against gastropods and for brachyurans; therefore, this predator would deplete the brachyuran population while having a relatively smaller effect on gastropod population. Spatial distributions of different taxonomic groups would diverge through selective feeding, rather than become more similar if all larvae were preyed upon equally. Food availability is likely not playing a role in determining horizontal patterns in distribution in my study since fluorescence showed greater vertical than horizontal variance. For example, throughout the entire bay, fluorescence measurements ranged from 0.08 to 0.17 at 3 m, while at a single site at different depths, the range was from 0.08 to 0.31. The vertical distribution of a broad range of planktotrophic larval species (bryozoans, carideans and some gastropods) is positively related to fluorescence (Lloyd et al. 2012a; b), suggesting that they aggregate where there is high food availability. However, this does not appear to be the case in my study since the abundance of some species were negatively correlated with fluorescence. Lastly, if the location of larval source was the dominant driver of observed patterns, one would expect to see that: 1) different taxonomic groups might have different regions of high abundance; and 2) larval distributions would be stable over a timescale of days since the benthic adult source population is effectively sessile. Therefore, it is unlikely that larval source affects the observed spatial distributions of larvae over the time scale of days to a week. Consequently, I propose that events occurring after the gamete/larval release, such as dispersal by currents, determined the observed horizontal patterns. Additionally, I suggest that dispersal by currents may have been more important than mortality due to predators, food availability or environmental variables (salinity, temperature, etc) in determining the observed horizontal patterns.

The degree of similarity in spatial distribution among taxonomic groups or species within a sampling date suggests that bay-scale patterns of larval abundance are related to some extent to swimming ability. Gastropods and bivalves have almost identical swimming speeds, while decapods have much higher swimming speeds than the other groups. The distributions of gastropods and bivalves were most strongly correlated, whereas that of decapods was generally weakly correlated with that of other groups. Unexpectedly, decapods were significantly correlated with bryozoans, but this pattern does not appear to be temporally consistent for a particular species of decapod, suggesting that the relationship between decapods and bryozoans may be spurious. This overall pattern was also observed at small-scales (< 10 km) in St. George's Bay (Daigle et al. unpublished data) suggesting that swimming ability is critical to the formation of spatial patterns in the larval distribution at scales from 0.5 up to at least 40 km (the extent of this study).

I have shown with the aggregation-diffusion model that larval horizontal swimming of larvae does not lead to aggregations of appropriate strength under even modest diffusion. Yet, I have also shown that distribution patterns are related to swimming ability. I propose that the horizontal spatial patterns in larval distributions in St. George's Bay are driven mainly by the interaction of swimming with physical features in the water column. Aggregations can form through interaction with internal waves and tidal bores (Shanks 1983; Pineda 1991), by swimming upwards in a downwelling flow (DiBacco et al. 2011), or resulting from filamentation and eddy-eddy interactions (Harrison et al. 2013). In all these aggregation-forming mechanisms, larvae swim against the vertical current and maintain their vertical position, thereby accumulating in the

upwelling or downwelling current. If larvae are able to maintain position in downwelling or upwelling flow, larvae accumulate in these areas like flotsam accumulating in windrows due to Langmuir circulation (Langmuir 1938). However, any larval patchiness generated by Langmuir circulation would be on the order of 100 - 300 m, while the observed spatial scale of larval patches in St. Georges Bay in Aug 2009 was ~3 km (Daigle et al. unpublished data). Additionally, the length of my net tows (~500 m) would not resolve patchiness at that fine a scale. Mesoscale eddies (10 - 100 km) are too large to be responsible for the aggregations I observed, but the related twisting and folding of water masses can produce patterns at scales relevant to my observations (Lévy et al. 2012; Harrison et al. 2013). Submesoscale fronts (1 - 10 km) also occur at a relevant scale, but they only last a few days.

I can estimate the feasibility of larval aggregations forming at scales of a few kilometres in just a few days, by assuming that the median abundance is equal to the non-aggregated background level of larval abundance. In my study, the maximum observed larval abundance was 5, 41, 34 and 13 times more aggregated than the background abundance for bryozoans, bivalves, gastropods and decapods, respectively. If during an event of vertical flux, such as upwelling/downwelling, all larvae are transported to a particular depth by swimming, fully developed aggregations would form within a tidal period (12 h). For example, for bivalves, where the maximum abundance was 41 times larger than the background, there must be a vertical flux of 41 m^3 every 1 m^3 over 12 h. This would require vertical transport of 0.78 mm s^{-1} [41 m / 12 h converted to mm s^{-1} or 41 m × 1000 mm m^{-1} / (12 h × 3600 s h^{-1})]. At the other extreme, bryozoans would require vertical transport of 0.12 mm s^{-1} [5 m × 1000 mm m^{-1} / (12 h × 3600 s h^{-1})] over

the same time period, or fully developed aggregations could develop in under 2 h given a vertical transport of 0.78 mm s^{-1}. This range of vertical current speeds is within the range that I measured with the ADCP (0.07 (± 2.3) mm s^{-1} to 0.83 (± 5.0) mm s^{-1}).

Since the interactions between swimming and current velocity occur at fairly small scales (< 3 km), I believe that the most effective method of measuring larval dispersal will occur at these small scales, most often along the vertical axis (i.e. over depth). I propose that large scale meroplankton surveys can be a useful tool to study patterns in biogeography, but not the most effective method to measure larval dispersal. Instead, both smaller scale field studies and laboratory experiments could be useful to evaluate behavioural (*i.e.* swimming) interactions among physical features in the water column on the vertical axis.

CHAPTER 6: CONCLUSIONS

Overall, this thesis has increased our understanding of mechanisms that influence larval dispersal in marine benthic invertebrates, particularly in the absence of strong oceanographic features. I demonstrated that: 1) the larval response to environmental cues can be modelled if the behavioural model is appropriately parameterized, and 2) it is likely that larval dispersal and aggregation are primarily affected by physical processes. These findings will improve current bio-physical models, which are the best tool available to model realistic dispersal trajectories. To be successful, such a model should 1) incorporate relevant larval behaviours, and 2) resolve physical features with which larvae may interact at relevant scales. This thesis addresses the first attribute by identifying thermal stratification as one mechanism that can regulate larval vertical distributions either by acting as a barrier to vertical migration or because the temperature can modulate vertical swimming velocities. I addressed the second attribute by eximing the mechanisms that affect larval distributions, as well as by quantifying the spatial scale and level of aggregation of these larval distributions.

In **Chapter 2**, I demonstrated that thermal stratification affects the vertical distribution of larval *S. droebachiensis*, *A. rubens* and *A. irradians*. For *A. irradians*, the thermal gradient acted as a barrier to migration, effectively preventing most larvae from swimming to the top layer of the water column. Conversely, in both species of echinoderms, the presence or strength of the thermal gradient did not appear to be as important in regulating vertical distribution as the temperature experienced by the larvae. In **Chapter 3**, I developed a random walk based model using *S. droebachiensis* as a model organism to demonstrate the mechanism responsible for the effects observed in

Chapter 2. In this case, the key to successfully simulating larval response to temperature was determining the temperature-dependent distribution of vertical swimming velocities and the temporal autocorrelation in these velocities.

In **Chapters 4 & 5**, the most striking and consistent pattern was that the larval distributions for species and taxonomic groups with similar swimming abilities were significantly correlated to one another at all scales (0.5 to 40 km). This suggests a common mechanism, related to larval swimming ability, which greatly influences the horizontal larval distribution. In **Chapter 5**, I suggest that these patterns are not primarily related to predation, food availability, environmental variables (salinity, temperature, etc) or the location of the larval source, but instead are likely related to dispersal and aggregation due to currents. In **Chapter 4**, I presented evidence which suggests that the spatial scale of variability in larval distributions (~ 3 km) matches that in both the environmental variables and of coherent structures in current velocities (i.e. the tidal excursion). In **Chapter 5**, I demonstrated that horizontal larval swimming could not be responsible for the observed level of aggregation in the larval horizontal distributions. Together, these 2 chapters provide compelling evidence that horizontal distributions are largely affected by physical processes, even in the absence of strong oceanographic features. I suggest that these horizontal patterns are the result of 1) an aggregative process (*i.e.* larvae swimming against a vertical current maintaining their vertical position) and 2) a diffusive process which scales the aggregations to the scale of the coherent structures in current velocity (*i.e.* tidal excursion). Structures that are smaller than that scale will be effectively homogenized by flow structures with low coherence.

Within the overall CHONe goals this thesis provides useful information comparing the roles of larval behaviour and dispersal on larval distributions between weaker swimmers and the stronger swimming larvae (*Homarus americanus*). Similarly, comparisons between dispersal trajectories of simulated larvae (including their behaviours) and those of magnetically attractive particles will prove interesting. Given that these particles are slightly positively buoyant, they should aggregate in areas of downwelling. This means that if my suggestions in **Chapter 5** indeed apply, a high of number sampled particles should coincide with a high abundance of larvae since similar aggregation mechanisms may be at work. There is a substantial amount of data on the vertical distribution of benthic invertebrate larvae in St. George's Bay (Lloyd et al. 2012a; b). Combining the data available on vertical distributions, a bio-physical model of St. George's Bay which models larval behavioural mechanisms identified in **Chapters 2 & 3** as well as the identified deterministic processes that affect horizontal distributions in **Chapters 4 & 5,** could prove powerful in the simulation of realistic larval dispersal trajectories.

Specifically, I propose to examine the roles of vertical swimming and vertical distribution on larval dispersal and aggregation using a bio-physical model. The model can be seeded with simulated larvae (SL) with either a static depth distribution, or, if possible, by "reverse engineering" larval behaviour based on the vertical distributions and known environmental cues. For this reverse engineering, I would use the vertical velocity autocorrelation relationship from **Chapter 3** and I would rely on the idea that the PDF of vertical swimming velocities is cue dependent. I will compare dispersal distance and rentention in the bay among species with contrasting larval behaviours and vertical

distributions. Patterns in aggregation and pattern formation can be examined by seeding the model with SL of different swimming abilities and different responses to downwelling, and upwelling. Modelling results can be compared to the levels of larval aggregation and spatial autocorrelation patterns that were empirically determined in **Chapter 4** & **5**.

In conclusion, this thesis and the proposed work will increase our understanding of larval behaviour and its effects on larval dispersal. **Chapters 2** & **3** can serve as a case study in which a model that could be used in a bio-physical model is developed from observations of vertical distributions and larval behaviour. In **Chapters 4** & **5**, I have highlighted mechanisms which affect larval dispersal (diffusion scaled to coherent structures in flow, and aggregation by vertical swimming against vertical currents) that are broadly applicable to marine benthic invertebrate larvae and likely other planktonic organisms. For example, such universally applicable mechanisms would tremendously simplify the task of estimating population connectivity for all species within a network of MPAs since the functional diversity of behaviours that affect dispersal trajectories is effectively reduced.

References

Banas, N. S., P. S. McDonald, and D. A. Armstrong. 2009. Green Crab Larval Retention in Willapa Bay, Washington: An Intensive Lagrangian Modeling Approach. Estuaries and Coasts **32**: 893–905.

Banse, K. 1986. Vertical distribution and horizontal transport of planktonic larvae of echinoderms and benthic polychaetes in an open coastal sea. Bulletin of Marine Science **39**: 162–175.

Bartumeus, F., M. G. E. Da Luz, G. M. Viswanathan, J. Catalan, and F. R. B. Artumeus. 2005. Animal search strategies: a quantitative random-walk analysis. Ecology **86**: 3078–3087.

Benhamou, S., and P. Bovet. 1989. How animals use their environment: a new look at kinesis. Animal Behaviour **38**: 375–383.

Botsford, L. W., F. Micheli, and A. Hastings. 2003. Principles for the design of marine reserves. Ecological Applications **13**: S25–S31.

Boudreau, B., Y. Simard, and E. Bourget. 1992. Influence of a thermocline on vertical distribution and settlement of post-larvae of the American lobster Homarus americanus Milne-Edwards. Journal of Experimental Marine Biology and Ecology **162**: 35.

Bradbury, I. R., and P. V. R. Snelgrove. 2001. Contrasting larval transport in demersal fish and benthic invertebrates: the roles of behaviour and advective processes in determining spatial pattern. Canadian Journal of Fisheries and Aquatic Sciences **58**: 811–823.

Browman, H. I., K. I. Stergiou, C. H. I. Browman, P. M. Cury, R. Hilborn, S. Jennings, H. K. Lotze, P. M. Mace, S. Murawski, D. Pauly, M. Sissenwine, and D. Zeller. 2004. Perspectives on ecosystem-based approaches to the management of marine resources. Marine Ecology Progress Series **274**: 269–303.

Brown, R. 1828. A brief account of microscopical observations made in the months of June, July and August, 1827, on the particles contained in the pollen of plants; and the general existence of active molecules in organic and inorganic bodies. Philosophical Magazine **4**: 161–173.

Burdett-Coutts, V., and A. Metaxas. 2004. The effect of the quality of food patches on larval vertical distribution of the sea urchins Lytechinus variegatus (Lamarck) and Strongylocentrotus droebachiensis (Mueller). Journal of Experimental Marine Biology and Ecology **308**: 221–236.

Chan, K., and D. Grünbaum. 2010. Temperature and diet modified swimming behaviors of larval sand dollar. Marine Ecology Progress Series **415**: 49–59.

Chia, F.-S., J. Buckland-Nicks, and C. M. Young. 1984. Locomotion of marine invertebrate larvae: a review. Canadian Journal of Zoology **62**: 1205–1222.

Cianelli, D., M. Uttieri, J. R. Strickler, and E. Zambianchi. 2009. Zooplankton encounters in patchy particle distributions. Ecological Modelling **220**: 596–604.

Codling, E. A., M. J. Plank, and S. Benhamou. 2008. Random walk models in biology. Journal of the Royal Society: Interface **5**: 813–34.

Corell, H., P. Moksnes, a Engqvist, K. Döös, and P. Jonsson. 2012. Depth distribution of larvae critically affects their dispersal and the efficiency of marine protected areas. Marine Ecology Progress Series **467**: 29–46.

Cowen, R. K., G. Gawarkiewicz, J. Pineda, S. R. Thorrold, and F. Werner. 2002. Population Connectivity in Marine Systems Population Connectivity in Marine Systems.

Cowen, R. K., G. Gawarkiewicz, J. Pineda, S. R. Thorrold, and F. E. Werner. 2007. Population connectivity in marine systems: an overview. Ocean **20**: 14–21.

Cowen, R. K., and S. Sponaugle. 2009. Larval Dispersal and Marine Population Connectivity. Annual Review of Marine Science **1**: 443–466.

Cox, D. R., and P. A. W. Lewis. 1966. The statistical analysis of series of events, CRC Monographs.

Cronin, T. W., and R. B. Forward Jr. 1986. Vertical migration cycles of crab larvae and their role in larval dispersal. Bulletin of Marine Science **39**: 192–201.

Daigle, R. M., and A. Metaxas. 2011. Vertical distribution of marine invertebrate larvae in response to thermal stratification in the laboratory. Journal of Experimental Marine Biology and Ecology **409**: 89–98.

Daigle, R. M., and A. Metaxas. 2012. Modeling of the larval response of green sea urchins to thermal stratification using a random walk approach. Journal of Experimental Marine Biology and Ecology **438**: 14–23.

Dekshenieks, M. M., E. E. Hofmann, J. M. Klinck, E. N. Powell, and E. Hofmannl. 1996. Modeling the vertical distribution of oyster larvae in response to environmental conditions. Marine Ecology Progress Series **136**: 97–110.

DiBacco, C., H. L. Fuchs, J. Pineda, and K. Helfrich. 2011. Swimming behavior and velocities of barnacle cyprids in a downwelling flume. Marine Ecology Progress Series **433**: 131–148.

DiBacco, C., and L. a. Levin. 2000. Development and application of elemental fingerprinting to track the dispersal of marine invertebrate larvae. Limnology and Oceanography **45**: 871–880.

DiBacco, C., D. Sutton, and L. McConnico. 2001. Vertical migration behavior and horizontal distribution of brachyuran larvae in a low-inflow estuary: implications for bay-ocean exchange. Marine Ecology Progress Series **217**: 191–206.

Dobretsov, S. V, and G. Miron. 2001. Larval and post-larval vertical distribution of the mussel Mytilus edulis in the White Sea. Marine Ecology Progress Series **218**: 179–187.

Edwards, K. P., J. A. Hare, F. E. Werner, and H. Seim. 2007. Using 2-dimensional dispersal kernels to identify the dominant influences on larval dispersal on continental shelves. Marine Ecology Progress Series **352**: 77–87.

Einstein, A. 1956. Investigations on the Theory of Brownian Movement, Courier Dover Publications.

Epifanio, C. E., C. C. Valenti, and A. E. Pembroke. 1984. Dispersal and recruitment of blue crab larvae in Delaware Bay, USA. Estuarine, Coastal and Shelf Science **18**: 1–12.

Folt, C. L., and C. W. Burns. 1999. Biological drivers of zooplankton patchiness. Trends in Ecology & Evolution **14**: 300–305.

Forward Jr, R. B., R. A. Tankersley, and J. M. Welch. 2003. Selective tidal-stream transport of the blue crab Callinectes sapidus: an overview. Bulletin of Marine Science **72**: 347–365.

Fuchs, H. L., M. G. Neubert, and L. S. Mullineaux. 2007. Effects of turbulence-mediated larval behavior on larval supply and settlement in tidal currents. Limnology and Oceanography **52**: 1156–1165.

Gaines, S., and J. Roughgarden. 1985. Larval settlement rate: A leading determinant of structure in an ecological community of the marine intertidal zone. Proceedings of the National Academy of Sciences of the United States of America **82**: 3707–11.

Gallager, S. M., J. L. Manuel, D. a. Manning, and R. K. O'Dor. 1996. Ontogenetic changes in the vertical distribution of giant scallop larvae, Placopecten magellanicus, in 9-m deep mesocosms as a function of light, food, and temperature stratification. Marine Biology **124**: 679–692.

Gregory, D. 2004. Climate: a database of temperature and salinity observations for the northweat Atlantic. Fisheries & Oceans Canada, Science, Canadian Science Advisory Secretariat

Grosberg, R. K., and D. R. Levitan. 1992. For adults only? Supply-side ecology and the history of larval biology. Trends in ecology & evolution **7**: 130–3.

Halpern, B. 2003. The impact of marine reserves: do reserves work and does reserve size matter? Ecological applications **13**: S117–S137.

Harper, F. M., and M. W. Hart. 2005. Gamete compatibility and sperm competition affect paternity and hybridization between sympatric Asterias sea stars. The Biological bulletin **209**: 113–26.

Harrison, C. S., D. A. Siegel, and S. Mitarai. 2013. Filamentation and eddy−eddy interactions in marine larval accumulation and transport. Marine Ecology Progress Series **472**: 27–44.

Hughes, T. P., A. H. Baird, E. A. Dinsdale, N. A. Moltschaniwskyj, M. S. Pratchett, J. E. Tanner, B. L. Willis, and M. Biology. 2000. Supply-side ecology works both ways: the link between benthic adults, fecundity, and larval recruits. Ecology **81**: 2241–2249.

Hurlbert, S. 1990. Spatial distribution of the montane unicorn. Oikos **58**: 257–271.

Jillett, J. B. 1976. Zooplankton associations off otago peninsula, south-□eastern New Zealand, related to different water masses. New Zealand Journal of Marine and Freshwater Research **10**: 543–557.

Jonsson, P. R. 1989. Vertical distribution of planktonic ciliates - an experimental analysis of swimming behaviour. Marine Ecology Progress Series **52**: 39–53.

Jørgensen, C. B., P. S. Larsen, and H. U. Riisgård. 1990. Effects of temperature on the mussel pump. Marine Ecology Progress Series **64**: 86–87.

Kaplan, D. 2006. Alongshore advection and marine reserves: consequences for modeling and management. Marine Ecology Progress Series **309**: 11–24.

Kashenko, S. D. 2005. Responses of Embryos and Larvae of the Starfish Asterias amurensis to Changes in Temperature and Salinity. Russian Journal of Marine Biology **31**: 294–302.

Kingsford, M. J., J. M. Leis, A. L. Shanks, K. C. Lindeman, S. G. Morgan, and J. Pineda. 2002. Sensory environments, larval abilities and local self-recruitment. Bulletin of Marine Science **70**: 309–340.

Kinlan, B. P., S. D. Gaines, and S. E. Lester. 2005. Propagule dispersal and the scales of marine community process. Diversity and Distributions **11**: 139–148.

Langmuir, I. 1938. Surface motion of water induced by wind. Science **87**: 119–123.

Largier, J. L. 2003. Considerations in estimating larval dispersal distances from oceanographic data. Ecological Applications **13**: 71–89.

Larsen, P. S., C. V Madsen, and H. U. Riisgård. 2008. Effect of temperature and viscosity on swimming velocity of the copepod Acartia tonsa, brine shrimp Artemia salina and rotifer Brachionus plicatilis. Aquatic Biology **4**: 47–54.

Legendre, P., and L. Legendre. 1998. Numerical ecology, 2nd Englis. Elsevier.

Levin, L. A. 2006. Recent progress in understanding larval dispersal: new directions and digressions. Integrative and comparative biology **46**: 282–97.

Lévy, M., R. Ferrari, P. J. S. Franks, A. P. Martin, and P. Rivière. 2012. Bringing physics to life at the submesoscale. Geophysical Research Letters **39**: L14602.

Lloyd, M. J., A. Metaxas, and B. DeYoung. 2012a. Patterns in vertical distribution and their potential effects on transport of larval benthic invertebrates in a shallow embayment. Marine Ecology Progress Series **469**: 37–52.

Lloyd, M. J., A. Metaxas, and B. DeYoung. 2012b. Physical and biological factors affect the vertical distribution of larvae of benthic gastropods in a shallow embayment. Marine Ecology Progress Series **464**: 135–151.

López-Duarte, P. C., H. S. Carson, G. S. Cook, F. J. Fodrie, B. J. Becker, C. Dibacco, and L. a Levin. 2012. What Controls Connectivity? An Empirical, Multi-Species Approach. Integrative and comparative biology **52**: 1–14.

López-Duarte, P. C., and R. a. Tankersley. 2007. Circatidal swimming behavior of brachyuran crab zoea larvae: implications for ebb-tide transport. Marine Biology **151**: 2037–2051.

Ma, H., J. P. Grassle, and R. J. Chant. 2006. Vertical distribution of bivalve larvae along a cross-shelf transect during summer upwelling and downwelling. Marine Biology **149**: 1123–1138.

Mackas, D. L. 1984. Spatial Autocorrelation of Plankton Community Composition in a Continental Shelf Ecosystem. Limnology and Oceanography **29**: 451–471.

Manuel, J. L., and R. K. O'Dor. 1997. Vertical migration for horizontal transport while avoiding predators: I. A tidal/diel model. Journal of Plankton Research **19**: 1929–1947.

Manuel, J. L., C. M. Pearce, D. A. Manning, and R. K. O'Dor. 2000. The response of sea scallop (Placopecten magellanicus) veligers to a weak thermocline in 9-m deep mesocosms. Marine Biology **137**: 169–175.

Martin, A. P. 2003. Phytoplankton patchiness: the role of lateral stirring and mixing. Progress In Oceanography **57**: 125–174.

McArdle, B. H. 1988. The structural relationship: regression in biology. Canadian Journal of Zoology **66**: 2329–2339.

McConnaughey, R. A., and S. D. Sulkin. 1984. Measuring the effects of thermoclines on the vertical migration of larvae of Callinectes sapidus (Brachyura: Portunidae) in the laboratory. Marine Biology **81**: 139–145.

McEdward, L. 1995. Ecology of marine invertebrate larvae, M.J. Kennish and P.M. Lutz [eds.]. CRC Marine Science Series, 6 CRC Press.

Meidel, S. K., and R. E. Scheibling. 1998. Annual reproductive cycle of the green sea urchin, Strongylocentrotus droebachiensis , in differing habitats in Nova Scotia, Canada. Marine Biology **131**: 461–478.

Menge, B. A., F. Chan, K. J. Nielsen, E. Di Lorenzo, and J. Lubchenco. 2009. Climatic variation alters supply-side ecology: impact of climate patterns on phytoplankton and mussel recruitment. Ecological Monographs **79**: 379–395.

Metaxas, A., and V. Burdett-Coutts. 2006. Response of invertebrate larvae to the presence of the ctenophore Bolinopsis infundibulum, a potential predator. Journal of Experimental Marine Biology and Ecology **334**: 187–195.

Metaxas, A., L. S. Mullineaux, and J. Sisson. 2009. Distribution of echinoderm larvae relative to the halocline of a salt wedge. Marine Ecology Progress Series **377**: 157–168.

Metaxas, A., and M. I. Saunders. 2009. Quantifying the "bio-" components in biophysical models of larval transport in marine benthic invertebrates: advances and pitfalls. The Biological bulletin **216**: 257–72.

Metaxas, A., and C. M. Young. 1998. Behaviour of echinoid larvae around sharp haloclines: effects of the salinity gradient and dietary conditioning. Marine Biology **131**: 443–459.

Miller, B. A., and R. B. Emlet. 1997. Influence of nearshore hydrodynamics on larval abundance and settlement of sea urchins Strongylocentrotus franciscanus and S. purpuratus in the Oregon upwelling. Marine Ecology Progress Series **148**: 83–94.

Miller, S., S. Morgan, J. White, and P. Green. 2013. Interannual variability in an atlas of trace element signatures for determining population connectivity. Marine Ecology Progress Series **474**: 179–190.

Morgan, S. G. 1995. Life and Death in the Plankton: Larval Mortality and Adaptation, p. 279–322. *In* L. McEdwards [ed.], Ecology of Marine Invertebrate Larvae. CRC Press.

Morisita, M. 1959. Measuring of the dispersion of individuals and analysis of the distributional patterns. Memoirs of the Faculty of Science, Kyushu University, Series E **2**.

North, E. W., Z. Schlag, R. R. Hood, M. Li, L. Zhong, T. Gross, and V. S. Kennedy. 2008. Vertical swimming behavior influences the dispersal of simulated oyster larvae in a coupled particle-tracking and hydrodynamic model of Chesapeake Bay. Marine Ecology Progress Series **359**: 99–115.

O'Connor, M. I., J. F. Bruno, S. D. Gaines, B. S. Halpern, S. E. Lester, B. P. Kinlan, and J. M. Weiss. 2007. Temperature control of larval dispersal and the implications for marine ecology, evolution, and conservation. Proceedings of the National Academy of Sciences of the United States of America **104**: 1266–71.

Oksanen, J., F. G. B. R. Kindt, P. Legendre, P. R. Minchin, R. B. O'Hara, G. L. Solymos, S. Peter, M. Henry, H. Stevens, and H. Wagner. 2012. Community Ecology Package.

Okubo, A. 1977. Horizontal dispersion and critical scales for phytoplankton patches, p. 21–42. *In* J.H. Steele [ed.], Spatial Pattern in Plankton Communities. Plenum Press.

Olson, R. R. 1985. The consequences of short-distance larval dispersal in a sessile marine invertebrate. Ecology **66**: 30–39.

Olson, R. R., and M. H. Olson. 1989. Food limitation of planktotrophic marine invertebrate larvae: does it control recruitment success? Annual Review of Ecology and Systematics **20**: 225–47.

Omori, M., and W. M. Hamner. 1982. Patchy distribution of zooplankton: behavior, population assessment and sampling problems. Marine biology **72**: 193–200.

Palumbi, S. R. 2003. Population genetics, demographic connectivity, and the design of marine reserves. Ecological applications **13**: 146–158.

Palumbi, S. R. 2004. MARINE RESERVES AND OCEAN NEIGHBORHOODS: The Spatial Scale of Marine Populations and Their Management. Annual Review of Environment and Resources **29**: 31–68.

Pennington, J. T., and R. B. Emlet. 1986. Ontogenetic and diel vertical migration of a planktonic echinoid larva, Dendraster excentricus (Eschscholtz): Occurrence, causes, and probable consequences. Journal of Experimental Marine Biology and Ecology **104**: 69–95.

Pennington, J. T., and R. R. Strathmann. 1990. Consequences of the Calcite Skeletons of Planktonic Echinoderm Larvae for Orientation, Swimming, and Shape. Biological Bulletin **179**: 121.

Petrie, B., and K. Drinkwater. 1978. Circulation in an open bay. Journal of the Fisheries Board of Canada **35**: 1116–1123.

Pineda, J. 1991. Predictable upwelling and the shoreward transport of planktonic larvae by internal tidal bores. Science **253**: 548.

Podolsky, R. D. 1994. Temperature and water viscosity: physiological versus mechanical effects on suspension feeding. Science **265**: 100–103.

Podolsky, R. D., and R. B. Emlet. 1993. Separating the effects of temperature and viscosity on swimming and water movement by sand dollar larvae (Dendraster excentricus). Journal of Experimental Biology **176**: 207–221.

Porch, C. E. 1998. A theoretical comparion of the contributions of random swimming and turbulence to absolute dispersal in the sea. Bulletin of Marine Science **62**: 31–44.

Poulin, E., A. T. Palma, G. Leiva, D. Narvaez, R. Pacheco, A. Navarrete, J. C. Castilla, and S. A. Navarrete. 2002. Avoiding offshore transport of competent larvae during upwelling events : The case of the gastropod Concholepas concholepas in Central Chile. Limnology and Oceanography **47**: 1248–1255.

Queiroga, H., and J. Blanton. 2005. Interactions between behaviour and physical forcing in the control of horizontal transport of decapod crustacean larvae.,.

Rangel, T. F., J. A. F. Diniz-Filho, and L. M. Bini. 2010. SAM: a comprehensive application for Spatial Analysis in Macroecology. Ecography **33**: 46–50.

Rothlisberg, P. C., J. A. Church, A. M. G. Forbes, and J. A. Churcb. 1983. Modelling the advection of vertically migrating shrimp larvae. Journal of Marine Research **41**: 511–538.

Rumrill, S. S. 1990. Natural mortality of marine invertebrate larvae. Ophelia **32**.

Ryland, J. S. 1977. Taxes and tropisms of bryozoans, p. 441–436. *In* R.M. Woollacott and R.L. Zimmer [eds.], Biology of Bryozoans. Academic Press.

Sameoto, J. A., and A. Metaxas. 2008a. Can salinity-induced mortality explain larval vertical distribution with respect to a halocline? The Biological bulletin **214**: 329–38.

Sameoto, J. A., and A. Metaxas. 2008b. Interactive effects of haloclines and food patches on the vertical distribution of 3 species of temperate invertebrate larvae. Journal of Experimental Marine Biology and Ecology **367**: 131–141.

Saunders, M. I., and A. Metaxas. 2010. Physical forcing of distributions of bryozoan cyphonautes larvae in a coastal embayment. Marine Ecology Progress Series **418**: 131–145.

Scheltema, R. S. 1986. On dispersal and planktonic larvae of benthic invertebrates: an eclectic overview and summary of problems. Bulletin of Marine Science **39**: 290–322.

Shanks, A. 1983. Surface slicks associated with tidally forced internal waves may transport pelagic larvae of benthic invertebrates and fishes shoreward. Marine Ecology Progress Series **13**: 311–315.

Shanks, A. L. 1995. Orientated swimming by megalopae of several eastern North Pacific crab species and its potential role in their onshore migration. Journal of Experimental Marine Biology and Ecology **186**: 1–16.

Shanks, A. L. 2009. Pelagic larval duration and dispersal distance revisited. The Biological bulletin **216**: 373–85.

Shanks, A. L., and L. A. Brink. 2005. Upwelling , downwelling , and cross-shelf transport of bivalve larvae : test of a hypothesis. Marine Ecology Progress Series **302**: 1–12.

Shanks, A. L., J. L. Largier, L. A. Brink, J. Brubaker, and R. Hooff. 2002. Observations on the distribution of meroplankton during a downwelling event and associated intrusion of the Chesapeake Bay estuarine plume. Journal of Plankton Research **24**: 391–416.

Shanks, A. L., J. L. Largier, L. Brink, and J. Brubaker. 2000. Demonstration of the onshore transport of larval invertebrates by the shoreward movement of an upwelling front. Limnology and Oceanography

Sharqawy, M. H., J. H. Lienhard, and S. M. Zubair. 2010. The thermophysical properties of seawater: A review of existing correlations and data. Desalination and Water Treatment **16**: 354–380.

Short, J., A. Metaxas, and R. M. Daigle. 2012. Predation of larval benthic invertebrates in St George's Bay, Nova Scotia. Journal of the Marine Biological Association of the United Kingdom 1–9.

Sokal, R. R. 1978. Spatial autocorrelation in biology 2. Some biological implications and four applications of evolutionary and ecological interest. Biological Journal of the Linnean Society **10**: 199–228.

Stanley, R., P. V. R. Snelgrove, B. Deyoung, and R. S. Gregory. 2012. Dispersal Patterns, Active Behaviour, and Flow Environment during Early Life History of Coastal Cold Water Fishes. PloS one **7**: e46266.

Steele, J. H. 1976. Patchiness, *In* D.H. Cushing and J.J. Walsh [eds.], The Ecology of the Seas. W. B. Saunders Co.

Stephens, R. E. 1972. Studies on the development of the sea urchin Strongylocentrotus droebachiensis. I. Ecology and normal development. The Biological Bulletin **142**: 132–144.

Strathmann, R. R. 1971. The feeding behavior of planktotrophic echinoderm larvae: mechanisms, regulation, and rates of suspensionfeeding. Journal of Experimental Marine Biology and Ecology **6**: 109–160.

Tamaki, A., S. Mandal, Y. Agata, I. Aoki, T. Suzuki, H. Kanehara, T. Aoshima, Y. Fukuda, H. Tsukamoto, and T. Yanagi. 2010. Complex vertical migration of larvae of the ghost shrimp, Nihonotrypaea harmandi, in inner shelf waters of western Kyushu, Japan. Estuarine, Coastal and Shelf Science **86**: 125–136.

Tapia, F. J., C. DiBacco, J. Jarrett, and J. Pineda. 2010. Vertical distribution of barnacle larvae at a fixed nearshore station in southern California: Stage-specific and diel patterns. Estuarine, Coastal and Shelf Science **86**: 265–270.

Tapia, F. J., and J. Pineda. 2007. Stage-specific distribution of barnacle larvae in nearshore waters: potential for limited dispersal and high mortality rates. Marine Ecology Progress Series **342**: 177–190.

Team, R. C. 2012. R: A language and environment for statistical computing. R Foundation for Statistical Computing

Tettelbach, S., and E. Rhodes. 1981. Combined effects of temperature and salinity on embryos and larvae of the northern bay scallop Argopecten irradians irradians*. Marine biology **256**: 249–256.

Thompson, C., R. York, and S. Gallager. 2012. Species-specific abundance of bivalve larvae in relation to biological and physical conditions in a Cape Cod estuary. Marine Ecology Progress Series **469**: 53–69.

Tremblay, M. J., and M. M. Sinclair. 1988. The vertical and horizontal distribution of sea scallop (Placopecten magellanicus) larvae in the Bay of Fundy in 1984 and 1985. Journal of Northwest Atlantic Fishery Science **8**: 43–53.

Tremblay, M. J., and M. M. Sinclair. 1990. Sea scallop larvae Placopecten magellanicus on Georges Bank: Vertical distribution in relation to water column stratification and food. Marine Ecology Progress Series **61**: 1–15.

Underwood, A., and P. Fairweather. 1989a. Supply-side ecology and benthic marine assemblages. Trends in Ecology & Evolution **4**: 16–20.

Underwood, A. J. 1997. Experiments in Ecology: Their Logical Design and Interpretation Using Analysis of Variance, Cambridge University Press.

Underwood, A. J., and P. G. Fairweather. 1989b. Supply-side ecology and benthic marine assemblages. Trends in Ecology & Evolution **4**: 16–20.

Vázquez, E., J. Ameneiro, S. Putzeys, C. Gordo, and P. Sangrà. 2007. Distribution of meroplankton communities in the Bransfield Strait , Antarctica. Marine Ecology Progress Series **338**: 119–129.

Weersing, K., and R. Toonen. 2009. Population genetics, larval dispersal, and connectivity in marine systems. Marine Ecology Progress Series **393**: 1–12.

Wehrtmann, I. 1994. Larval production of the caridean shrimp, Crangon septemspinosa, in waters adjacent to Chesapeake Bay in relation to oceanographic conditions. Estuaries and Coasts **17**: 509–518.

Wing, S. R., J. L. Largier, L. W. Botsford, J. F. Quinn, M. Cisneros, K. Arico, L. Morgan, and K. Higgins. 1995. Settlement and transport of benthic invertebrates in an intermittent upwelling reg :) ion. **40**: 316–329.

Yamazaki, H. 1993. Lagrangian study of planktonic organisms: perspectives. Bulletin of Marine Science **53**: 265–278.

Young, C. M. 1995. Behavior and locomotion during the dispersal phase of larval life, p. 249–277. *In* L. McEdward [ed.], Ecology of Marine Invertebrate Larvae. CRC Press.

Zar, J. H. 1999. Biostatistical analysis, Upper Saddle River, N.J, Prentice Hall.

Appendix I: Copyright Permissions

Copyright licence transfer from the Journal of Experimental Marine Biology and Ecology

Request:

April 20, 2013

Journal of Experimental Marine Biology and Ecology
Dr. Simon F. Thrush, Editor-in-Chief
National Institute of Water and Atmospheric Research (NIWA),
Hamilton, New Zealand

I am preparing my PhD thesis for submission to the Faculty of Graduate Studies at Dalhousie University, Halifax, Nova Scotia, Canada. I am seeking your permission to include a manuscript version of the following paper(s) as a chapter in the thesis:

Daigle, R. M., and A. Metaxas. 2011. Vertical distribution of marine invertebrate larvae in response to thermal stratification in the laboratory. Journal of Experimental Marine Biology and Ecology 409: 89–98.

Daigle, R. M., and A. Metaxas. 2012. Modeling of the larval response of green sea urchins to thermal stratification using a random walk approach. Journal of Experimental Marine Biology and Ecology 438: 14–23.

Canadian graduate theses are reproduced by the Library and Archives of Canada (formerly National Library of Canada) through a non-exclusive, world-wide license to reproduce, loan, distribute, or sell theses. I am also seeking your permission for the material described above to be reproduced and distributed by the LAC(NLC). Further details about the LAC(NLC) thesis program are available on the LAC(NLC) website (www.nlc-bnc.ca).

Full publication details and a copy of this permission letter will be included in the thesis.

Yours sincerely,

Rémi M. Daigle

Permission is granted for:

a) the inclusion of the material described above in your thesis.
b) for the material described above to be included in the copy of your thesis that is sent to the Library and Archives of Canada (formerly National Library of Canada) for reproduction and distribution.

Name: Title:

Signature: Date:

Response 1

ELSEVIER LICENSE
TERMS AND CONDITIONS

May 07, 2013

This is a License Agreement between Remi M Daigle ("You") and Elsevier ("Elsevier") provided by Copyright Clearance Center ("CCC"). The license consists of your order details, the terms and conditions provided by Elsevier, and the payment terms and conditions.

All payments must be made in full to CCC. For payment instructions, please see information listed at the bottom of this form.

Supplier	Elsevier Limited The Boulevard,Langford Lane Kidlington,Oxford,OX5 1GB,UK
Registered Company Number	1982084
Customer name	Remi M Daigle
Customer address	502-1239 Barrington St Halifax, NS B3J 1Y3
License number	3143771055296
License date	May 07, 2013
Licensed content publisher	Elsevier
Licensed content publication	Journal of Experimental Marine Biology and Ecology
Licensed content title	Vertical distribution of marine invertebrate larvae in response to thermal stratification in the laboratory
Licensed content author	Rémi M. Daigle,Anna Metaxas
Licensed content date	1 December 2011
Licensed content volume number	409
Licensed content issue number	1–2
Number of pages	10
Start Page	89
End Page	98
Type of Use	reuse in a thesis/dissertation
Portion	full article
Format	both print and electronic

Are you the author of this Elsevier article?	Yes
Will you be translating?	No
Order reference number	
Title of your thesis/dissertation	EFFECTS OF LARVAL SWIMMING BEHAVIOUR ON THE VERTICAL AND HORIZONTAL DISTRIBUTION PATTERNS OF MARINE INVERTEBRATE LARVAE
Expected completion date	May 2013
Estimated size (number of pages)	200
Elsevier VAT number	GB 494 6272 12
Permissions price	0.00 USD
VAT/Local Sales Tax	0.0 USD / 0.0 GBP
Total	0.00 USD

Response 2

ELSEVIER LICENSE
TERMS AND CONDITIONS

May 07, 2013

This is a License Agreement between Remi M Daigle ("You") and Elsevier ("Elsevier") provided by Copyright Clearance Center ("CCC"). The license consists of your order details, the terms and conditions provided by Elsevier, and the payment terms and conditions.

All payments must be made in full to CCC. For payment instructions, please see information listed at the bottom of this form.

Supplier	Elsevier Limited The Boulevard,Langford Lane Kidlington,Oxford,OX5 1GB,UK
Registered Company Number	1982084
Customer name	Remi M Daigle
Customer address	502-1239 Barrington St Halifax, NS B3J 1Y3
License number	3143771421870
License date	May 07, 2013
Licensed content publisher	Elsevier
Licensed content publication	Journal of Experimental Marine Biology and Ecology
Licensed content title	Modeling of the larval response of green sea urchins to thermal stratification using a random walk approach
Licensed content author	Rémi M. Daigle,Anna Metaxas
Licensed content date	30 December 2012
Licensed content volume number	438

Licensed content issue number	
Number of pages	10
Start Page	14
End Page	23
Type of Use	reuse in a thesis/dissertation
Intended publisher of new work	other
Portion	full article
Format	both print and electronic
Are you the author of this Elsevier article?	Yes
Will you be translating?	No
Order reference number	
Title of your thesis/dissertation	EFFECTS OF LARVAL SWIMMING BEHAVIOUR ON THE VERTICAL AND HORIZONTAL DISTRIBUTION PATTERNS OF MARINE INVERTEBRATE LARVAE
Expected completion date	May 2013
Estimated size (number of pages)	200
Elsevier VAT number	GB 494 6272 12
Permissions price	0.00 USD
VAT/Local Sales Tax	0.0 USD / 0.0 GBP
Total	0.00 USD

Appendix II: Source Codes

Vertical position random walk model

```
%% modifiable model parameters
clear

ts=1;                           %timestep length (s)
n=3600/ts;                      %number of timesteps (set for 1h)
npart=300;                      %number of particles
rep=100;                        %number of replicates
B=3:3:9;                        %temperature of bottom layer (°C)
DT=[0,3,6,12];


swimsd20=sqrt(0.0988)*10^-3;                            %magnitude of
random larval swimming displacement (m s^-1) ->std of residual
swimsd15=sqrt(0.0175)*10^-3;
swimsd10=sqrt(0.0122)*10^-3;
swimsd5=sqrt(0.0053)*10^-3;
swimsd3=sqrt(0.0067)*10^-3;
prob20=(1-exp(-0.1075*ts))*(0.0988/0.1^2);              %probability of
larvae changing swimming speeds more than 0.1 mm/s -> slope
prob15=(1-exp(-0.1141*ts))*(0.0175/0.1^2);
prob10=(1-exp(-0.1170*ts))*(0.0122/0.1^2);
prob5=(1-exp(-0.0893*ts))*(0.0053/0.1^2);
prob3=(1-exp(-0.0990*ts))*(0.0067/0.1^2);



%% create/reset variables

binlog=[];
zcmlog=[];
swimavg=zeros(20,n);
freq=nan(1000,20,3);
velocities=[2:-0.1:-2]'*10^-3;
bins=[-0.25:0.01:0.25];
probfaster1=zeros(length(velocities),20);
probfaster2=ones(length(velocities),20);
probfaster=zeros(length(velocities),20);
driftfix=load('driftfix.txt'); driftfix(:,2)=driftfix(:,2)*ts;


%% create temperature, swimsd and prob table

tsdprob=ones(20,3);tsdprob(:,1)=1:20; tsdprob(3,2:3)=[swimsd3, prob3];
tsdprob(5,2:3)=[swimsd5, prob5]; tsdprob(10,2:3)=[swimsd10, prob10];
tsdprob(15,2:3)=[swimsd15, prob15]; tsdprob(20,2:3)=[swimsd20, prob20];
tsdprob(4,:)=tsdprob(3,:)/2+tsdprob(5,:)/2;
for i=1:5
    tsdprob(i+5,:)=tsdprob(5,:)/5*(5-i)+tsdprob(10,:)/5*i;
    tsdprob(i+10,:)=tsdprob(10,:)/5*(5-i)+tsdprob(15,:)/5*i;
    tsdprob(i+15,:)=tsdprob(15,:)/5*(5-i)+tsdprob(20,:)/5*i;
end
```

```
%% create tables
% create cdf table

freq(:,3,:)=load('freq3.txt');freq(:,5,:)=load('freq5.txt');freq(:,10,:
)=load('freq10.txt');freq(:,15,:)=load('freq15.txt');freq(:,20,:)=load(
'freq20.txt');
pdf=ones(length(velocities),20);

for t=[3,5,10,15,20]
    for r=1:3;

pdfr(:,r)=ksdensity(freq(:,t,r),velocities*10^3,'width',0.1)/sum(ksdens
ity(freq(:,t,r),velocities*10^3,'width',0.1));
        pdf(:,t)=mean(pdfr');
    end
end

pdf(:,4)=pdf(:,3)/2+pdf(:,5)/2;
for i=1:5
    pdf(:,i+5)=pdf(:,5)/5*(5-i)+pdf(:,10)/5*i;
    pdf(:,i+10)=pdf(:,10)/5*(5-i)+pdf(:,15)/5*i;
    pdf(:,i+15)=pdf(:,15)/5*(5-i)+pdf(:,20)/5*i;
end

cdf=ones(length(velocities),20);
for i=1:length(velocities)
    for j=3:20
        cdf(i,j)=sum(pdf(1:i,j));
    end
end
cdf(:,1)=velocities;


% create table for probability of going faster



for i=2:length(cdf)
    for j=[3,5,10,15,20]
        if pdf(i,j)<0.001; if i<20; probfaster1(i,j)=0; else
probfaster1(i,j)=1; end;
        else
            probfaster1(i,j)=(1-probfaster1(i-1,j))*pdf(i-
1,j)/pdf(i,j);
        end
    end
end
for i=length(cdf)-1:-1:1
    for j=[3,5,10,15,20]
        if pdf(i,j)<0.001; if i<20; probfaster2(i,j)=0; else
probfaster2(i,j)=1; end;
        else
            probfaster2(i,j)=1-probfaster2(i+1,j)*pdf(i+1,j)/pdf(i,j);
        end
```

```
    end
end

probfaster(1:20,:)=probfaster1(1:20,:);
probfaster(21:41,:)=probfaster2(21:41,:);

probfaster(:,4)=probfaster(:,3)/2+probfaster(:,5)/2*i;
for i=1:5
    probfaster(:,i+5)=probfaster(:,5)/5*(5-i)+probfaster(:,10)/5*i;
    probfaster(:,i+10)=probfaster(:,10)/5*(5-i)+probfaster(:,15)/5*i;
    probfaster(:,i+15)=probfaster(:,15)/5*(5-i)+probfaster(:,20)/5*i;
end


%% set temperatures
for bottom=B
for diff=DT

top=bottom+diff;                    %temperature of top layer (°C)

if top==21; top=20; end             %21°C is beyond experimental limits
if bottom==21; bottom=20; end


%% temperature profile

prof=[(-0.25:0.01:0.25)', [ones(20,1).*bottom;ones(11,1) ;
ones(20,1)*top]];
for i=1:11
    prof(20+i,2)=round(bottom/11*(11-i)+top/11*i);
end


%% random walk
    % replication
    count=0;


for R=1:rep
    z=unifrnd(-0.25,-0.24,npart,1)*ones(1,n+1);
    swim=zeros(npart,1);                                    %initialize
swim vector
    r=unifrnd(0,1,npart,1);
    for i=1:npart
        for j=1:length(cdf)
            if r(i)>cdf(j,bottom)
                swim(i)=(cdf(j,1)-unifrnd(0,0.1*10^-3))*ts;
            end
        end
    end

    SV=(tsdprob(bottom,2).*randn(npart,1))*ts;
%initialize swimsd
    swimlog=ones(npart,n);
```

```
    for t=1:n                                                   % time steps
        swimlog(:,t)=swim(:);


        ztemp=z(:,t);                                           % "old"
positions
        z(:,t+1)=z(:,t)+swim+SV;                                % random
walk

        z(z<-0.25)=-0.25;                                       % solid
boundary conditions
        z(z>0.25)=0.25;

        T0=prof(round(ztemp*100+25)+1,2);
        T1=prof(round(z(:,t)*100+25)+1,2);

        r1=unifrnd(0,1,npart,1);                                % identifies
larvae that randomly change swim velocity (autocorrelated)
        randAC=[];
        for i=1:npart
            SV(i)=(tsdprob(find(tsdprob(:,1)==T0(i)),2)*randn)*ts;
            if tsdprob(T1(i),3)>r1(i)
                randAC=[randAC; i];
            end
        end




        r2=unifrnd(0,1,npart,1);
        change=[randAC];                                % AC change in swim
speed
        for i=1:length(change)
            j=round((ceil(swim(change(i))*10^4)/10^4-0.0021)/-0.0001);
            if r2(i)<probfaster(j,T1(change(i)))

swim(change(i))=(ceil(swim(change(i))*10^4)/10^4+0.1*10^-3-
unifrnd(0,0.1*10^-3))*ts;
            else
                swim(change(i))=(ceil(swim(change(i))*10^4)/10^4-
0.1*10^-3-unifrnd(0,0.1*10^-3))*ts;
            end
        end




        swimavg(bottom,t)=mean(swim)+swimavg(bottom,t);

        % drift fix
        swim=swim-driftfix(T1,2);
```

```
        swim(swim>0.002)=0.002;
        swim(swim<-0.002)=-0.002;

    end


    % stats
    bin60(:,R)=(hist(z(:,n+1),bins))';
    zcm(:,R)=sum(bin60(:,R)/npart.*(bins*-100+25)');
    R
end

zcmlog=[zcmlog;[bottom top zcm]];
binlog=[binlog, [bottom*ones(1,rep); top*ones(1,rep); bin60]];
beep
bottom
top

end
end

swimavg=swimavg/rep;
```

Horizontal larval aggregation-diffusion model

```
clear
clf
% create empty data logs
log=[]
log2=[]

%replicate
for rep=1:5
    vmlog=[]
    Imlog=[]
    %% create larval distributions along transect
    l=40000;                                                    %transect
length (m)
    time=24*30;                                                 %time
elapsed (h)
    a=[14.14, 32.5, 43.98, 1.92];                               %mean
larval ('Bryozoans','Bivalves','Gastropods','Decapods') abundance (no.
m^-3)
    s=[(0.4+1.1)/2, (1.6+1.1)/2, 1.3, (6+20)/2]/1000*3600;  %mid-range
swimming speeds
    net=pi()*(0.75/2)^2;                                        %net area
(m^2)
    n=round(l*a*net);                                           %total
number of larvae in the transect
    dist=nan(max(n),4);                                         %create
distribution matrix (all NaN's)
    for sp=1:4
        dist(1:n(sp),sp)=rand(n(sp),1);
    end
    dist=sort(dist)*l;



    %% diffusion
    for coeff=0:50                                          %diffusion
coefficient (m^2 s^-1)
        %coeff=3.9 %m^2/s
        k=sqrt(2*coeff*3600);                                   %SD of
the random kick
        %% time steps and sampling
        for t=1:time
            sites=11;
            samples=rand(sites,4).*(l-500);
            for sp=1:4
                for i=1:length(samples)

x(sp,i)=sum((dist(:,sp)>samples(i,sp))&(dist(:,sp)<(samples(i,sp)+500))
)/500/net*100;
                end
                %calculate Morisita's index ("quadrat size" is 100 m^3)
                Im(sp,t)=(sites*sum(x(sp,:).*(x(sp,:)-
1)))/(sites*mean(x(sp,:))*(sites*mean(x(sp,:))-1));
            end
            %calculate variance/mean ratio
```

```
            vm(:,t)=nanvar(x'/100)./nanmean(x'/100);

            %swim to nearest "point of attraction" (every 3000 m)
            for sp=1:4
                index=mod(round(dist(:,sp)/3000),2);
                index(index==0)=-1;
                dist(:,sp)=dist(:,sp)+s(sp)*index+k*(randn(max(n),1));
                dist(dist(:,sp)<0,sp)=abs(dist(dist(:,sp)<0,sp));
                dist(dist(:,sp)>l,sp)=l+(l-dist(dist(:,sp)>l,sp));
            end
            [rep coeff t/time*100]
        end
        vmlog=[vmlog;coeff vm(:,time)'];
        Imlog=[Imlog;coeff Im(:,time)'];
    end
    log=[log;ones(coeff+1,1)*rep Imlog];
    log2=[log2;ones(coeff+1,1)*rep vmlog];
    save('clump_results.mat')
end




%calculate mean and SE of Morisita's and var/mean
Imbarlog=[];ImSElog=[];vmbarlog=[];vmSElog=[];
for i=1:size(Imlog,1)
    Imbarlog(i,:)=nanmean(log(log(:,2)==i-1,3:6));
    ImSElog(i,:)=nanstd(log(log(:,2)==i-1,3:6))/sqrt(rep);
    vmbarlog(i,:)=nanmean(log2(log2(:,2)==i-1,3:6));
    vmSElog(i,:)=nanstd(log2(log2(:,2)==i-1,3:6))/sqrt(rep);
end

%plot
errorbar(Imbarlog,ImSElog)
xlabel('Diffusion Coefficient (m^2 s^-^1)')
ylabel('Morisitas Index')
legend('Bryozoans','Bivalves','Gastropods','Decapods')

errorbar(vmbarlog,vmSElog)
xlabel('Diffusion Coefficient (m^2 s^-^1)')
ylabel('Dispersal Index')
legend('Bryozoans','Bivalves','Gastropods','Decapods')
```